Ordering Geniculate Input Into Primary Visual Cortex

D. Phil Thesis

by Kristine Krug

Christ Church

University of Oxford

Michaelmas 1997

LIFE SCIENCE LIBRARY OX
DEPOSITED
1 8 JUN 1998
THESIS

ABSTRACT

Ordering Geniculate Input Into Primary Visual Cortex
Kristine Krug
Christ Church, Oxford
Doctor of Philosophy
Trinity 1997

Precise point-to-point connectivity is the basis of ordered maps of the visual field in the brain. One point in the visual field is represented at one locus in the dLGN and one locus in primary visual cortex. A fundamental problem in the development of most sensory systems is the creation of the topographic projections which underlie these maps. Mechanisms ranging from ordered ingrowth of fibres, through chemical guidance of axons to sculpting of the map from an early exuberant input have been proposed. However, we know little about how ordered maps are created beyond the first relay. What we do know is that a topological mismatch requires the exchange of neighbours in the geniculo-cortical projection and that manipulating the input to the primary relay can affect the geniculo-cortical topography. Taking advantage of the immaturity of the newborn hamster's visual system, I studied the generation of an ordered map in primary visual cortex during the time of target innervation in normal and manipulated animals. I also investigated the patterning of neuronal activity prior to natural eye-opening.

Paired injections of retrograde fluorescent tracers into visual cortex reveal that geniculate fibres are highly disordered at the time of invasion of the cortical plate. Topography in the geniculo-cortical projection emerges out of an unordered projection to area 17 in the first postnatal week. Furthermore, I show that manipulating the peripheral input can alter the topographic map which arises out of the early scatter. Removal of one eye at birth appears to slow the process of geniculo-cortical map formation ipsilateral to the remaining eye and at the end of the second postnatal week, a double projection between thalamus and cortex has formed. If retinal activity is blocked during this time, this double projection does not emerge. The results implicate retinal activity as the signal that induces the development of a different topographic order in the geniculo-cortical projection.

It is generally believed that visual experience can influence development only after eye-opening. However, the final part of my thesis shows that neurons in the developing visual cortex of the ferret can not only be visually driven at least 10 days before natural eye-opening, but are also selective for differently oriented gratings presented *through the closed eye-lid*. Thus, visually-driven neuronal activity could influence development much earlier than previously assumed in many developmental studies.

Meiner Mutter, meiner Oma
und meinem Vater.

Acknowledgments

I would like to thank

Ian Thompson	who was my supervisor and whom I would definitely choose again.
Andrew Parker	who always made time for me to discuss new ideas.
Pat Cordery	who taught me everything about Histology and who is a wonderful friend.
Bruce Cumming	who supported me in - amongst many other things - the C programming.
Ken Stratford	who wrote patiently so many versions of the nearest neighbour analysis.
"my lab"	who made the three years fun, especially Gary, Anita and Darragh.
Christ Church	which provided support and which is a wonderful place to live.
the Wellcome Trust and the Studien-stiftung	which both supported me exceedingly well throughout the three years and opened up many great opportunities for me.
and my family	my mum, dad, granny and brother who have always been there for me.

The work presented in this thesis is my own. However, some of the first cortical bead injections, a small number of introcular TTX injections and all enucleations were done by my supervisor Dr. Ian Thompson.

No part of this thesis has been submitted for another degree in this University or elsewhere. This thesis conforms to the regulations of the General Board and the Board of the Faculty of Physiological Sciences governing the examination of students for the degree of Doctor of Philosophy as set in the Examination Decrees and Regulations (1993) OUP.

Kristine Krug
21. December 1997

CONTENT

I. Introduction 1

1. Ordered maps in the brain: an overview 2

2. The development of topographic maps 7

   2.1 The thalamo-cortical projection 9
   2.2 Manipulating topographic mapping in cortex 11
   2.3 A role for retinal activity in the development of topography 13

3. Micro-mapping in primary visual cortex 16

   3.1 Early neuronal activity and the development of orientation-selectivity 16

II. Anatomical Methodology 20

1. Animals and anaesthesia 22

2. The tracers 23

3. Manipulating retinal activity during development 27

4. Data Acquisition and basic measures 28

5. Analysis 29

   5.1 Area of dLGN labelled - density analysis 30
   5.2 Nearest neighbour analysis 31
   5.3 Vector analysis 33
   5.4 Cluster analysis 34

III. Development of Geniculo-Cortical Topography in the Hamster 37

1. Introduction 38

2. Material and Methods 41

3. Results 43

3.1 Retrograde labelling of the geniculo-cortical projection by paired injections visualizes the emergence of topography. 43
3.2 Retrograde labelling of geniculate projection neurons by heterochronic injections suggests little role for cell death in map formation. 48

4. Discussion 50

4.1 Assessing order of geniculo-cortical topography 50
4.2 Where is the thalamo-cortical topography generated? A comparison with the somatosensory system. 51
4.3 A role for cell death? 53
4.4 Implications for map formation in the cortex 54

IV. Development of abnormal geniculo-cortical topography after monocular enucleation at birth. 57

1. Introduction 58

2. Material and Methods 61

3. Results 62

3.1 Qualitative assessment of the development of the ipsilateral geniculo-cortical map after monocular enucleation at birth. 62
3.2 The quantitative analyses confirm increased scatter in the ipsilateral map from P4 onwards. 64
3.3 A quantitative test for the double focus. 68

4. Discussion 70

4.1 How does removal of one eye at birth affect the development of the geniculo-cortical map? 70
4.2 How relevant is the "retinal signal" to normal development? 76
4.3 About the role and the nature of "the retinal signal". 77

V. Retinal activity and the development of geniculo-cortical topography after monocular enucleation at birth. 79

1. Introduction 80

2. Material and Methods 82

3. Results 83

3.1 The effect of retinal activity blockade on the development of abnormal topography ipsilateral to the remaining eye. 83
3.2 The effect of retinal activity blockade on the development of normal topography contralateral to the remaining eye. 86

4. Discussion 89

4.1 Is retinal activity essential for abnormal map formation after enucleation? 90
4.2 Is retinal activity necessary for normal development of geniculo-cortical topography? 91
4.3 Implications 92

VI. Visual driving of cortical neurons through the unopened eyelids in ferrets 94

1. Introduction 95

2. Material and Methods 97

2.1 Animals 97
2.2 Surgery and Anaesthesia 97
2.3 Recordings 99
2.4 Analysis 100

3. Results 103

3.1 Neurons in primary visual cortex respond to light through the naturally closed eyelid 103
3.2 At least a third of the visually-responsive neurons respond differentially to orientation 104
3.3 Directionality of responses 107

4. Discussion 108

4.1 The nature of the response 108
4.2 The origin of the oriented response 110
4.3 Development of orientation- and direction-tuning 111
4.4 Implications 113

VII. Conclusions 115

1. Map formation in area 17 117

2. Early activity in visual development 121

References 124

I. Introduction

1. Ordered maps in the brain: an overview

2. The development of topographic maps

2.1 The thalamo-cortical projection

2.2 Manipulating topographic mapping in cortex

2.3 A role for retinal activity in the development of topography

3. Micro-mapping in primary visual cortex

3.1 Early neuronal activity and the development of orientation-selectivity

1. Ordered maps in the brain: an overview

In the sensory systems, most projections are topographically organized. The general order of representations is often based on the primary receptor sheet. In the retinotopic map, two points close to each other on the retina will be mapped close to each other at progressive levels of processing, similarly two points close to each other on the body surface will usually be mapped close to each other in the somatosensory thalamus and cortex. In the auditory system, the receptor sheets provides only one axis of central representations based on iso-frequency bands, across which other features are mapped. However, in the olfactory system, the order of the receptor-sheet seems to be lost in the primary relay and a new order is created. Another, well-studied example of a sensory map which is not implicit in the spatial arrangement of the peripheral receptor sheet is the auditory space map in the superior colliculus. It represents the location of a sound source, for the computation of which binaural timing and intensity cues as well as frequency modulations by the pinna are used.

From the retina, visual information is basically relayed in such a way that one point in visual space is represented at one locus on a retina, one locus in the dorsal lateral geniculate nucleus (dLGN) and one locus in primary visual cortex. However, the basic receptor map is not passively relayed but transformed and recreated at each level. Firstly, different projections containing either the whole or just a partial map can be dispatched from the same structure. The retina not only projects to the dLGN but also to the superior colliculus. Ascending information in the somatosensory information in the spinal cord is

divided into multiple tracts, like the medial-lemniscal and the antero-lateral tract. They represent different submodalities of the somatosensory system like touch and pain and have different central targets. The cochlear nerve bifurcates sending information in parallel to the three subdivisions of the cochlear nucleus. Also, before most sensory projections reach the thalamus they decussate completely or partially. In the somatosensory system with its almost complete cross-over, each half of the body is represented in the contralateral hemisphere. There is no decussation of the primary sensory projection in the olfactory system. In the visual system, the contralateral hemifield is mapped in each thalamus and this requires a partial decussation of visual fibres at the chiasm. In the dLGN, although the input from the two eyes is aligned, there is not a single topographic map but multiple ones which are registered in layers. In the visual system, in particular in cortex, the functional visual map is often described as visuotopic, since the anatomical retinotopic map gives rise to an ordered functional representation of the contralateral hemifield. Other features like orientation-selectivity maps or ocular dominance columns have to be mapped within the framework of this topographic map, such that over a small range within the map topography breaks down (see below).

Much of the work on the development of primary sensory maps has focussed on the retino-tectal or retino-collicular projection. However, for the thalamo-cortical topography most studies have been done in the somatosensory system of rodents, since the topographic order is easily visualised in the form of "barrels" in the cortex, which represent individual whiskers (Woolsey and Van der Loos, 1970). The pattern of barrels can be manipulated during development by removal of whiskers and hair-follicles (Van der Loos and Woolsey,

1973). For these reasons and the above outlined similarities, these are the major two areas of research I will focus on in particular in relationship to my own work. Primary thalamo-cortical projections provide also the best evidence for reorganization in development and the functional significance of ordered maps in cortex. Work in the somatosensory system of the macaque (Florence et al., 1996) shows that if a peripheral nerve is severed prenatally, the cortical map can rearrange into an ordered representation despite the disordered regeneration of the peripheral nerve. Later on, the plasticity of cortex appears limited. Performance in perceptual tasks like discrimination appears correlated to the degree to which the topographic map in cortex could reorder. An ordered representation of the incoming information seems to be a prerequisite for appropriate processing.

Topographic maps can be studied with various tools. Traditionally, single, small injections of retrograde tracers, like WGA-HRP were used. For a topographic projection, a discrete focus of back-labelled cells was expected to be found in a predictable region of the projecting structure. However, single injections by themselves cannot provide information about the orientation of a map. Also, the size of the labelled cluster of cells is very much dependent on the size of the injection site. In order to control for spread of tracer, paired injection of differently coloured fluorescent tracers have been used more recently (see anatomical methods). With two or more different tracers more information about the relative orientations of two maps to each other can be obtained. Problems occur if those tracers do not have similar uptake properties or are not accurately enough placed, ie. a second injection is made unknowingly into an adjacent brain area. Another way, to study topographic mapping is by anterograde tracing of fibres, using, for example DiI or

HRP. Thus, the trajectory of fibre fascicles or single axons can be studied. The shape and the extent of their terminal arbors as well as how they course in relationship to each other can give some indication of disorder in a projection. For example fibres bundled in a tight fascicle should be more ordered than if fibres interdigitate.

Another way to study a map is by recording receptive fields along the different axes of the map. The anatomical and the physiological map would be expected to be congruent, i.e. if there is a point-to point connectivity between different structures, receptive fields of neurons that project to each other would be expected to overlap in most cases. Within an ordered visual map, receptive fields should shift in an ordered fashion across the visual field or, in the somatosensory system, across the body surface. However, focussing down in visual cortex onto clusters of neurons, topography appears to break down and local topographic scatter can be found. The minimum distance between two perpendicular electrode penetrations in primary visual cortex that record adjacent non-overlapping aggregate receptive fields demarks a hypercolumn. Within the hypercolumn, local topographic scatter is created by the representation of different features like for example orientation columns. But the clustered representation of these features down to the individual neurons requires again specialised, precise input. Orientation-selectivity in simple cells needs the precise alignment of receptive fields from geniculate neurons to create this emergent property of cortical cells. The generation of orientation-tuning of cortical neurons will be discussed in the last section of the introduction in connection with patterns of early activity in primary visual cortex. Early neuronal activity could influence

the development of the topographic map as well as the generation of micro-mapping in primary visual cortex of rodents and carnivores.

2. The development of topographic maps

In the visual or the somatosensory system, the visual field or the body surface is represented in topographic maps at multiple levels of processing. One of the fundamental problems of development is the creation of the necessary precise point-to-point connectivity between consecutive layers of processing. There have been three main complementary ideas about how to order a specific input onto its target. One is the chemo-specificity hypothesis (Sperry 1963), in which a chemical signal or gradient guides the growing fibres to their correct target. Another suggests that axon-to-axon interactions preserve the order in developing projections (Horder and Martin, 1978, but see Scholes, 1979). The third is regressive self-organization based on Hebbian synapses, which sculpts the correct order from exuberant ingrowth (Hebb, 1949; Willshaw and von der Malsburg, 1976). All three could contribute to map formation: to reliably create an ordered map with a predictable polarity, the global axes of the map need to be defined and often further local refinement will be needed.

A well studied example of topographic map formation is the retino-tectal, or retino-collicular, projection. In this map, the axis perpendicular to the direction of fibre ingrowth is crudely laid out in the ingrowing fibre bundle in many species (Scholes, 1979 - fish; Torrealba et al., 1982 - cat; Simon and O'Leary, 1991 - rat; Reese and Baker, 1993 - ferret; Chan and Guillery, 1994 - rat). In rodents and in carnivores, this is the medio-lateral axis and represents the ventro-dorsal axis of the retina. For the rostro-caudal axis representing the temporo-nasal retinal axis, molecular gradients of molecules have been proposed to lay-

out the basic polarity. The notion that precise, localised chemical signals must be involved in axon guidance stems from experiments on the regeneration of the retino-tectal projection in amphibians (Sperry, 1963). For example, if an eye is rotated in the orbit, visuo-motor coordination recovers, but is inverted. Therefore, most axons have found their original targets again. An in vitro stripe-assay demonstrated a signal in the caudal tectum that repels temporal axons (Walter et al., 1987a; Walter et al., 1987b). Appropriate gradients of expression patterns have been identified in the rostro-caudal axis of the tectum and complementary to this in the retina, which have been tested in vitro and in vivo (Drescher et al., 1995; Cheng et al., 1995; Nakamoto et al., 1996). But this does not necessarily mean a single growth cone is directed precisely to its final target by molecular guidance. Indeed, there is evidence that retinal fibres overshoot and reorganise to find their target (Simon and O'Leary, 1992 - rat; Nakamura and O'Leary, 1989 - chick). Also retino-tectal axons have been shown to send out multiple short collaterals over some extent of the optic tectum in the chick (Yates et al, 1996). These twigs could either test a molecular gradient and/or be selected and/or rearrange by an activity-dependent signal. In the rodent retino-collicular map, it has been shown that an initially very crude projection is topographically organised during a period of terminal rearrangement and retinal ganglion cell death (O'Leary et al., 1986; Simon and O'Leary, 1992). Furthermore, activity seems to be important for this refinement, and there is evidence that NMDA-receptors may be one effector of the "Hebbian Synapse" that seems to be involved (Simon et al., 1992). However, it has been proposed that not all retinal maps start disordered: in carnivores like the cat, the initial retino-collicular map appears to be more ordered (Chalupa et al., 1996).

Not much is known about the development of retino-geniculate topography. Most studies have examined the time course of crossed and uncrossed segregation and the emergence of the monocular segment, which is a basic requirement for a binocularly congruent map. In both the rodent and the ferret this happens postnatally (So et al., 1984; Linden et al., 1981). But Jeffery (1985) shows that early monocular retino-geniculate topography exists before the segregation of the input from the two eyes.

2.1 The thalamo-cortical projection.

Once the input from the two eyes is aligned, it might seem conceivable that the mapping at the following stage, from geniculate onto visual cortex, could be achieved by preserving the thalamic map in the growing projection (Blakemore and Molnar, 1990; Kennedy et al., 1994). Indeed, results from retrograde tracing of thalamic axons in the somatosensory system of rodents suggest that the earliest projections to the subplate and lower cortical layers are topographically ordered (Catalano et al., 1996; Agmon et al., 1995). However, a topological mismatch of the polarities of the maps in the thalamo-cortical relay nuclei and the primary sensory areas in cortex renders a passive relay of the map impossible. An exchange of neighbours somewhere along the trajectory is required (Connolly and Van Essen, 1984; Nelson and LeVay, 1985; Adams et al., 1997). Nelson and LeVay (1985) suggested the subcortical white matter as the place for the exchange of neighbours, since they observed defasciculation and crossing there. In cats and ferrets, there is also a so-called "waiting period" for geniculate fibres in the subplate, which would give them time to reorganize (Ghosh and Shatz, 1992). The existence of a waiting period

in the rodent thalamo-cortical projection is disputed (Catalano et al., 1996). The cortico-thalamic projection must also reorganise and Adams et al. (1997) have proposed the region in or close to the internal capsule, including the perireticular nucleus, as the relevant site. Again fibres defasciculate in this structure and form a dense fibre meshwork, which could signify the reorganization of the map. An alternative hypothesis to the exchange of neighbours in the subplate is the "handshake theory" in which thalamo-cortical and cortico-thalamic fibres meet in the internal capsule and "guide" each other to the correct target (Molnar and Blakemore, 1995). However, evidence is sparse for this theory. Furthermore, thalamo-cortical and cortico-thalamic tracts have been described to travel separately along most of the internal capsule in the rodent (Miller et al.,1993).

So, if the exchange of neighbours does indeed take place underneath cortex, what do we know about fibre order in the subplate and in the lower cortical layers? As outlined above, a retrograde tracing study with DiI in the rat somatosensory system suggested that at E18 thalamo-cortical fibres project in an ordered fashion to the subplate and lower cortical layers. Yet it is not clear whether this projection would also be topographically correct for the adult thalamo-cortical map. Also anterograde tracing of thalamo-cortical fibres describes at least local disorder with horizontally coursing fibres in the subplate (Catalano et al., 1996 - rat) and the lower cortical layers (Agmon et al., 1993 - mouse). The state of topography in the projection to area 17 in the subplate and the lower cortical layers is not known. The only data available is again anterograde fibre tracing with HRP and since the tracer placements were made into the white matter, the origin of the labelled fibres could be either geniculo-cortical or cortico-cortical. Naegele et al. (1988) describe

fibres running horizontally in the subplate with multiple twigs, which project vertically into cortex. This phenotype suggests that ingrowing fibres are testing multiple sites for a signal.

The available data suggest at least local disorder when geniculate fibres reach visual cortex, but the extent of the disorder has not been established. Therefore, it is also not clear if the subplate is the place of exchange of nearest neighbours. The apparent confusion may be due the choice of species in some studies: in most rodents and carnivores, geniculate fibres have reached their target by birth and it is not too surprising that the geniculo-cortical projection is topographically ordered (Kennedy et al., 1994). The hamster and the ferret are two exceptions - the bulk of the projection enters cortex only postnatally (Miller et al., 1993; Krug et al., submitted; Smith and Thompson, submitted). A major part of this thesis is the documentation, qualitatively and quantitatively, of considerable topographic disorder in the early geniculo-cortical projection to the subplate and lower cortical layer. Disorder that disappears in the first postnatal week (Chapter III).

2.2 Manipulating topographic mapping in cortex.

To obtain a better understanding of the mechanisms guiding map formation, many researchers have studied ways in which topographic mapping can be manipulated. For example in cortex, one classic example are albino strains which have a genetic deficiency in melanin. In albino animals, more fibres than normal cross to the contralateral hemisphere at the optic chiasm which results in a much narrower strip of temporal retina sending axons to the ipsilateral dLGN (Guillery and Kaas, 1971). The map in the dLGN is abnormal, such that in most parts of the dLGN the lines of projection through the layers

no longer represent a single point in visual space. If this abnormal map was relayed via an unchanged geniculo-cortical projection, certain parts of visual cortex would represent two locations far apart in visual space. However, if the geniculo-cortical map was influenced by the altered retinal input, it might be possible to recreate a continuous map of the visual field in cortex. Amazingly both outcomes are found, but usually not in the same animal (Kaas and Guillery, 1973; Hubel and Wiesel, 1971; Huang and Guillery, 1985; Guillery et al., 1984). However, there are also reports of both patterns in the same animals (Cooper and Blasdel, 1980; Thompson, *personal communication*). Thus, basic geniculo-cortical topography is sometimes produced independently of altered retinal input, but sometimes is able to rearrange and form a novel cortical map. It is not known what determines the course which is eventually taken.

The influence of abnormal retinal mapping for geniculo-cortical topography is underlined in enucleation experiments. In the hamster, removal of one eye at birth leads to a double map of the geniculo-cortical projection ipsilateral to the remaining eye (Trevelyan and Thompson, 1992). The abnormalities in the adult are twofold. There is a physiological double representation of the visual field of the ipsilateral temporal retina. Also, the topography between geniculate and cortex is anatomically abnormal: a single very lateral or very medial point in area 17 receives input from two distinct parts in the dLGN (this can be visualized by paired cortical injections of differently coloured retrograde tracers). To yield this pattern of connectivity, again a combination of retina-dependent and retina-independent mechanisms seems to be at work. The basic duplicated map is most likely present in the dLGN (see Thompson, 1979) and is relayed by an anatomically normal

mapping rule to cortex. However, it is hypothesized that if the two points in the geniculate get their input from the same site in the retina, they also can feed into the same cortical location.

How much can these manipulations tell us about normal map formation? The development of altered topography has not been studied. The question is: does rearranged geniculo-cortical topography develop with the same time-scale and in a similar process to the normal topography? In chapter IV of this thesis, I will investigate the time-course of the development of the abnormal ipsilateral geniculo-cortical map after monocular enucleation. The abnormal topography develops out of the same initial disordered projection to visual cortex, albeit on a slower time-scale.

2.3 A role for retinal activity in the development of topography.

Manipulation of retinal input suggests a possible role of a retinal signal in the development of the geniculo-cortical projection. The nature of that signal is not known. One likely candidate is retinal activity, but the fact that the blockade of activity often has little effect on normal, surgically unperturbed development in mammals renders its importance still elusive. However, evidence from amphibians and fish demonstrate an important role of retinal activity for refinement of the retino-tectal topography in development and regeneration (Cline, 1991, for review). In general, patterned neuronal activity, either visually driven or intrinsic, could drive retinotopic map formation by ensuring that neighbouring retinal ganglion cells fire together. A Hebbian process would consolidate inputs that are synchronously active. Visual driving does this by default, since

neighbouring ganglion cells represent overlapping or adjacent parts of the visual field. Intrinsic, spontaneous activity spreading in waves across in the neonatal retina of the ferret achieve the same effect (Meister et al., 1991; Wong et al., 1993). But what are the consequences of blockade of retinal activity in development? A topographically normal geniculo-cortical map develops in the complete absence of retinal input as studies on binocularly enucleated or congenitally anophthalmic animals have shown (Godement et al, 1979, Kaiserman-Abramof et al., 1980; Guillery et al., 1985). However, it is not entirely clear whether there might be increased local disorder and scatter in the geniculo-cortical projection in these animals.

Evidence from the somatosensory thalamo-cortical projection in rodents suggests that activity does not determine basic topographic mapping itself. Rather it is involved in adaptive changes in the cortical map after disruption of the peripheral receptor sheet. For example the expansion of adjacent barrels after whisker removal can be prevented by blocking NMDA-receptor-activity in barrel cortex (Schlaggar et al., 1994). Also the more localised refinement of the map appears activity-dependent (Fox et al., 1996). Blocking neuronal activity or a component of it interferes with the rearrangement and refinement of the thalamo-cortical map. In the first example, the thalamo-cortical map was studied after peripheral whisker removal. This paradigm is similar to the enucleation experiment in as far as the input to the thalamo-cortical projection was altered. But there is only an expansion of the map in the thalamo-cortical projection, while after enucleation basic topography is also altered. However, if the results from the somatosensory thalamo-cortical map are transferable to the geniculo-cortical projection, blocking retinal input

should interfere with the abnormal changes in the map which result from the peripheral manipulation. Thus, if the above hypothesis is correct, the altered anatomical mapping of geniculate onto cortex after monocular enucleation at birth should be prevented. This will be tested in Chapter V.

3. Micro-mapping in primary visual cortex

Zooming in on the level of clusters of neurons or even single neurons in primary visual cortex, the problem of mapping reappears. In order to generate ocular dominance (OD) columns in layer IV, fibres from the two eyes need to be segregated for individual topographic locations and mapped at regular intervals in layer IV. One way to generate properties of single neurons like orientation tuning or binocular disparity is through the specific input of a set of geniculate neurons with appropriately aligned receptive fields (Hubel and Wiesel, 1962; Barlow et al., 1967). Indeed basic orientation-tuning in primary visual cortex has been shown recently to be a function of the geniculate input to layer IV cells (Reid and Alonso, 1995; Ferster et al., 1996). Again the question is how geniculate afferents become mapped precisely onto their cortical target.

3.1 Early neuronal activity and the development of orientation-selectivity

The influence of visual experience on the development of visual cortex was demonstrated first by the effects of monocular deprivation on ocular dominance columns in primary visual cortex of kittens (Hubel and Wiesel, 1963a). Hubel and Wiesel themselves generally believed that most features of neurons in primary visual cortex are innate, and in their hands neurons could be classified as simple or complex cells and showed orientation-tuning and directionality at eye-opening in kittens (Hubel and Wiesel, 1963b). However, in the 1970s the idea that visual experience shapes development became very popular. This arose for basically three reasons. For one, many experiments were

carried out that showed dark-rearing, stroboscopic lights and patterned environments could indeed influence receptive field properties in primary visual cortex. For example, exposure of kittens to a striped environment led to a higher proportion of neurons in primary visual cortex tuned to the same orientation as the stripes, at the expense of other orientations (Blakemore and Van Sluyters, 1975). Secondly, it was found that at the time of eye-opening some properties like disparity-tuning and orientation-tuning seemed less developed and were found in fewer neurons (Barlow and Pettigrew, 1971; Blakemore and Van Sluyters, 1975). Thirdly, it was such a seemingly beautiful and simple hypothesis, especially in the absence of any other good idea of how mapping was controlled innately.

The distinction between experience-dependent and innate factors influencing development saw a new twist in the late eighties with the first description of correlated spontaneous activity in the developing retinal ganglion cell layer before eye-opening and even before birth (Maffei and Galli-Resta, 1990), followed by the observation of intrinsically generated waves travelling across the retina, which are transmitted to the dLGN (Wong et al., 1993; Mooney et al., 1996). These waves provide a patterned activity signal that could provide spatial and temporal information for development. Thus, retinal activity could be important before natural eye-opening. Retinal waves have been implicated for example in the ON-/OFF-layer formation in the dLGN of ferrets, in particular, since it appears that ON and OFF-retinal ganglion cells fire at different rates (Wong et al., 1996). However, it is not clear how they would be involved in the shaping of orientation-tuning.

The nineties see a trend towards the innateness again. Many studies employed binocular suture paradigms or recording and imaging techniques in development to investigate whether experience is or is not necessary for the development of characteristics of primary visual cortex in carnivores (see examples below). Concentrating on orientation-tuning, Chapman and Stryker (1993) recorded from neurons in primary visual cortex of ferrets after artificially opening their eyelids. Since they could detect orientation-selective units before natural eye-opening, they concluded basic orientation-tuning must arise independent of experience. It is not clear, however, if those orientation-tuned units are generated spontaneously or develop through some kind of genetically programmed mechanism. Infusion of TTX into visual cortex from P21 for 3 weeks shows that retinal activity seems to be necessary for the maturation and sharpening of orientation-tuning (Chapman and Stryker, 1993). As a new tool, optical imaging has been much used to investigate the development of maps of orientation-tuning in visual cortex. Interestingly, these maps can only be recorded days or weeks after eye-opening in area 17 and 18 of ferrets and cats (Chapman et al., 1996; Gödecke and Bonhöffer, 1996; Gödecke et al., 1997). This could have two reasons: either they develop only at that time or the signal is too weak to be picked up early on. In kittens, reverse suturing experiments show no effect on the alignment of the maps of orientation columns through the two eyes (Gödecke and Bonhöffer, 1996). Also, the development of the orientation map in area 18 is not affected by binocular suturing (Gödecke et al., 1997). The idea that most features are innate is so prevailing that authors have claimed for example that binocularity develops independent

of experience basing their interpretation on results from three-week-old kittens (Freeman and Ohzawa, 1992). Kittens open their eyes at the beginning of the second postnatal week.

The tacit assumption in all the papers cited above is that visual experience can influence development only after eye-opening, and even then some find this doubtful. However, there are some indications in the literature that neurons in primary visual cortex of the cat can be driven before natural eye-opening (Huttenlocher, 1967). In the last part of my thesis, I show visual driving well before natural eye-opening in three to four week old ferrets through *the unopened eyelids*. The patterning of neuronal responses, in particular orientation-selectivity, at this early age, is investigated.

II. Anatomical Methodology

1. Animals and anaesthesia

2. The tracers

3. Manipulating retinal activity during development

4. Data Acquisition and basic measures

5. Analysis

5.1 Area of dLGN labelled - density analysis

5.2 Nearest neighbour analysis

5.3 Vector analysis

5.4 Cluster analysis

Anatomical Methodology

The following sections provide an overview and discussion of the basic procedures and techniques used for the experiments on the anatomical development of the geniculo-cortical projection in the hamster (Chapters III, IV, and V). In particular, the analytical tools with which different aspects of topography were quantified are introduced. Also, results on properties of tracers and their uptake were included, when they are relevant to the three anatomical chapters. Some experiments required additions to or deviations from the methodology described here, these will be described in the relevant chapters. Electrophysiological techniques are explained entirely in the methods section to chapter VI.

All the anatomical work on the development of the geniculo-cortical projection has been undertaken on the golden hamster (*Mesocricetus auratus*). The hamster was chosen because it is born relatively immature in comparison to most other rodents as well as most carnivores, after a gestation period of only 15-16 days (Wolfensohn and Lloyd, 1994). The eyes open about 14-15 days after birth. Most geniculo-cortical fibres only invade visual cortex postnatally (Miller et al., 1993; Krug et al., submitted), rendering the hamster an ideal experimental subject to study the development of topography in primary visual cortex.

1. Animals and anaesthesia

All anatomical experiments were carried out on hamster pups of time-mated females. The day of birth was counted as postnatal day zero (P0). Some hamster pups had one eye removed on the day of birth. This procedure as well as intraocular injections of tetrodotoxin (TTX) or saline before P7 were carried out under ether anaesthesia. For cortical bead injections up to P6, hamsters were anaesthetized with a dilute solution (1 in 10 in 0.9% sterile saline) of alphaxalone 0.9% and alphadolone acetate 0.3% (Saffan, Pitman-Moore, Uxbridge, UK; i.m., equivalent dose of 0.5 ml/kg at full concentration). Older animals (P12) were injected i.p. with a 1 in 2 dilution of pentobarbitone sodium (Sagatal, RMB Animal Health Limited, Dagenham, UK; 60 mg/kg at full concentration). For perfusions an overdose of Sagatal was given i.p. at all ages.

All care of the animals, as well as all procedures, were carried out in accordance with home office regulations.

2. The tracers

Fluorescent latex microspheres. Latex microspheres (beads) filled with either rhodamine or fluorescent green (LumaFluor, Naples, Florida) are fast and bright retrograde tracers *in vivo*. They are ideal for double tracer studies since despite their different wavelength they have very similar uptake and labelling properties (Katz and Iarovici, 1990). The diameter of the beads ranges between 0.02 - 0.2 μm. They are assumed to be taken up actively at terminals and growth cones and retrogradely transported to the cell soma by fast axonal transport, but the precise mechanisms are as yet unknown (Katz et al., 1984). After injections into area 17, the labelled cell bodies in the dLGN appear distinct and clearly visible through the appropriate fluorescence filter with a x25 objective, which I commonly used to analyse sections. Fibres of passage do not appear to take up the tracer, since injections into the white matter label only few or no cells in the dLGN (Trevelyan, 1992; Chapter III, Results).

At certain postnatal ages (P2, P4, P6 or P12) anaesthetized hamsters received paired or single injections of red and green fluorescent latex microspheres (diluted 1 in 10 in either distilled water or 0.9% saline) into area 17. The scalp was resected and discrete placements of the retrograde tracer were made perpendicular to the cortical surface either through pinpricks in the skull at ages P2 to P6 or after craniotomy at P12. Paired injections were spaced medio-laterally, 300 μm to 800 μm apart (Table II.1). Injections at P2 were placed roughly level with lambda and 1.5 mm to 2.3 mm laterally. With progressing age injection sites were placed up to 1 mm forward to lambda and up to 3.5 mm laterally.

According to age between 25 nl and 100 nl of the tracer were injected through glass pipettes (inside tip diameter 10 - 25 µm) under air pressure. The scalp was resutured and animals were allowed to recover in an incubation box. They were normally sacrificed after 18-24 hours for P2 injections or 24-48 hours for the older hamsters, which were returned to their litter mates, to allow for transport of the tracer. For heterochronic experiments, the red and the green tracer were injected at different times at the same cortical location. Animals received a single injection at P2 and then, after identification of the original site under UV-light, a second injection of a different colour at either P6 or P12. These animals were sacrificed 24-48 hrs after the second injection.

	number of animals	Injections - ML separation	Injection size in %Area 17
P2	7	575 µm ±160.5	1.66% ±1.2
P4	3	550 µm ±50	
P6	8	481 µm ±185	1.29% ±0.78
P12	7	557 µm ±203	1.27% ±0.47

Table II.1. Injection sites. This table contains measurements of the medio-lateral separation of paired injections and the size of their single injection sites (in %area of layer IV). The analysed material is taken from Chapter III. To calculate the percentage area of area 17 injected, I used measurements of the extent of layer IV obtained with transneuronal labelling (Krug at al., submitted). The bold values represent mean values, underneath is their standard deviation.

In fixed sections, injection sites appear discrete and in the case of the paired injections non overlapping. They occupy roughly 1-2% of the area of area 17 (see Table II.1). Up to and including P6, the bead injections usually penetrated the cortical plate and the subplate. Only at P12 was it possible to restrict most injection sites to the cortical plate (Figure II.1). Previous work on single injections suggests that the beads are not taken up

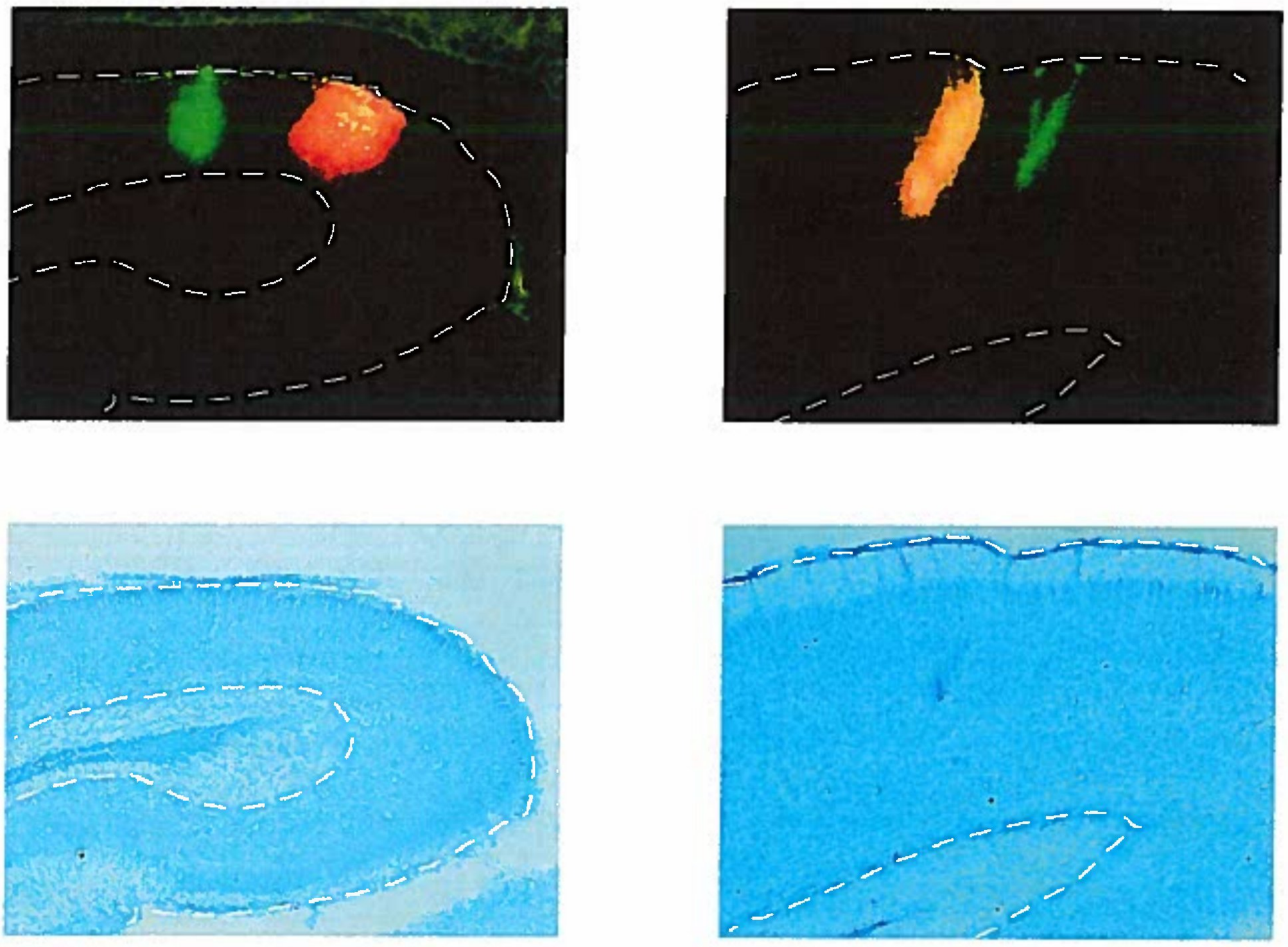


Figure II.1. The photomicrographs at the top of the page depict injection sites in area 17. The picture on the left shows paired injections at P2, the one on the right injections at P12. The corresponding Nissl sections are underneath. The pial surface and the border between subplate and white matter were marked in the Nissl sections with a white dashed line, then the outlines were transferred to the fluorescent photomicrographs. At P2, injection sites penetrated the cortical plate as well as the subplate, while at P12, both injections were restricted to the cortical plate.

beyond the visible injection site (Katz et al., 1984). My closely spaced, paired injections of red and green microbeads also control for lateral spread of the beads in cortex, since we can determine the number of double-labelled cells. If, for example in very young animals, the diffusion of tracer was much greater than the apparent injection sites, the two injections would overlap. This would generate a high proportion of the double-labelled cells, which is not the case (see Chapter III, Discussion).

After the appropriate survival time, animals were perfused through the heart with PBS followed by 4% paraformaldehyde in 0.1 M phosphate buffer. After postfixation, brains were removed from the skull and soaked in 30% sucrose (in distilled water or in 4% paraformaldehyde) until they sank. Then coronal sections were cut at 50μm on a freezing microtome. One in two series were mounted on gelatinized slides. After brief washes in 100% ethanol and xylene (20-30 seconds in each), one series was coverslipped using Fluoromount medium. The other series was stained with cresyl violet and coverslipped with DPX.

Wheatgerm agglutinin conjugated with horseradish peroxidase (WGA-HRP). In order to ascertain the basic size and shape of the dLGN on coronal sections at P2 (Figure II.2), when it is more difficult to identify the dLGN from Nissl stain, hamsters received an intraocular injection of WGA-HRP at P0 (4% in sterile saline containing 0.02% Fast Green FCF; 150-200 nl). After 48 hours survival, they were perfused with PBS followed by a mixture of 1% paraformaldehyde/1.25% glutaraldehyde in 0.1 M phosphate buffer followed again by PBS. Slide-mounted 50 μm fixed coronal tissue sections were reacted

dLGN at P2

500 μm



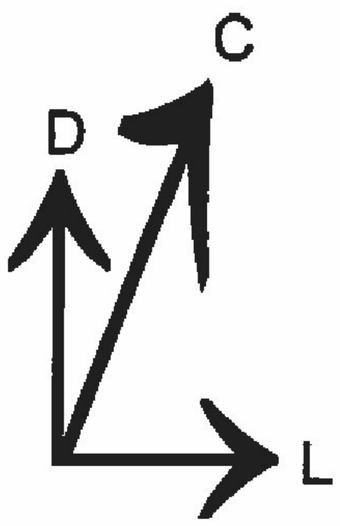


Figure II.2.
These photomicrographs depict a one in two series of sections through a dLGN at P2. The dLGN was labelled antero-gradely with WGA-HRP, injected at P0 into the contra-lateral eye. Sections are 50 μm thick and run caudo-rostrally from the top to the bottom of the page. The fibres from the optic tract enter the dLGN laterally. The borders of the dLGN are clearly visible (see arrows), even at this early age.

D -dorsal, **C** - caudal, **L** - lateral.

with tetramethylbenzidine by a modified standard procedure (Mesulam, 1982). The pattern of label was compared to P2 Nissl stained sections.

3. Manipulating activity during development

Intraocular injections of tetrodotoxin (TTX). In some hamsters which had an eye removed at birth the role of retinal activity in map formation was investigated. Starting at P2, the pups received daily injections of 10^{-3} M tetrodotoxin (TTX) in citrate buffer (volume 25 - 100 nl, depending on age) into the remaining eye (Thompson & Holt, 1989). The volume is roughly adjusted to estimates of the eye volume at the particular ages to yield a final concentration in the eye of around 10^{-6} M. This concentration was shown to block visually elicited responses in the superior colliculus (SC) at P16 (Thompson and Holt, 1989). Until P7 hamster pups were anaesthetized with ether, later Sagatal was used (see 1. Animals and anaesthesia). At P12, animals received bilateral paired bead injections of red and green fluorescent latex microspheres (injection volume 75 nl; medio-lateral separation 400-600 µm) under Sagatal anaesthesia (see 2. Tracers). For the controls the same protocol was carried out, but instead of the TTX only the citrate buffer (pH4.3) was injected.

4. Data Acquisition and basic measures.

Geniculate neurons retrogradely labelled with fluorescent tracers were sampled with a computer program. Using a Zeiss fluorescent microscope, a *camera lucida* view of the display screen was optically superimposed onto the coronal section. The outlines of the dLGN were drawn into the computer at low magnification (x 2.5 objective) and a sample grid (200 x 200 μm) superimposed. Labelled cells were drawn at a higher magnification (x 25 objective) using a 200 x 200 μm sample box, thus ensuring that all the labelled cells within the dLGN were counted. Only cells in which the retrograde tracer defined the cell soma were drawn. For each sample box, the locations of all cells of one colour were marked in first. Then the display screen was cleared and the filter set was changed so that the population of cells labelled with the second tracer could be drawn independently. The computer package then identifies as candidates for double-labelled cells red and green profiles whose centres were less than 10 pixels (= 5.8 μm) apart. These were subsequently assessed visually and classified as double- or single-labelled. The dLGN borders were verified from the Nissl stained sections. The program contains information about the absolute locations of cells labelled by the two tracers and the positions of dLGN borders.

This data was then imported into SYSTAT (for DOS or Version 5 for Windows; SYSTAT, Evanston, Illinois) for visualisation, printouts and further analysis.

5. Analysis

The analysis was carried out in the coronal plane. In the adult hamster, a column running roughly rostro-caudally feeds into one point in cortex (Dursteler et al., 1979). Medio-laterally spaced injections in cortex label foci that are separate in the coronal plane, representing slices through the columns (Figure II.3). A medial injection into area 17 usually labels cells lateral in the dLGN and a lateral injection labels a more medial part of dLGN. The relationship between the two columns of label, and thus between the two foci on each section, depends on the injection site parameters as well as on the precision in the topographic map. Keeping the injection parameters as constant as possible (see above), I studied the development of topography in the geniculo-cortical map during the first two postnatal weeks. Coronal sections were taken through the whole dLGN and most of the observed refinement during this phase of development could be seen in individual sections. All labelled cells within a section were counted and their x and y coordinates determined by superimposing a Cartesian coordinate system. The order in the geniculo-cortical projection was quantified in three ways, by a density analysis estimating the percentage labelled area of dLGN, a nearest neighbour analysis looking at the segregation of input to the two cortical injection sites, and by a vector analysis testing for the overall columnar organisations of the projection. For studies on the abnormal geniculo-cortical projection seen ipsilateral to the remaining eye in enucleated animals (Chapter IV and V)), a cluster analysis was also employed.

Figure II.3. A 6-day-old hamster received paired injections of red and green microbeads into area 17. The injection sites were separated by about 500 µm along the medio-lateral axis. The photomicrograph depicts a coronal section through the brain. At the top, the red and the green injection sites are visible in visual cortex. In the bottom right-hand corner, the slightly darker outlines of dLGN can be seen. The two cortical injections label cells in two discrete columns in the dLGN. On coronal sections, these are visible as two discrete foci of label: the red and the green arrows point to the red and the green focus respectively. The two foci lie dorsally in the dLGN, as it would be expected from a more caudal section. The medio-lateral relationship of the two foci is reversed to that of the cortical injection sites.

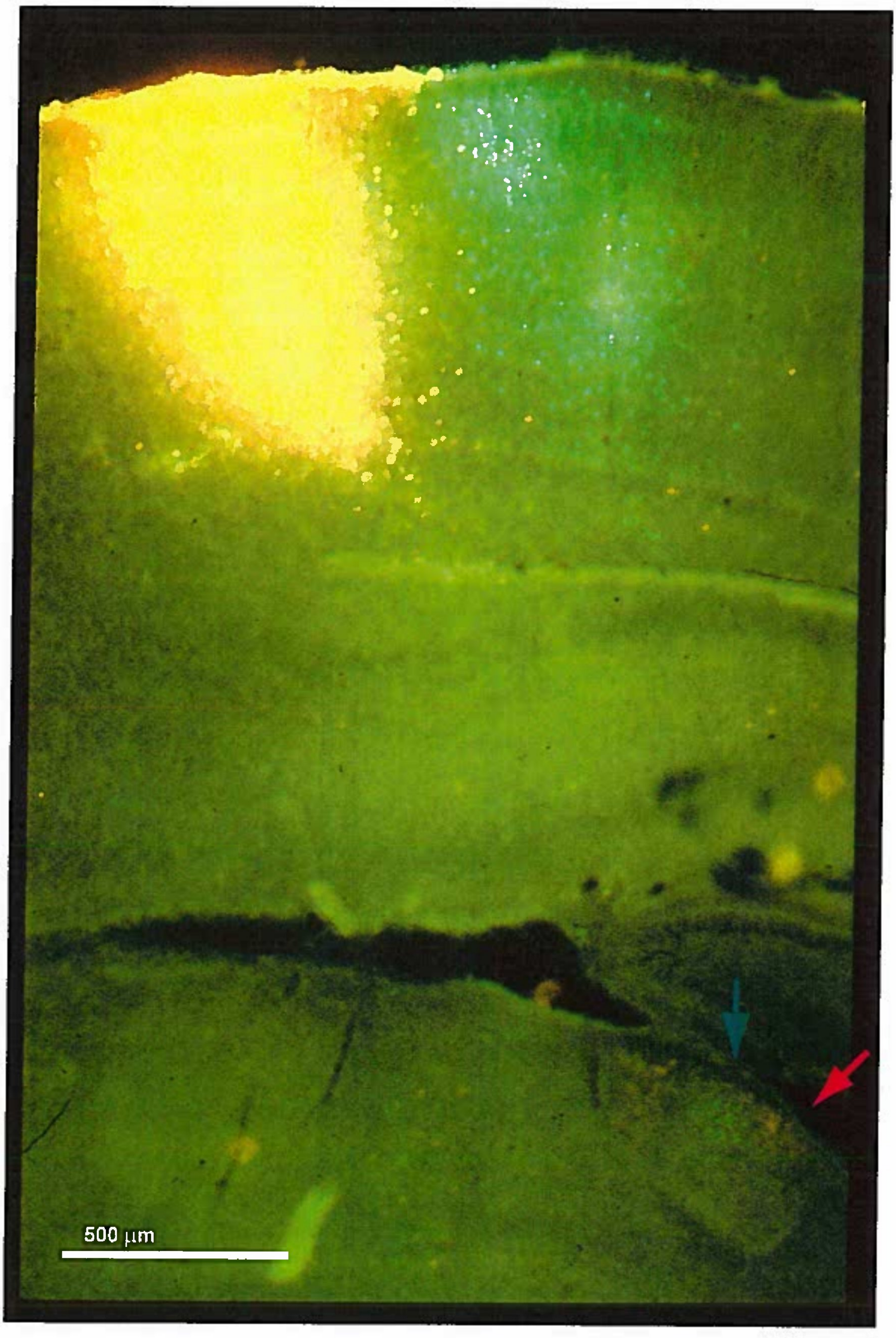


Figure II.3

5.1 Area of dLGN labelled - density analysis

The extent of dLGN labelled by a single injection was estimated with isodensity contours. A program written in "C", calculated local densities (cells mm^{-2}) by convolving the x-y array of one population of cells in each section with a 2D-Gaussian (standard deviation SD = 21 μm). This was evaluated at 6μm intervals across the section with the following equation:

$$density = k * \sum [e^{-\frac{1}{2}(\frac{\sqrt{(x_i-a)^2+(y_i-b)^2}}{SD})^2}]/2*\pi*SD^2$$

This formula evaluates the density at the position (a, b). If the SD of the Gaussian is large relative to the cluster size, it could blur the cluster boundary. If the SD of the Gaussian is too small, the density measures become noisy. However, there is a substantial range over which changes in the SD were found to have little effect, and the value chosen (21 μm) was in the centre of that range. The evaluation grid and the standard deviation were chosen, so that for simulated and real data, changes of the two in either direction would produce very stable labelled area measurements at a given criterion, i.e. the results plateau around these values. The criterion for area labelled was selected at 10% of the peak density; this criterion produces estimated area values that match the known area of the simulated data sets most closely.

The peak density for each type of label in a given dLGN, across all sections, was determined. Then the program calculated the area in each section which contained label

equal to or more than 10% of the peak density. The results across all sections of one dLGN were summed and the sum was divided by the total area of the sampled dLGN sections, which was measured by scanning calibrated printouts of the sections into Sigma-Scan (Version 3.90 for DOS, Jandel Scientific). Since the injection sites occupy a fairly constant proportion of the area of primary visual cortex (see Table II.1), the percentage dLGN labelled gives an estimate of the proportion of the dLGN which converges onto a given small point in cortex. Thus we can estimate the scatter in the projection and look at the change of convergence during development.

Isodensity contours can be visualized by adding all the collated density values of a single population of cells in a single section, using a Matlab routine. The density measures at which contours are desired can be entered directly into the routine. In order to reveal local areas of high density those contour lines can be superimposed on the original sections, as was done for the heterochronic experiments (Chapter III, Results).

5.2 Nearest neighbour analysis

The nearest neighbour analysis estimated the degree of segregation between two populations of labelled cells by determining the probability that a given labelled cell has as its nearest neighbour a cell of the same colour. A Pascal Program (written by Dr. K. Stratford) ran through each population of labelled cells on each geniculate section and noted whether a labelled cell has as nearest neighbour a cell of the same ("1") or a different colour ("0"). If a neuron had as its nearest neighbour a double-labelled cell, its neighbour

relation was noted as "0.5". Double-labelled cells themselves received a value of "0.5", because they represent their own nearest neighbours. These values were summed and averaged separately for the red and the green populations in each section: if the two populations were totally segregated a value of 1.0 would be expected but if the two populations were distributed at random, the value would be 0.5. Because the individual sections contained different numbers of labelled cells, the resulting neighbour values for each section were weighted according to the relative number of red or green cells on that particular section. The weighting was done separately for the red and the green populations to account for the possibility that segregation was occurring not in the plane of the section but across sections. This gave two neighbour values for the whole dLGN, one for the red and one for the green population. These two values were then averaged to give a final single neighbour value for each dLGN, which was expressed as a percentage. The reason for this final average is because the nearest neighbour measure is sensitive to imbalances in the total numbers of red and green cells. For instance, even if the two populations are truly randomly segregated, the neighbour value for the smaller population would deviate from 0.5 to 0 as the relative number of cells in that population declines. Similarly, the value for the larger group would approach 1.0 as it became relatively more numerous. But simulations of the effects of population size differences for different degrees of segregation, using naturally occurring cell number differences, revealed that there was a symmetrical deviation in the neighbour values for the two groups from the value seen when the two groups matched in size. The increase in the nearest neighbour value of the larger

population would mirror the decrease in the smaller one, for up to a 1:4 ratio in relative numbers (K.J. Stratford, *personal communication*). (Consequently only animals in which the ratio was equal to or greater than 1:4 were considered). The symmetric deviations allowed us to average the separate red and green nearest neighbour values to give a final nearest neighbour value for each analysed dLGN.

To be able to compare nearest neighbour values across the different ages studied, we used similar injection site separations in all animals (see Table II.1). Since the medio-lateral extent of area 17 expands in the first two postnatal weeks (Krug et al., submitted), the *relative* cortical spacing of the injection sites is even larger in the younger animals. The chosen injection site separations at 500-600 μm represent a sizeable proportion of the extent of area 17. At P12, this is about 25% of the maximum medio-lateral extent of area 17, but at P2, 35% (Krug et al., submitted). This should bias the early results towards a more segregated value, which is against the trend that I find (see Chapter III and IV).

5.3 Vector analysis

The spatial relationship between the two foci of labelled cells in any one section was determined by calculating the vector between their respective centres of gravity. First the orientations of sections were aligned, to match the dorso-ventral and medio-lateral axes (Figure II.4). The x, y coordinates of each cell were known. Sections with less than 10 cells in either population were excluded from the analysis. Then the mean x and y values were calculated for the red and the green population in each section. The origin of the vector was always taken as the centre of gravity of the population of cells labelled from the

more medial cortical injection. In the adult, such an injection always labels a more lateral population of cells, but this relationship was not always evident in younger animals. This strategy was adopted to determine if a bias towards the adult map can be revealed in the early highly scattered projection.

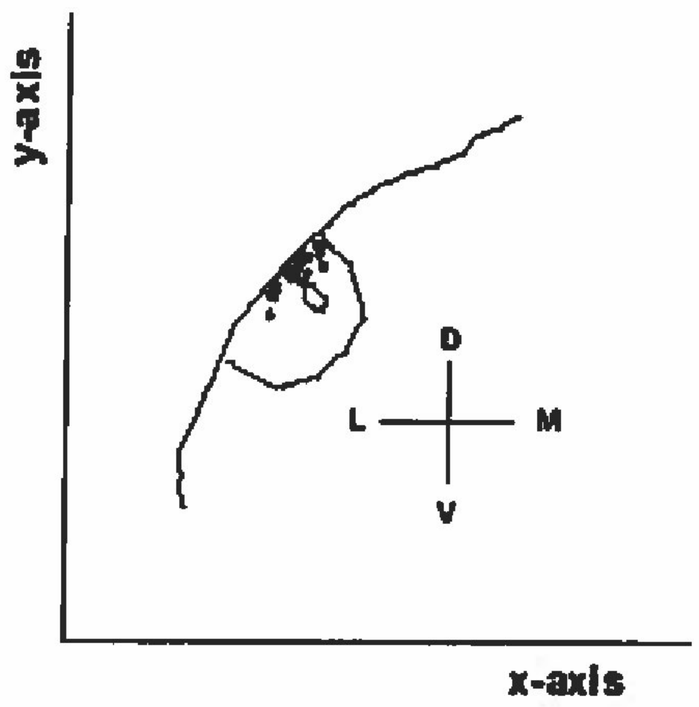


Figure II.4. For the vector analysis, all dLGN sections were aligned as shown on the left: the medio-lateral axis coincides with the x-axis and the dorso-ventral axis with the y-axis. Thus, the vectors could be directly compared. **D** - dorsal, **M** -medial, **V** - ventral, L-lateral.

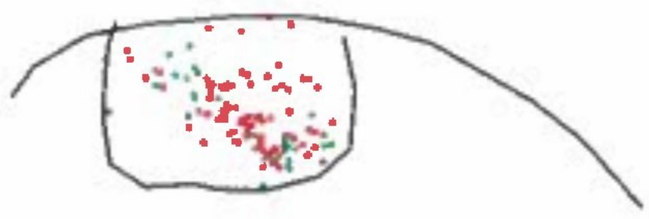
5.4 Cluster analysis

After monocular enucleation at birth, single tracer injections close to the 17/18 border have been described as yielding dual foci on coronal sections of the dLGN (Trevelyan and Thompson, 1992). To be able to determine if this pattern is present or not in individual sections, a cluster analysis was carried out using a "C" programme. First, the Euclidean distance of all cells of one colour from the centre of gravity was determined. The total variance of this distance for a single population of cells on a section was calculated. Then the cells were randomly distributed into two groups and the same calculations were performed for each group. The programme now used an iterative procedure to minimize the total variance of the two clusters by randomly moving individual

cells between the two groups until a stable minimum had been reached. Sections with two foci showed a sharper drop in variance from one to two groups than those with a single focus (Figure II.5).

In order to judge whether this change in variance is significant a Monte Carlo simulation was used. This determined the likelihood that a particular variance ratio could have been generated by chance by samples from a single Gaussian distribution. For each data set, 1000 random data sets were created containing the same number of cells drawn from a Gaussian distribution and with the same standard deviations for x and y as the original group of labelled cells. In the same procedure as above, they were divided into two groups and the total variance minimised. The percentage of data sets which show lower variances than the original data set gives an estimate of the probability (p) that the real variance ratio was yielded by sampling from a single Gaussian focus of cells. If less than 1% of the simulated data sets had variance ratios smaller than the real data, the null hypothesis that the cells were drawn from a single Gaussian focus is rejected.

This procedure could be misleading if a single cluster was elongated and slanted relative to the coordinate axes, since the Gaussian distribution is only defined by the standard deviations for x and y. This artefact was eliminated by rotating the dLGN, so the pial surface of the dLGN was roughly horizontal (Figure II.6). This way any elongation of a single focus of label would be mostly parallel to the x axis or the y axis. In mature, normal geniculo-cortical pathways almost all foci of label can be described as samples of a single Gaussian (Chapter IV, Results). This Monte Carlo simulation can detect if there is more than one cluster of labelled cells on a section.



oh677-1l

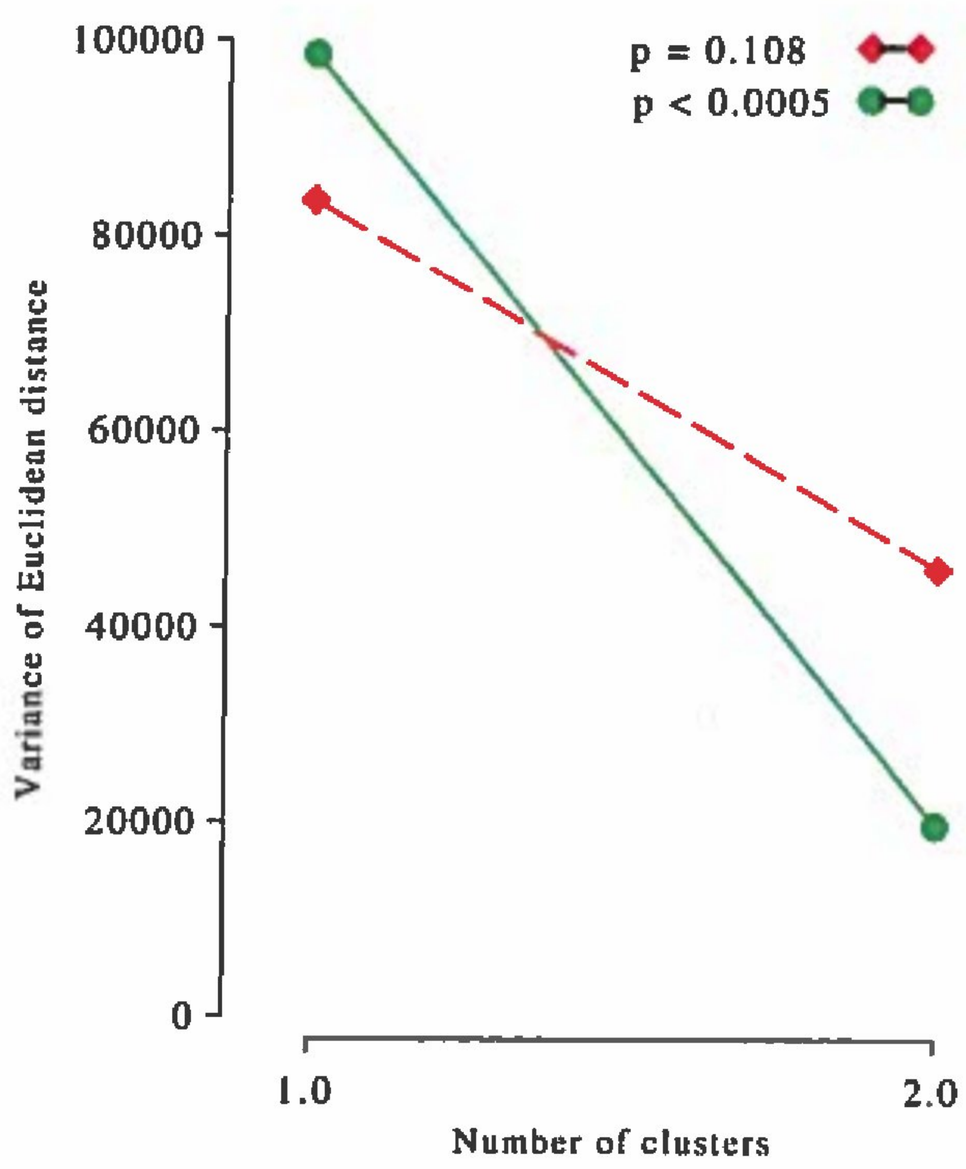


Figure II.5. For the section on the top of the sheet, the variance of the Euclidean distance between all red cells and between all green cells was separately calculated. Then the two populations of cells were cut into two clusters each and the combined variance of the two clusters determined. The graph compares the variance for a single cluster with the minimum variance for two clusters. There is a steeper drop in variance for the green cells from one to two clusters than for the red cells. Furthermore, the Monte Carlo analysis shows that the drop in variance is significant ($p<0.01$) for the green but not for the red cells. Therefore, the green population of cells represents two Gaussian clusters, the red cells are a single one.

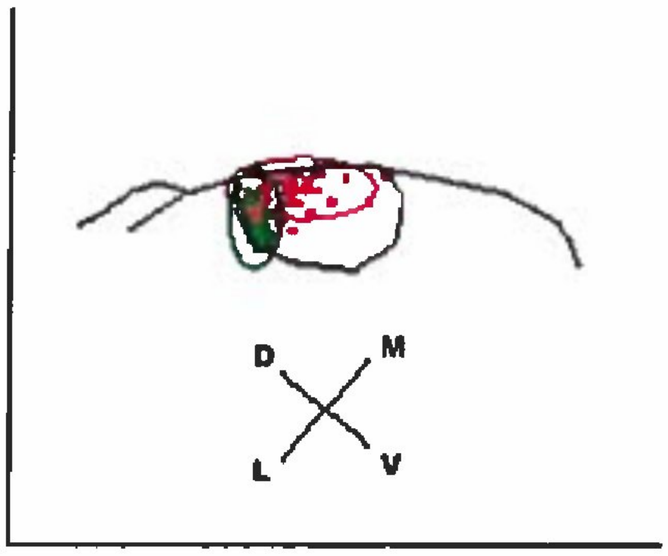


Figure II.6. For the cluster analysis, sections were rotated in such a way that the pial surface is parallel to the x-axis. Thus, most distortions of a single focus would be along the coordinate axes (see red and green ellipses). The Gaussian is defined by the standard deviation of the labelled cells in the x and the y direction. Therefore, after the rotation, a group of labelled cells would not falsely be classified as dual foci by the cluster analysis if it was only an elongated single focus. **D** - dorsal, **M** - medial, **V** - ventral, **L** -lateral.

III. Development of Geniculo-Cortical Topography in the Hamster

1. Introduction

2. Material and Methods

3. Results

3.1 Retrograde labelling of the geniculo-cortical projection by paired injections visualizes the emergence of topography.

3.2 Retrograde labelling of geniculate projection neurons by heterochronic injections suggests little role for cell death in map formation.

4. Discussion

4.1 Assessing order of geniculo-cortical topography

4.2 Where is the thalamo-cortical topography generated?

A comparison with the somatosensory system.

4.3 A role for cell death?

4.4 Implications for map formation in the cortex

1. Introduction

Most sensory representations in the mammalian brain are organised topographically, the sensory map reflecting the arrangement of the primary receptor sheet. These maps are a feature not just of the initial relay, but underpin the structure of sensory areas at different levels throughout the brain. Various developmental mechanisms have been proposed for the creation of the precise point-to-point connectivity which underlies topographic maps. At one extreme, the maps could be sculpted out of an initially random projection by regressive events; at the other extreme, the map in the target may already be laid out in the invading fibre bundle. The work described in the chapter investigates how geniculo-cortical topography is generated in the hamster.

Studies on the primary retinal projections have demonstrated that both mechanisms can play a role in defining the retinotopic map. Topographic fibre order in the optic tract may contribute to order in the target (Scholes, 1979; Torrealba et al., 1982; Simon and O'Leary, 1991; Reese and Baker, 1993), whereas the retino-collicular map in the rodent, but not in the cat, emerges after a period of axonal rearrangement and ganglion cell death (O'Leary et al., 1986; Simon and O'Leary, 1992; Chalupa et al., 1996). It might be argued that once the map has been generated in the thalamus, a simple relay of fibres to cortex, in which neighbours in the thalamus remain as neighbours in the pathway, will create topography. This is not the case. The relative polarities of sensory thalamic and primary cortical maps require an exchange of neighbours within the projection for map creation

(Connolly and Van Essen, 1984; Nelson and LeVay, 1985; Adams et al., 1997).

Exactly where and how this exchange occurs is not certain. Work by Agmon and colleagues (1993, 1995) on mouse somatosensory cortex shows that at birth, when thalamic axons have invaded the lower cortical layers, the thalamo-cortical projection is topographically ordered. At this age, the most advanced axons are growing radially through layer V. However, in the deepest cortical layers and in subplate, fibres course tangentially (Agmon et al., 1993; Catalano et al., 1991, 1996). Such a pattern might imply that the earliest fibres to invade cortex would have a disordered topography. Whether, the disorder is simply local or is the result of the re-ordering of thalamic fibres that is necessary to generate the cortical map is not clear. I have quantified the topographic organisation of the early thalamic input into visual cortex by making paired injections of red and green fluorescent latex microspheres in newborn hamsters. In the Syrian hamster, the bulk of the thalamic afferents does not enter primary visual cortex until after birth (Crossland and Uchwat, 1982; Miller et al., 1993; Krug et al., submitted). In a previous study using single injections of WGA-HRP, Naegele et al. (1988) found that the pattern of retrograde label in the dLGN refined from a general gradient of labelled cells to a discrete column of cells within the first two postnatal weeks. The use of microspheres permits very restricted injection sites in neonatal tissue, and the paired injections allow to control for any lateral spread of the tracer. They also allow the assessment of the precision of the topography by examining both the extent of double-labelling of individual geniculate cells and the degree of segregation of the two retrogradely labelled populations. My results indicate massive changes in geniculo-cortical topography in the neonatal hamster. By allowing back-

labelled cells to survive through the period of map formation, it is shown that selective cell death makes little contribution to the development of geniculo-cortical topography.

2. Material and Methods

At certain postnatal ages (P2, P4, P6 or P12) anaesthetized hamsters received paired injections of red and green fluorescent latex microspheres. For the heterochronic experiments, a specific group of animals was injected with only one tracer at P2 and, subsequently, either at P6 or at P12, a differently coloured tracer was injected at the same site (for details see Chapter II).

Some hamster pups had one eye removed on the day of birth under ether anaesthesia (for further details see Trevelyan & Thompson, 1992). In these cases, the geniculo-cortical projection contralateral to the remaining eye was examined - this side retains 95% of its input and has been shown to develop normal adult topography (Trevelyan and Thompson, 1992). For the quantitative measures of topography we employed in this study (nearest neighbour analysis and percentage of dLGN labelled - see Chapter II) no significant difference between operated and unoperated hamsters could be detected (two-way ANOVA, $p \leq 0.076$ and $p \leq 0.506$) while the changes with age for the pooled data were highly significant ($p < 0.0005$ in both cases). Therefore, we have pooled the data from unoperated animals with the results from the contralateral side of monocular enucleated animals.

I have not attempted to estimate total counts of labelled cells. It is difficult and unreliable to reconstruct true cell numbers from sections of a 3D-structure such as the dLGN, if stereological tools are not used in the sampling strategy. Furthermore any changes in cell counts in developmental experiments, as seen in my raw data (Table III.1),

are subject to various influences: such as maturation of the topography, changes in cell density and the growth of the brain that, apart from topographic changes, could affect labelled cell numbers. The analyses described in Chapter II investigate more specifically different aspects of the maturing topography and often employ proportional measures, e.g. %dLGN labelled. Also, since most changes studied occur in the coronal plane they are also less prone to sectioning artefacts. All factors predict a drop in labelled cell numbers, which is what I observe in the raw cell counts (Table III.1).

	number of animals	number of cells labelled per injection
P2	**7**	**742 ±302**
P4	**3**	**587 ±131**
P6	**8**	**521 ±369**
P12	**7**	**351 ±244**

Table III.1. Unmodified cell counts.

The cell counts are raw cell counts per injection site added over an entire one in two series of a dLGN (section thickness = 50 µm). No correction factors have been applied. The bold values represent means, next to them are their standard deviation.

3. RESULTS

3.1 Retrograde labelling of the geniculo-cortical projection by paired injections visualizes the emergence of topography.

Paired injections of red and green latex microspheres were made to determine the topographic organization of the projection. Injections were placed perpendicular to the cortical surface. Injection sites included cortical plate and subplate in the younger animals, only at P12 was it possible to restrict the tracer placements systematically to the cortical plate. The injections were separated medio-laterally: similar ranges (300 - 800 μm) were used at all ages, and the mean separations are comparable (Table III.2). However, it should be noted that area 17 has a smaller medio-lateral extent in the younger animals (Krug et al., submitted), so that the relative medio-lateral separation is wider in these neonates.

(i) At P2, the geniculo-cortical projection is scattered. Two discrete injections of red and green tracer into area 17 at P2 retrogradely label cell bodies throughout the ipsilateral dLGN with considerable intermingling of red- and green-labelled cells on any one coronal section. Inspection of Figure III.1, shows that labelled cells of a single colour can be found throughout the entire dLGN. We have quantified the spread of retrograde labelling by measuring the area of each coronal section that contains labelled cells at a density of at least 10% of the peak density seen in that dLGN (see Chapter II, 5). Nearly three-quarters of the dLGN is labelled at this or a higher density of label (see below).

Although labelled from separate cortical sites, the red and the green population of cells appear congruent in the P2 dLGN. This result is confirmed by an analysis of the

	n	Injections ML separation	Injection size in %area 17	Double label	Percentage dLGN labelled	Percentage nearest neighbour same
P2	7	575 µm *±160.5*	1.66% *±1.20*	16% *±6*	73% *±7.6*	48.8% *±4.6*
P4	3	550 µm *±40.5*		7% *±3*	38% *±5.2*	66.7% *±14.2*
P6	8	481 µm *±185.0*	1.29% *±0.78*	8% *±6*	19% *±8.0*	80.8% *±7.4*
P12	7	557 µm *±203.0*	1.27% *±0.47*	6% *±7*	13% *±8.1*	90.6% *±5.1*

Table III.2. Summary Data

This table summarises the data from the retrograde labelling experiments on normal geniculo-cortical development. While medio-lateral separations and the relative size of injection sites as well as the percentage of double labelled cells stay fairly constant across the ages, a dramatic decrease in the back-labelled area together with progressive segregation of the neurons projecting to different injection sites can be seen during the first two postnatal weeks. The bold numbers are means with the standard deviation underneath in italics.

Figure III.1. The pattern of geniculate back-label during the first two postnatal weeks. The upper part of the figure shows cortical injections of red and green fluorescent tracers, seen in coronal sections. Injections were placed at P2, P4, P6 and P12. The white dashed contours mark the pial surface and the border between subplate and white matter. The calibration bars represent 500 µm. Underneath are representations of series of coronal sections through the dLGN (50 µm thick, one in two series). The sections run caudo-rostrally from top to bottom. Each coloured dot indicates the location of a neuron back-labelled with either the red or the green tracer (double-labelled cells were drawn twice, once in each color).

The dLGN sections on the left depict the pattern of back-label as generated by paired medio-laterally spaced injections at P2. Two days after birth, the distribution of the retrograde label is diffuse, in every section there are red cells intermingled with green cells and vice versa. Next follows a P4 dLGN. The back-labelled cells appear to cluster more, although many of them are still widely scattered. The third column of sections stem from an animal injected at P6 and show an ordered map: the lateral, green cortical injection produces a distinct medial focus of labelled cells, while the medial red injection back-labels an adjacent lateral focus of cells. At P12, there is little obvious change from the pattern at P6.

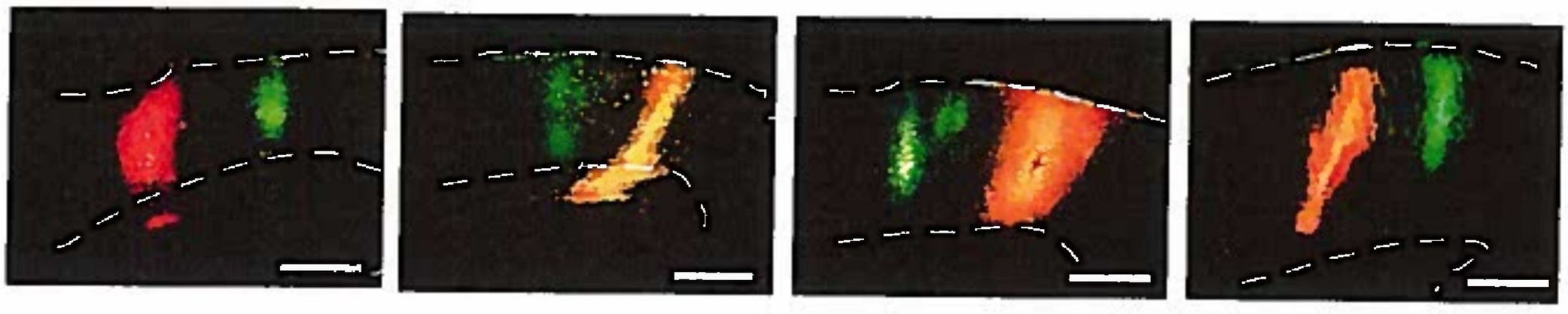


Figure III.1

nearest neighbour for each labelled cell (see below). Despite the apparent overlap of the two populations of labelled cells, only a small percentage of neurons is back-labelled by both tracers (16% at P2, see Table III.2). The low fraction of double-labelled cells eliminates the possibility that the spread of retrograde label seen in Figure III.1 reflects a greater spread of tracer across the cortex than was apparent from the injection site. On visual inspection, injection sites were discrete and non-overlapping. Reconstruction of injection sites at P2 show that each occupies less than 2% of the visual cortical area at this age (Table III.2). For undetected spread alone to account for the extensive geniculate labelling, the effective injection sites would have to be much larger. The existing injections are 100 - 250 μm in diameter, so any substantial increase would generate overlap and increased double-labelling. Most cells are not double-labelled and the double-labelled cells are scattered throughout the dLGN.

Uptake by fibres of passage also cannot explain the diffuse pattern of back-label. After multiple injections of beads into cortical plate and subplate anterior to area 17, retrogradely labelled cells were restricted to the ventro-basal complex (VB). This is illustrated in the left-hand panels of Figure III.2. The green beads were injected deep in order to assess any labelling of fibres of passage running to more caudal cortical areas such as visual cortex. Green beads were not seen in dLGN neurons but back-labelled cells were found throughout VB. In this animal, a *single* small red injection was made into visual cortex (not shown): neurons labelled with red beads are found throughout dLGN. In older animals, it is easier to restrict bead injections to the upper cortical layers but injections that also invade the lower layers and subplate give the same pattern of geniculate back-label.

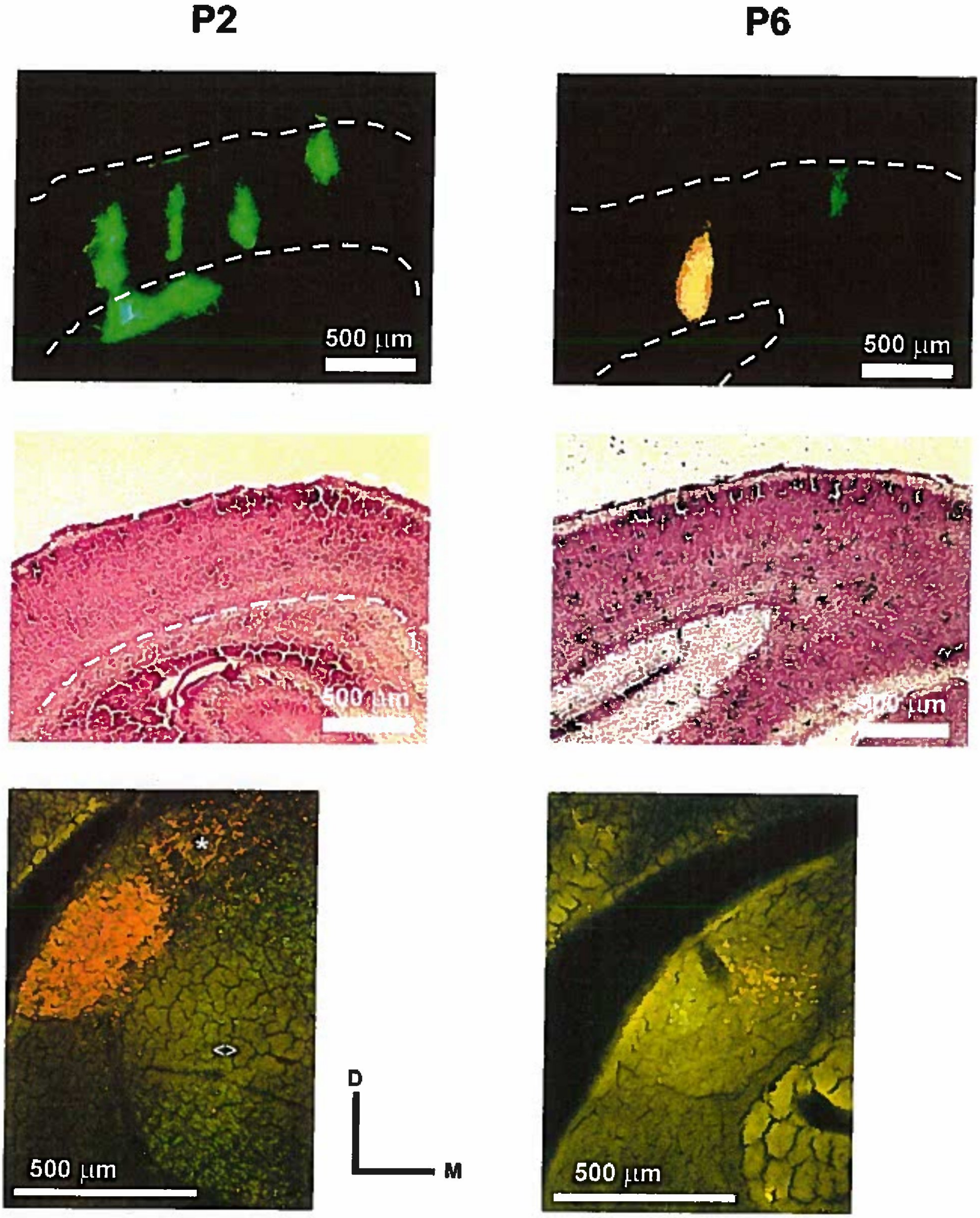


Figure III.2. Controls for uptake by fibres of passage. These photomicrographs of coronal sections through dLGN and cortex demonstrate that fibres of passage do not take up the red and green fluorescent micro-beads. At P2 (left), injections were placed into somatosensory cortex penetrating the cortical plate, the subplate and the marginal zone along a large medio-lateral extent. Such injections should involve geniculate axons running caudally to area 17. However, despite many green back-labeled cells in the ventrobasal complex (VB - <>), the dLGN contained less than a handful of green cells. The dLGN and the lateral posterior nucleus (LP - *) contain cells labeled from a single red bead injection into area 17 (not shown). At P6 (right), a superficial and a deep injection were made into area 17. Both injections back-label discrete foci of similar size in coronal sections of the dLGN. Thus horizontally running visual fibres deep to layer IV/V do not take up the beads, only the terminals. D - dorsal, M - medial, * - LP, <> - VB.

In the right-hand panels of Figure III.2, two similar foci of red and green labelled cells can be seen in the dLGN even though the red injection involved the deeper cortical layers and subplate. Thus, injections of beads made through micropipettes are not taken up significantly by geniculate fibres of passage deep in visual cortex. This confirms the observations of Trevelyan (1992) in adult hamsters: placements of red and green tracers along the same pipette track, one into the cortex and the other into the white matter, yield back-label in the dLGN almost exclusively from the cortical injection. The P2 injections in Figure III.2 also indicate quite accurate targeting of visual thalamic axons to visual cortex despite early disorder within the geniculo-cortical projections.

(ii) By the end of the first postnatal week, the projection appears ordered. Cortical injections were made at P4, P6 and P12; inspection of the pattern of labelling reveals that clear geniculo-cortical topography has emerged by the end of the first postnatal week. After injections on P4, although labelled cells of both colours are widely scattered across the dLGN, distinct condensations of red or green cell bodies can be discerned. At P6, the pattern of back-label looks essentially adult-like. On coronal sections, two discrete foci of labelled cells are visible, one red and one green (Figure III.1). These foci appear dorso-medially on the more caudal sections and move through the dLGN to the ventro-lateral margin in more rostral sections: thus forming an ordered column through the nucleus. The columns of red and green labelled cells are spatially separate, with very little overlap. In Figure III.1, the more medial column of green cells arose from a cortical injection of green beads placed laterally to the red tracer. The topography is that expected from the adult. Qualitatively, only small changes seem to take place over the following week: P6 and P12

injections yield a similar pattern of back-label.

(iii) Quantitative analysis of the developing geniculo-cortical projection. With a single tracer, it is possible to measure the extent of the dLGN occupied by retrogradely labelled cells by using a density analysis (see Chapter II). Having used two tracers, we were also able to measure both the percentage of double-labelled cells (indicating the spread of individual axonal arbors) and the nearest neighbour relations of the two populations (giving a measure of the spatial segregation of the two groups of cells).

Looking at the changes in percentage area of dLGN labelled, we get an estimate of the convergence in the projection onto one point in cortex. Our criterion of density ensures that we only assess the area of dLGN which contains a certain baseline of label. About 70% of the dLGN is labelled at or above 10% of the peak labelling density following a single injection at P2 (Figure III.3A). This value drops to about less than a quarter when injections are made at P6, although the relative injection sizes remain between 1.66% and 1.29% (Table III.2). Relatively little change with age is seen in the percentage of geniculate cells that are double-labelled (Figure III.3C). The small drop in the percentage of double-labelled cells we see between P2 and older animals could reflect changes in relative size of the injection (Table III.2) or changes in the number of collateral branches (see Discussion). At the same time, the probability that a cell has a nearest neighbour of the same colour increases. At P2, a labelled neuron is as likely to have as its nearest neighbour a cell filled by the same or a different tracer (Figure III.3B). This suggests a random distribution of label: the input to the two discrete injection sites is not segregated in the dLGN. The nearest neighbour value rises from approximately chance at P2 to about

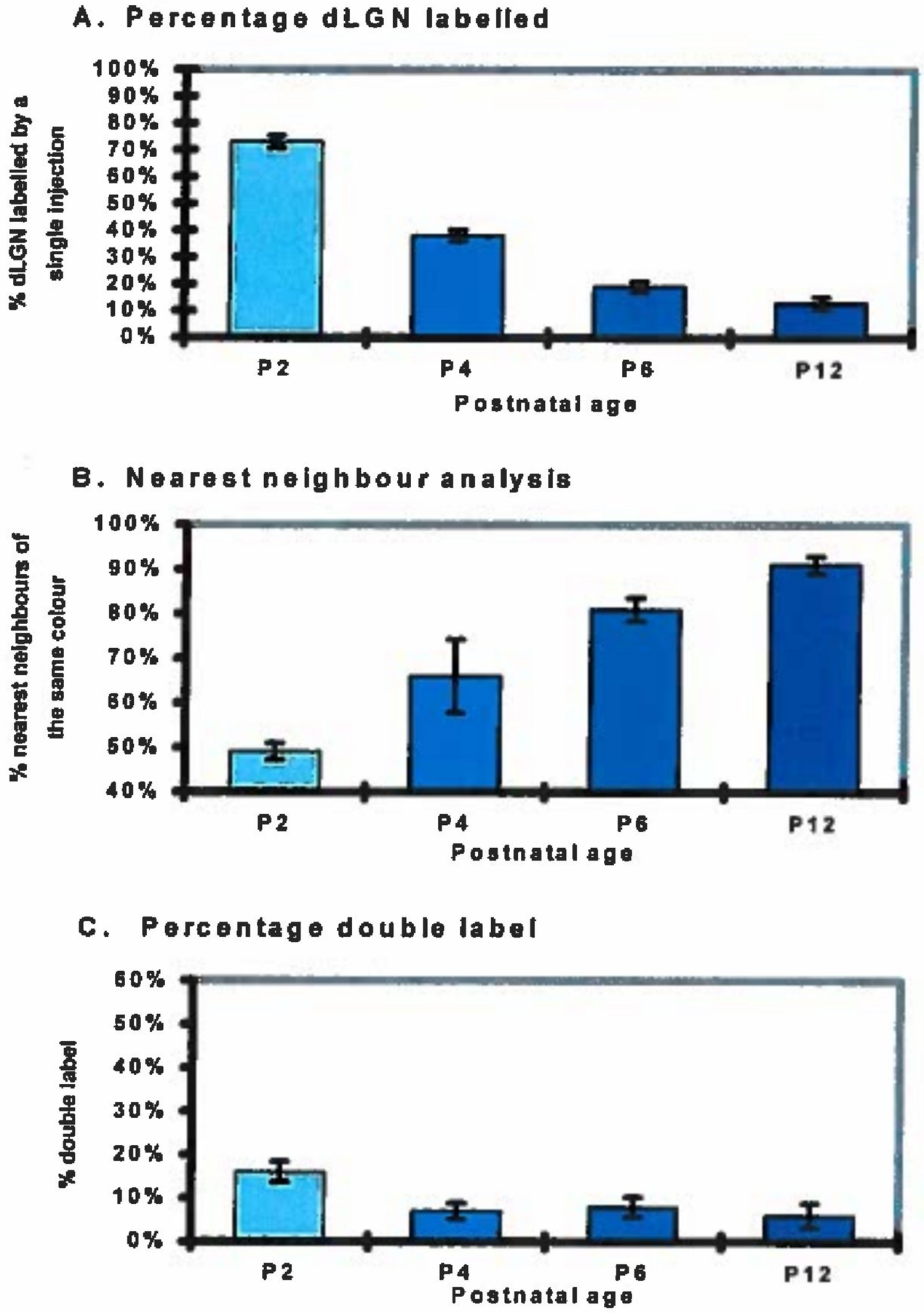


Figure III.3. Quantitative assessment of geniculo-cortical topography.

A. Percentage dLGN labelled by a single injection. For each coronal sections we measured the area which contained at least 10% of the peak density in this particular dLGN. The summed areas were expressed as a percentage of the total area of the dLGN sections. This analysis gives an estimate of the scatter of back-label throughout the dLGN, which is very high at P2 and then falls dramatically in the following week. These changes with age are highly significant (one-way ANOVA, $p<0.0005$).

B. Nearest neighbour analysis. In order to quantify the segregation in the projection, we estimated the probability that a labelled cell has as its nearest neighbour a cell of the same colour. A value around 50%, as we see it at P2, suggests that there is no segregation of the input to the two discrete injection sites. As the connection gets more ordered the value rises significantly (one-way ANOVA, $p<0.0005$).

C. Double label. The figure displays the percentage of cells double-labelled (with respect to the smaller of the two populations) against postnatal age. This measure stays fairly constant.

In each graph, the error bars depict the standard error of the mean.

80% at P6: the input to different points in cortex segregates (Figure III.3B). Between P6 and P12, the figures for the nearest neighbour analysis and the percentage of dLGN labelled reflect further refinement (t-test, $p < 0.05$), but on a smaller scale than before.

The nearest neighbour results suggest that the early projection to area 17 is random. To test whether there is any bias towards the adult columns in the early scatter, we calculated the vector from the centre of the population of cells labelled by the medial injection to the centre of the population labelled by the lateral injection. This was done for every section (Figure III.4). The size of the vector indicates the degree of segregation, its direction should be predictable from the adult pattern of columns: a medial cortical injection labels cells laterally in the dLGN, and vice versa. The plot shows that the two foci of label segregate more and more during the first two postnatal weeks. At P4 and later almost all vectors point to the right, i.e. medially. Because of the alignment of the projection columns (see Figure III.1), there is also a small dorso-ventral component to the vector. The length of the mean vector increases from P4 to P6 and again between P6 and P12. At P2, however, the vectors cluster around zero and some sections in all animals yield vectors which point laterally. Although there are sections with the correct bias in the pattern of label, there seems to be little overall bias for the adult-like columnar organisation. Thus, these measurements underline the picture of a random geniculate projection to the subplate and lower cortical layers at P2. At later ages the increase of the vector length between the two clusters, in conjunction with the reduction in the area of dLGN back-labelled, indicates greater segregation of the input to the two injection sites.

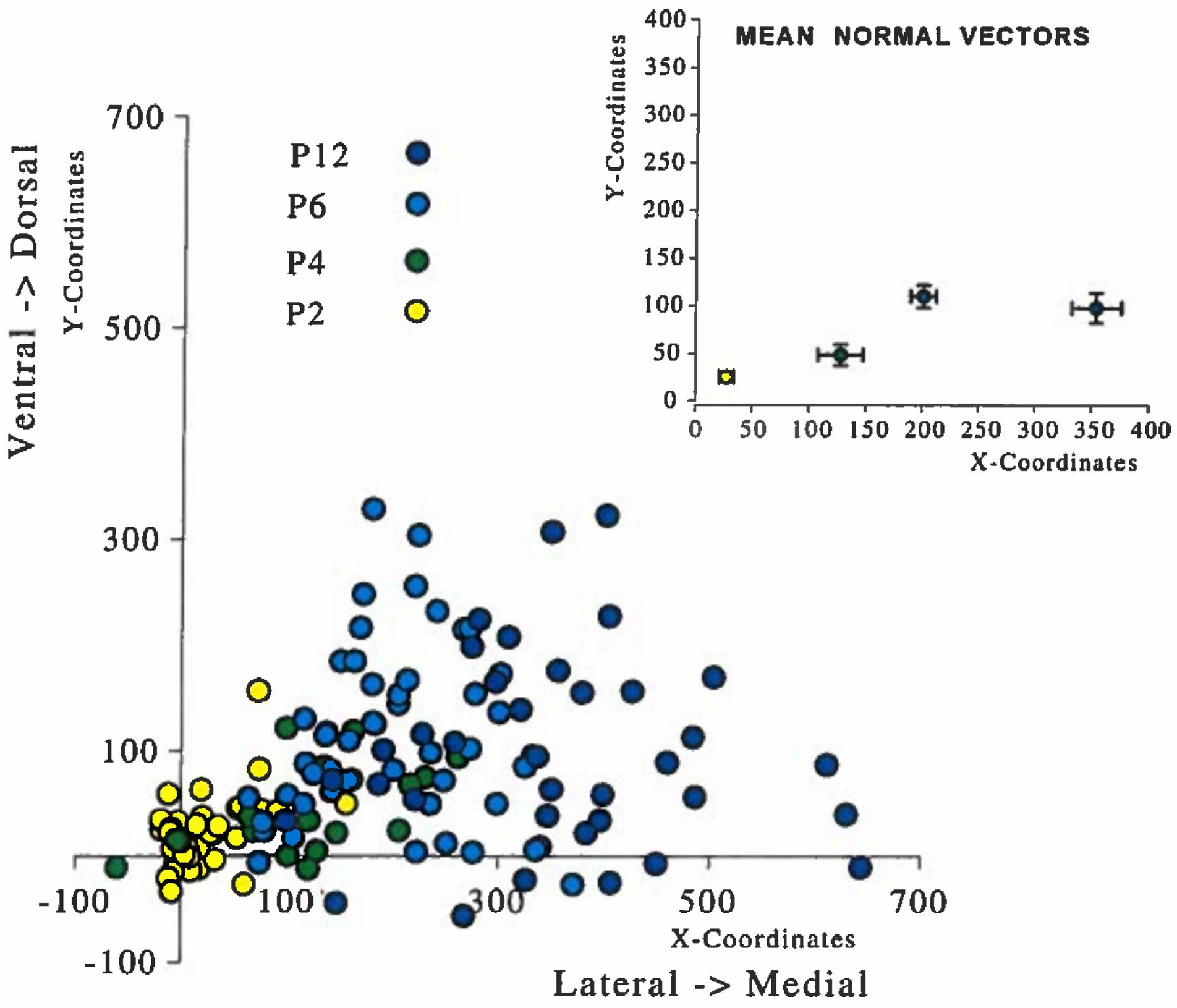


Figure III.4. The vector analysis confirms early disorder. This graph describes the spatial relationship between the two populations of label in each section. Brain sections were aligned along their dorso-ventral and medio-lateral axes. The vector was calculated from the centre of gravity of the population of cells labelled by the more medial cortical injection to the population labelled by the lateral injection. The larger graph shows the distribution of the individual results from each section, the smaller graph at the top represents the mean vectors at each age. In the adult, normal dLGN this vector goes lateral to medial (Dursteler et al., 1979). Except for the P2 vectors, almost all point medially as predicted. The result at P2 strongly indicates no overall bias towards the adult map in the early scatter.

The scatter along the dorso-ventral axis has three possible causes. One reason lies in the curvature of the dLGN, which affects the alignment of the projection columns: producing some separation in the dorso-ventral axis (cf. Figure 1, P6 and P12). Secondly, the dorso-ventral and medio-lateral axes of the sections are only approximately aligned. Finally, the scatter could be caused by a slight anterior-posterior offset of the paired injections.

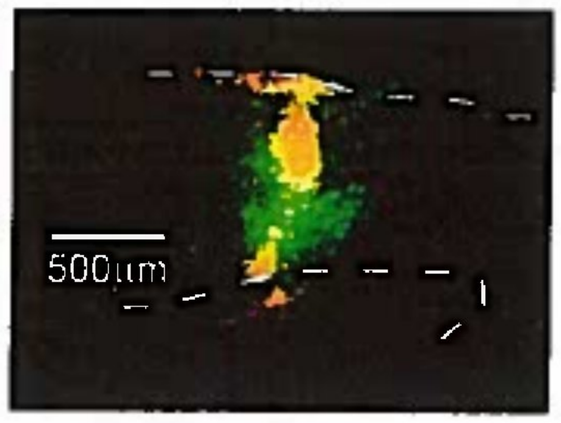
3.2 Retrograde labelling of geniculate projection neurons by heterochronic injections suggests little role for cell death in map formation. In order to reveal what part the selective death of inappropriately projecting geniculate neurons might play in the development of an ordered projection, we injected one tracer into area 17 at P2 - before topography is established - and allowed the animal to survive through the maturation of the geniculo-cortical map to P6 or P12. At either of these ages, an injection of the second tracer was placed into the same cortical site as the P2 injection. If selective cell death is the major mechanism sculpting the adult map from the early scattered projection, with two spatially superimposed heterochronic injections we should see two congruent populations of labelled geniculate cells, as all cells that had originally made inappropriate connections would have been eliminated. In contrast, any neurons which are labelled by the early injection but are outside the area labelled by the later tracer placement have survived despite making an initial projection to a topographically incorrect target.

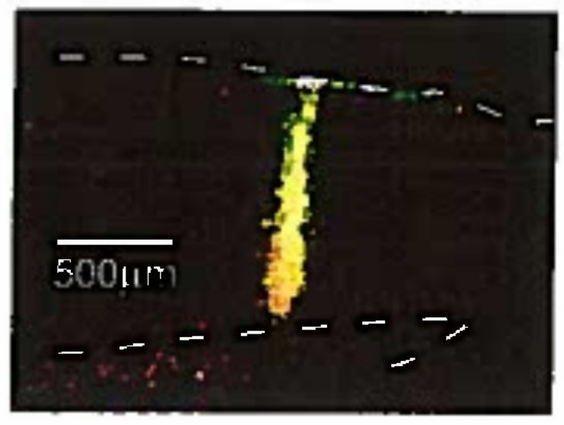
In Figure III.5 (right) a cortical injection at P2 labels cell bodies scattered throughout the dLGN although the animal survived until P12. The somas were clearly defined by the beads. This figure shows that the pattern of geniculate labelling seen after long-term survival following a P2 injection does not differ qualitatively from the P2 result seen after 18-24 hours survival. There is also no difference in the pattern of early back-label between survival to P6 and P12. At an age when the geniculo-cortical connectivity has reached an adult-like appearance, the percentage of dLGN labelled by the early injection was still comparable to the value obtained at P2 (Figure III.6). It appears that inappropriately targeted cells do not die selectively in order to yield the adult projection.

Figure III.5. This figure shows two heterochronic experiments. The photomicrographs at the top of the page depict the injection sites into area 17. The white dashed lines mark the pial surface and the border between subplate and white matter. Underneath are the respective patterns of back-label on coronal sections of the dLGN. The sections of the one in two series were 50 µm thick and run caudo-rostrally from top to bottom.

The dLGN on the right stems from an animal in which red beads were injected at P2, and at P12 green beads were placed at the same cortical site (in the double-exposure photomicrograph the spatially coincident injections appear yellow). The cells labelled with green form a tight focus moving through the nucleus, whereas the early labelled red cells remain diffusely distributed across the dLGN, not merely co-localised with the green cells. On the left-hand side, a green injection was placed into area 17 at P2 and a red injection was made at the same site at P6. Again the early projection labels cells throughout the nucleus whereas the later injection only labels a discrete focus of cells.

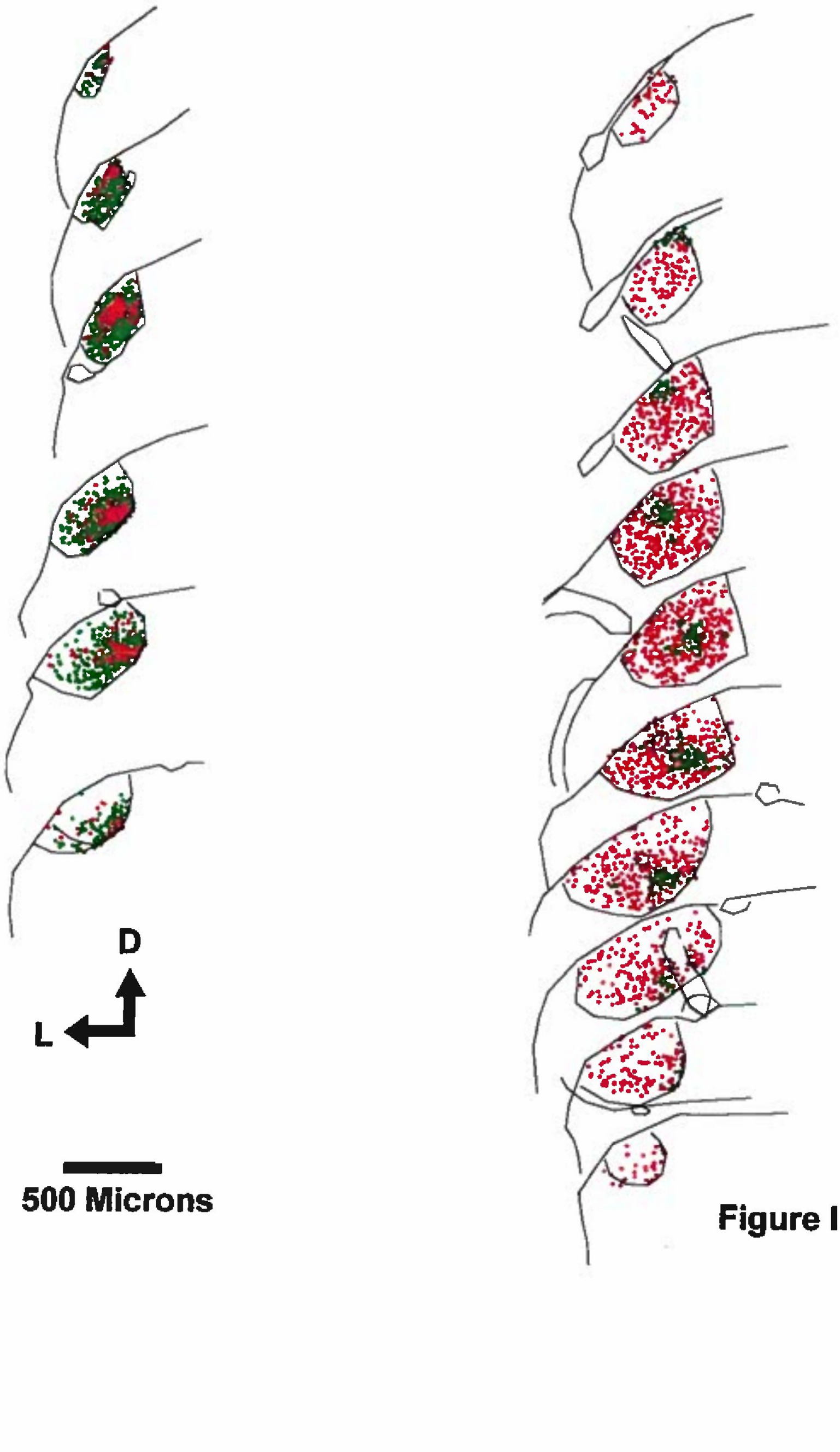
The persistence of cells labelled at P2 outside the second later focus shows that the early labelled cells which make inappropriate connections early in development survive the ordering of the projection.





P2 & P6

P2 & P12



500 Microns

Figure III.5

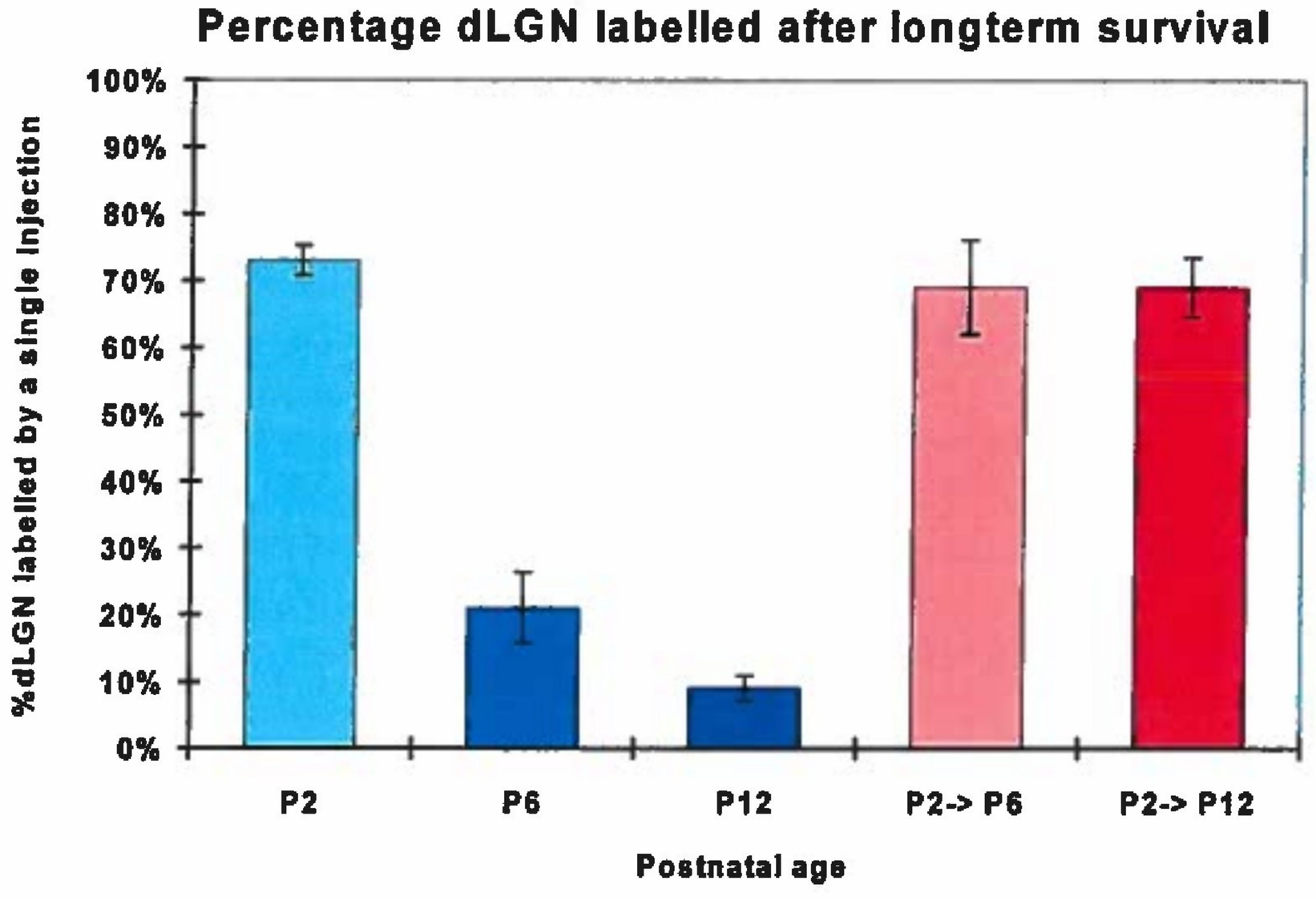


Figure III.6. Percentage of dLGN labelled by a single injection - after short or long term survival. The graph shows what percentage of the dLGN in the coronal plane is retrogradely labelled by a single injection into area 17 after varying survival times. The error bars represent the standard error of the mean. The three blue bars describe the results for single injections placed at P2, P6 or P12 respectively; in these cases the animals were sacrificed within the next 48 hours (n=6 in each age group). The decrease in labelled area with the maturation of the projection can be clearly seen. However, if after a P2 injection animals were allowed to grow up to P6 or P12 (red columns, n=7 in each group), the percentage of dLGN labelled still resembled the P2 result and not those animals which received injections at later times. Thus, most early labelled cells can survive the ordering of the projection, even if they make inappropriate connections in early development.

A change in the distribution of terminals can be demonstrated directly from the later placement, at P6 or P12, of a second tracer at the same cortical site. A green injection site of the same size as the earlier red placement, but made at P12, back-labelled only a tight and restricted focus of cells in the dLGN (see Figure III.5) comparable to a normal P12 injection. For P6 heterochronic injections, the result is similar.

Many of the cells labelled with the second tracer were also double-labelled with the first tracer: these neurons therefore made a topographically appropriate projection at P2 as well as P12. However, the fact that only a maximum of 35% of the population labelled by the second injection was double-labelled suggests that the majority of geniculate neurons at P2 fail to make a topographically correct connection. This suggests that active terminal re-arrangement rather than just selective stabilization of an existing collateral drives the formation of geniculo-cortical topography.

Iso-density contours were employed to investigate if there was any non-uniformity in the distribution of cells labelled at P2 but surviving to P12 that might coincide with the focus of back-label by the later injection. Figure III.7 shows that this holds true for a sizeable proportion of sections, in particular for more rostral sections. This bias towards the later map either could be present at P2 or be generated later by some cell death. Since in the early P2 projection, the vector analysis as well as the nearest neighbour analysis point to an unordered projection, the second possibility seems more likely. Since the central focus of label from the P2 injection appears to be constrained in the dorso-ventral as well as the medio-lateral direction, a small contribution of selective cell death to map formation seems likely, but the effect is weak and cannot be seen on all sections.

Figure III.7. Iso-density contours were superimposed on dLGN sections from an animal which received a red injection at P2 and a green injection at P12. The sections run caudo-rostrally from A to F. The area within each contour contains red cells, labelled by the P2 injection, above a certain density. Remarkably, the densest areas of the back-label by the early injection (blue and black contours) often coincide with the green focus of label by the second injection, in particular on the more rostral sections (D-F).

The colours of the contours in rising density: **yellow < pink < blue < black.**

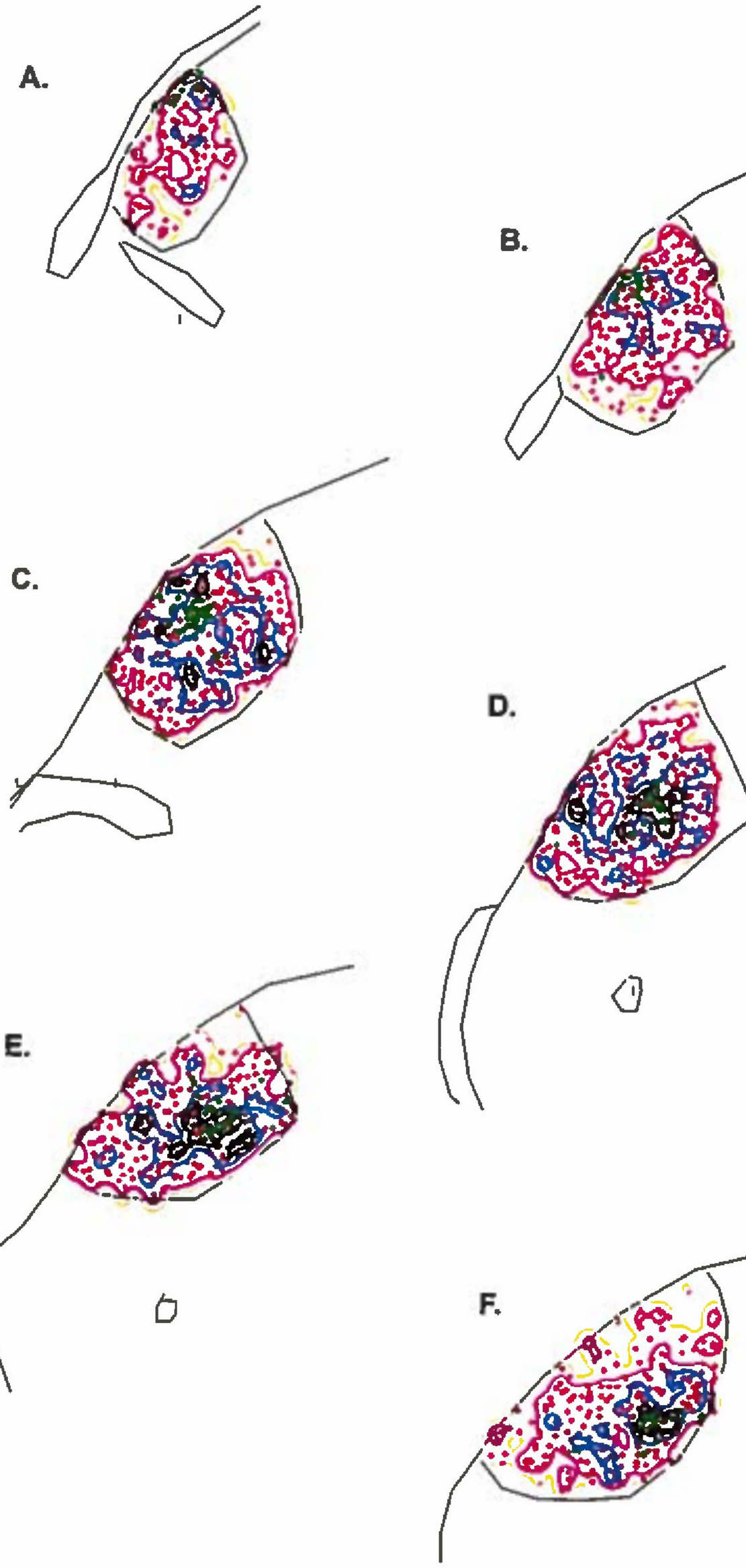


Figure III.7

DISCUSSION

The results in this chapter show that geniculo-cortical topography is sculpted from an initially scattered projection to area 17. By the time most geniculate axons are confined to layer IV, on P6 (Krug et al., submitted), the basic map is in place. Long-term survival experiments exclude selective cell death as a major factor in the formation of the topography. A combination of collateral withdrawal and axonal targeting are implicated in this process.

4.1 Assessing order of geniculo-cortical topography

Qualitatively and quantitatively, the early geniculo-cortical projection pattern in the hamster is disordered. A restricted injection into cortex on P2 labels cells throughout the dLGN, whereas a similar injection only four days later produces a well defined column of back-label. This observation and the controls illustrated in Figure III.2 strongly suggests that the early disorder cannot simply be attributed to a technical artefact such as uptake by fibres of passage. The use of paired injections, with low levels of double-label, also eliminates cortical spread of tracer as cause of the scatter. Uptake by fibres growing past the injection sites is also an unlikely explanation, since fibres coming from all parts of the dLGN would have to pass through two points around 500 µm apart, two points that do not even lie along the line of ingrowth. What is revealed is extensive mis-targeting of thalamic axons.

The lack of order in the early projection is confirmed by the quantitative analysis. The percentage of dLGN labelled gives an estimate of the scatter in the projection, whereas the nearest neighbour and vector analyses reflect the segregation of the geniculate input to discrete cortical points separated by an average distance of about 500 μm. The density analysis suggests that there is some minor bias in the projection, as only 70% of the dLGN contains labelled cells at the criterion density. However, both the nearest neighbour result and the vector analysis reveal that thalamic afferents at P2 do not distinguish between two cortical sites separated by one-third the width of striate cortex. The quantitative analyses do show that there is some refinement in topography after the map has emerged at P6 and leave open the possibility of further subtle changes after P12.

4.2 Where is the thalamo-cortical topography generated? A comparison with the somatosensory system.

My results might seem to conflict with studies on the development of topography in rodent somatosensory system. In mouse barrel cortex, thalamic afferents display a thalamotopic map at birth, when the fibres are still confined to the lower cortical layers (Agmon et al, 1993, 1995). Adult-like barreloid topography is seen at P2 when the thalamic fibres are established in layer IV. My results also show a topographic map at P6, at a time when the geniculo-cortical projection is well established in layer IV (Krug et al., submitted). But I find an absence of topography earlier when thalamic afferents are confined to the subplate and lower cortical layers (Miller et al., 1993; Krug et al., submitted). In their retrograde tracing at P0, however, Agmon et al. (1995) were careful

to place the DiI in the dense cortical plate. This ensured that they labelled only the thalamic axons advancing through layer V towards layer IV and avoided the tangential plexus of fibres in layer VI (Agmon et al., 1993). Catalano et al. (1996) also described tangentially running, as well as locally branching, thalamic axons in the subplate (layer VIb) and layer VI in prenatal and neonate rat somatosensory cortex. Such morphology implies topographic disorder, although retrograde tracing by Catalano et al. (1996) indicates that the order is local. I have concentrated on quantifying the precision of the thalamo-cortical map at a time when the bulk of the thalamic afferents are confined to subplate and the deepest cortical layers. My results show that at least for the geniculo-cortical system, the initial guidance of thalamic axons to cortex does not generate the adult map and imply that thalamic axons have to actively sort-out in the deepest layers of the cortex, before they target layer IV. It would be interesting to establish whether paired bead injections into somatosensory cortex at a comparable stage would reveal similar errors in early targeting.

My results also have implications for the morphology of the thalamic axons. If big, overlapping terminal arbors were responsible for disorder in the projection, one would expect a high percentage of double-labelled cells and some bias in the distribution of red and green cells. I find a small, but consistent, percentage of double-labelled cells: this could arise if individual axons had small, scattered collateral branches (a pattern that would also contribute to the topographic disorder). Such an axonal morphology was described in the newborn hamster by Naegele et al. (1988) after labelling single thalamic terminal arbors from HRP injections into the optic radiation. Between P0 to P2, axons extended

multiple short collaterals into subplate and lower regions of the cortical plate. It would be interesting to know what role these early collaterals play in the guidance of thalamic axons to their final targets.

4.3 A role for cell death?

The fact that the diffuse distribution of geniculate neurones labelled early in development persists into the second postnatal week eliminates selective cell death as the main mechanism generating geniculo-cortical topography. But the iso-density results indicate it might make a modest contribution to map formation. A comparison between the P2 nearest neighbour value after overnight survival and the value obtained after paired injections at P2 followed by longterm survival to P12 should show directly the extent of the contribution by selective cell death to topographic ordering. The heterochronic double-tracer injections also suggest that the map is not generated simply by the stabilisation of a topographically appropriate collateral. In this case, one would expect that all cells labelled by the second injection should also be labelled by the first injection. The fact that there is a relatively low rate of double-labelling with heterochronic injections indicates considerable terminal re-arrangement during cortical map formation. Thalamic cell death does occur in postnatal rodent. In the ventrobasal nucleus of the rat, over a quarter of all cells die during the first postnatal week, with a peak at the day of birth (Waite et al., 1992). Pyknotic cell counts in postnatal hamster dLGN indicate peaks of cell death around P5 and P8, particularly near the periphery of the nucleus (Sengelaub et al., 1985). Although a minor contribution of cell death to the establishment of topography is possible, my

observations make it seem more likely that cell death is involved in size matching rather than in the generation of the geniculo-cortical map.

4.4 Implications for map formation in the cortex

An exchange of neighbours in the thalamo-cortical projection is a necessary requirement for primary sensory map formation (Connolly and Van Essen, 1984; Nelson and LeVay, 1985; Adams et al., 1997). Nelson and LeVay suggested that the rearrangement of geniculate fibres takes place in the white matter underlying cortex. My results in conjunction with the known timing of cortical invasion by geniculate fibres strongly implicate the cortical subplate in map formation and therefore in the exchange of neighbours. These observations also leave little room for ordered ingrowth of the geniculate afferents or reciprocal guiding of geniculo-cortical and cortico-geniculate fibres in forming the topographic map in area 17, although the internal order in the fibre bundle could be well preserved up to the subplate. Despite disorder *within* the projection, my retrograde tracing suggests accurate targeting of area 17 as a whole by the thalamic axons from the dLGN. It is possible that quite different principles guide the accurate targeting of thalamus to a given cortical area and the generation of topographic order within this area. For instance, it has been suggested that axons from different parts of the thalamus fasciculate in distinct bundles and do not mix on their way to their cortical targets (Blakemore and Molnar, 1990). Indeed, the mapping of the whole thalamus onto neocortex could be achieved by ordered ingrowth, since there is no topological mismatch between these structures as a whole (Adams et al., 1997).

What mechanisms might guide the formation of cortical topography from the early disordered input we have shown? The balance between activity-independent and activity-dependent mechanisms needs to be investigated. In the retino-collicular system of the rodent, both mechanisms appear to contribute to the generation of the retinotopic map. Molecular gradients could lay out the basic polarity of a crude map, whereas Hebbian synapses would underlie the refinement of topography (Walter et al., 1987; Nakamoto et al., 1996; Simon et al., 1992). It is not known whether molecular gradients exist *within* cortical areas but certainly neural activity has been implicated in both the refinement of the basic somatosensory thalamo-cortical map (Fox et al., 1996), and in the initial arborization of the geniculate afferents in cat visual cortex (Herrmann and Shatz, 1995). The machinery for map refinement via neural activity appears to be present in the immature visual system. During the early development of visual pathways, waves of patterned spontaneous activity have been demonstrated in the rodent and carnivore retina (Maffei and Galli-Resta, 1990; Meister et al., 1991; Wong et al., 1993). This activity can be transmitted through the dLGN (Mooney et al., 1996) and could potentially activate subplate cells (Friauf et al., 1990), providing a substrate for Hebbian refinement. It will be interesting to see how activity-dependent and -independent mechanisms are balanced in the development of the geniculo-cortical map: a map in which order emerges from disorder. The importance of retinal influences on map formation is investigated in the following two chapters.

IV. Development of abnormal geniculo-cortical topography after monocular enucleation at birth.

1. Introduction

2. Material and Methods

3. Results

3.1 Qualitative assessment of the development of the ipsilateral geniculo-cortical map after monocular enucleation at birth.

3.2 The quantitative analyses confirm increased scatter in the ipsilateral map from P4 onwards.

3.3 A quantitative test for the double focus.

4. Discussion

4.1 How does removal of one eye at birth affect the development of the geniculo-cortical map?

4.2 How relevant is the "retinal signal" to normal development?

4.3 About the role and the nature of "the retinal signal".

1. Introduction

If geniculo-cortical topography is generated from an initially unordered map (Chapter III), then can any map be generated, and what are the cues that instruct the ordering of the geniculate input? The most interesting factor which has been proposed to influence the ordering of the thalamo-cortical map is the input to the thalamus itself. Such a mechanism can potentially link the visual input, or at least the retinal map, to the cortical mapping. As discussed in Chapter I, there is evidence that abnormal retinal input can result in altered anatomical or physiological topography in visual cortex of adult carnivores or rodents (Kaas and Guillery, 1973; Hubel and Wiesel 1971; Huang and Guillery, 1985; Trevelyan and Thompson, 1992). In this chapter, I will investigate the developmental consequences of manipulating retinal projections at birth for the geniculo-cortical projection in the hamster.

In the primary retinal targets, early monocular enucleation affects the remaining retinal projections in two ways: it can result in a change in the size of the projection, for example an expansion of the remaining input (Lund, 1973; So et al., 1984), but it can also cause topographic changes (Thompson, 1979; Jeffery and Thompson, 1986). Evidence from albino carnivores, where retinal topography is altered without changes in the size of the projection, suggests that the topographic changes in particular might influence mapping on the cortical level: in the so-called 'Boston' pattern, the anatomical mapping of geniculate onto cortex changes to reconstruct a continuous physiological map from a disrupted thalamic input (Hubel and Wiesel, 1971; Huang and Guillery, 1985). The

mechanics by which altered retinal input can re-route thalamic axons are unknown. My studies on the normal development (Chapter III) reveal an early diffuse map. Therefore, the abnormal geniculo-cortical topography could emerge out of the early disordered projection by stabilisation of a different population of axons. Consequently I have studied the development of the abnormal topography ipsilateral to the remaining eye after monocular enucleation at birth.

After eye removal at birth, a double projection between dLGN and visual cortex can be found ipsilateral to the remaining eye in the adult hamster (Trevelyan and Thompson, 1992). The dLGN in this hemisphere loses 95% of its retinal input. On the other side, which only loses 5%, a normal geniculo-cortical map develops. In these animals, a lateral injection of a retrograde tracer into area 17 close to the 17/18 border ipsilateral to the remaining eye does not reveal a single column of label as described in the previous chapter, but back-labels two distinct columns in the dLGN

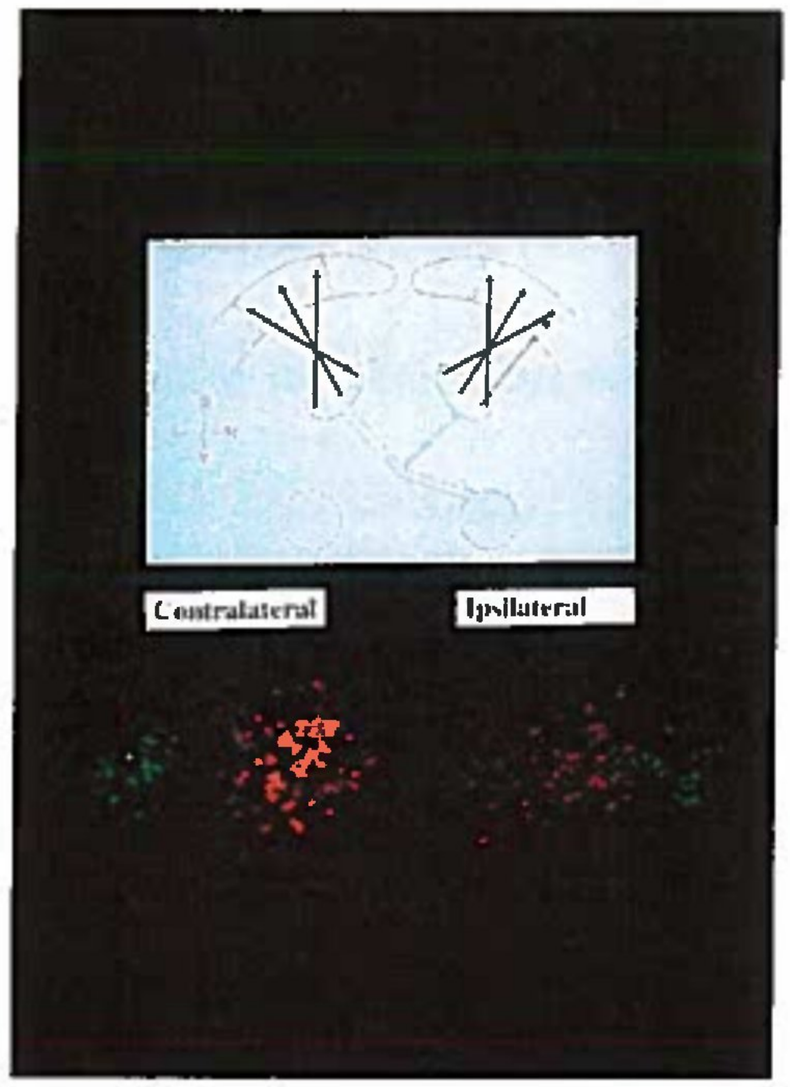


Figure IV.1. The drawing on top sketches the changes in the geniculo-cortical system after monocular enucleation at birth: ipsilateral to the remaining eye one point in cortex receives input from two discrete geniculate sites. Underneath are the patterns of back-label in the dLGN seen after paired bead injections into the visual cortex of each hemisphere. The left photomicrograph shows the normal projection with a single red and green focus of label, on the right, the two foci of green cells flanking a central red focus project both to the same cortical injection site. (Photos from Trevelyan 1992).

(Figure IV.1). Examining how this aberrant pattern of connectivity develops might answer questions about when and how retinal input can influence the development of the geniculo-cortical map. In order to pursue this question hamsters enucleated at birth received bilateral paired injections of red and green fluorescent retrograde tracers. The order of geniculate input ipsilateral to the remaining eye was studied during the first two postnatal weeks and the result compared to the normal development of the projection, which has been described in the previous chapter.

2. Material and Methods

Hamster pups had an eye removed on the day of birth under ether anaesthesia. Paired injections of fluorescent latex microspheres were placed into area 17 in both hemispheres at P2, P4, P6 or P12 (for details see Chapter II). The medio-lateral spacing of the injection sites was similar in both hemispheres and was also similar to the separations used in normal animals (see Table IV.1 and Chapter III). The projection contralateral to the remaining eye shows normal adult topography (Trevelyan and Thompson, 1992), and develops similarly to the map in unoperated animals (Chapter III, Methods). Therefore, in this chapter topography ipsilateral to the remaining eye is compared to the combined results from normal animals plus experiments on the side contralateral to the remaining eye in monocularly enucleated hamsters. For clarity, the combined results are referred to as "normal". This group is taken from the previous chapter.

	Ipsilateral to the remaining eye	**Contralateral and normal animals**
P2	**613 µm** ±110.9 n = 4	**575 µm** ±160.5 n = 7
P4	**575 µm** ±106.1 n=2	**550 µm** ±50 n = 3
P6	**467 µm** ±104.1 n = 3	**481 µm** ±185 n = 8
P12	**494 µm** ±142 n = 4	**557 µm** ±203 n = 7

Table IV.1 summarizes the medio-lateral spacing of injections sites in this chapter. The separations are comparable for injections done ipsilateral to the remaining eye in monocularly enucleated animals and injections done both on the contralateral side of monocular enucleates and in normal animals (values taken from Chapter III).

3. Results

3.1. Qualitative assessment of the development of the ipsilateral geniculo-cortical map after monocular enucleation at birth.

(i) At the end of the first postnatal week, the map ipsilateral to the remaining eye appears less ordered. Paired red and green bead injections were used to assess geniculo-cortical topography in hamsters which had an eye removed at birth. Similar injection site separations were used as in the study on normal development to be able to compare and contrast the development of order in the map (see Table IV.1).

The picture of back-label after injections at P2 is indistinguishable between the ipsilateral and contralateral side. In both cases, a small cortical injection back-labels cells in the dLGN which are dispersed across the entire nucleus. The two populations of cells are completely intermingled (Figure IV.2). The earliest stage by which eye removal first visually affects the development of topography is at P6. Contralaterally an adult-like map with two tight and segregated foci of label is revealed. However, ipsilateral to the remaining eye neither the abnormal adult pattern of back-label, with the double foci, nor normal, segregated foci of label are seen. Instead there are two large and overlapping foci of labelled cells, one red and one green (Figure IV.2).

Looking at coronal sections throughout the nucleus, at P2 red and green labelled cells can be found on all sections across the dLGN and throughout each section within the borders of the nucleus (Figure IV.3). At this age, no topographic order in the projection from dLGN to area 17 can be discerned. At P4 in the normal projection condensations of

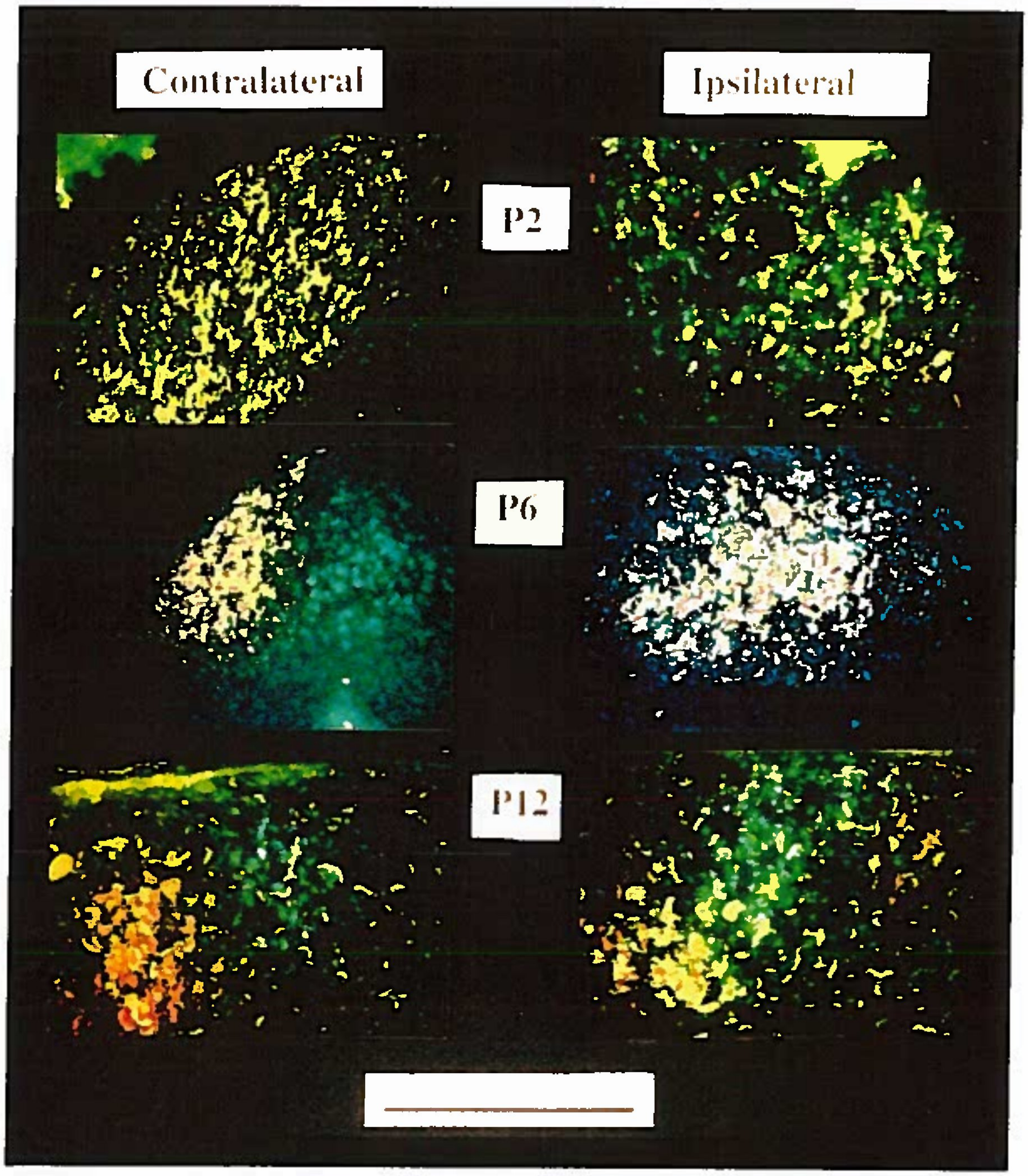


Figure IV.2. The photomicrographs depict coronal sections through the dLGN after bilateral cortical bead injections at P2, P6 or P12. The animals had one eye removed at birth. The sections on the left have been taken from the dLGN contralateral to the remaining eye, the ones on the right stem from the ipsilateral dLGN. No difference can be detected between the projections on each side at P2 - in both conditions the pattern of back-label seems equally scattered throughout the dLGN. However, at P6 the foci of label ipsilateral to the remaining eye are larger and more overlapping than on the corresponding contralateral section. Finally at P12, we see the typical double focus pattern ipsilaterally: two red foci by a single more lateral injection site, flanking a single green focus. The background of the two P12 sections shows some yellow auto-fluorescence because these sections were not cover-slipped.

Figure IV.3. This figure depicts 4 pairs of injections and their pattern of back-label in the dLGN on the side ipsilateral to the remaining eye. All animals were monocularly enucleated at birth and beads were injected at P2, P4, P6 and P12. The photomicrographs of the injection sites show white dashed contours marking the pial surface and the border between subplate and white matter. The scale bars measure 500 µm (NB. the magnification factor for the P12 injection sites differs from the rest).

On the far left, the injections placed at P2 label cells throughout most of the dLGN, the red and the green population appear intermingled. Two days later, at P4, although the label appears more restricted on some sections, it is still widely scattered and the red and green populations of labelled cells overlap greatly. Large and overlapping foci of label can be seen at P6. Although a clear double focus pattern, which is the hallmark for the adult ipsilateral projection, is not yet discernible, it appears possible it could be sculpted from the pattern seen on central sections at P6. The double focus is clearly visible at P12, but not on every section.



Figure IV.3

label have appeared, although many labelled cells are still scattered widely. On the ipsilateral side, the pattern of back-label appears more overlapping on some sections. However, many sections cannot readily be distinguished from their normal counterparts (Figure IV.3). By P6, on odd sections, the large foci of label might show a hint of a double focus, but the pattern is not clearly defined. In general, the pattern of back-label appears to be more scattered than in the normal projection at the same age (Figure IV.3)

(ii) A double-focus of back-label can be seen at P12. The double foci of label can now be seen on some coronal sections (Figure IV.2 and IV.3): paired injections close to the 17/18 border reveal a single focus of label from the more medial injection which is flanked by two discrete foci labelled by the more lateral injection. The double focus is - as in the adult - not equally visible on every section and the second focus is not found at every level of the dLGN (Figure IV.3). The second, lateral focus appears more rostrally in the nucleus and seems not to extend entirely down to the ventral surface of the dLGN. All foci of label appear tight and mostly segregated from each other. However, some dLGNs still show some scatter of back-label and the second medial focus can still be quite small. Further refinement might be required.

In summary, after removal of one eye at birth the projection ipsilateral to the remaining eye at P2 is similar to the normal pattern. At the end of the first postnatal week, the projection is more scattered than normal and the pattern of back-label less well segregated. The topography characteristic of the adult enucleated animal is first seen at P6

for the contralateral, i.e. normal, side, but the characteristic double focus in the ipsilateral projection appears later.

3.2. The quantitative analyses confirm increased scatter in the ipsilateral map from P4 onwards.

The qualitative data show variation of the pattern of back-label across sections and across animals. Therefore, quantitative analysis was employed to assess the pattern of back-label in the dLGN more objectively and more generally. The qualitative picture described above is underlined by the quantitative comparisons of the ipsilateral dLGN with the normal development investigated in the previous chapter (Figure IV.4 and Table IV.2). First the percentage of dLGN back-labelled by a single injection is assessed. At P2, in both conditions labelled cells are scattered to a similar extent throughout most of the dLGN (Figure IV.4A). The labelled area lies at just over 70%. Furthermore, the nearest neighbour values are in both cases around 50%: no segregation between the input to the two injection sites can be detected. Monocular enucleation does not induce any apparent deviation from the randomness of the connectivity from dLGN to area 17 at this age (Figure IV.4B). Looking at the vector from the centre of gravity of cells labelled by the more medial injection to the centre of gravity of the neurons labelled by the more lateral injection, those vectors are very short and point in all possible directions (Figure IV.5). This confirms the absence of the basic map. All the results mirror those of the previous chapter. At this stage in development there is no obvious difference between the ipsilateral and a normal projection.

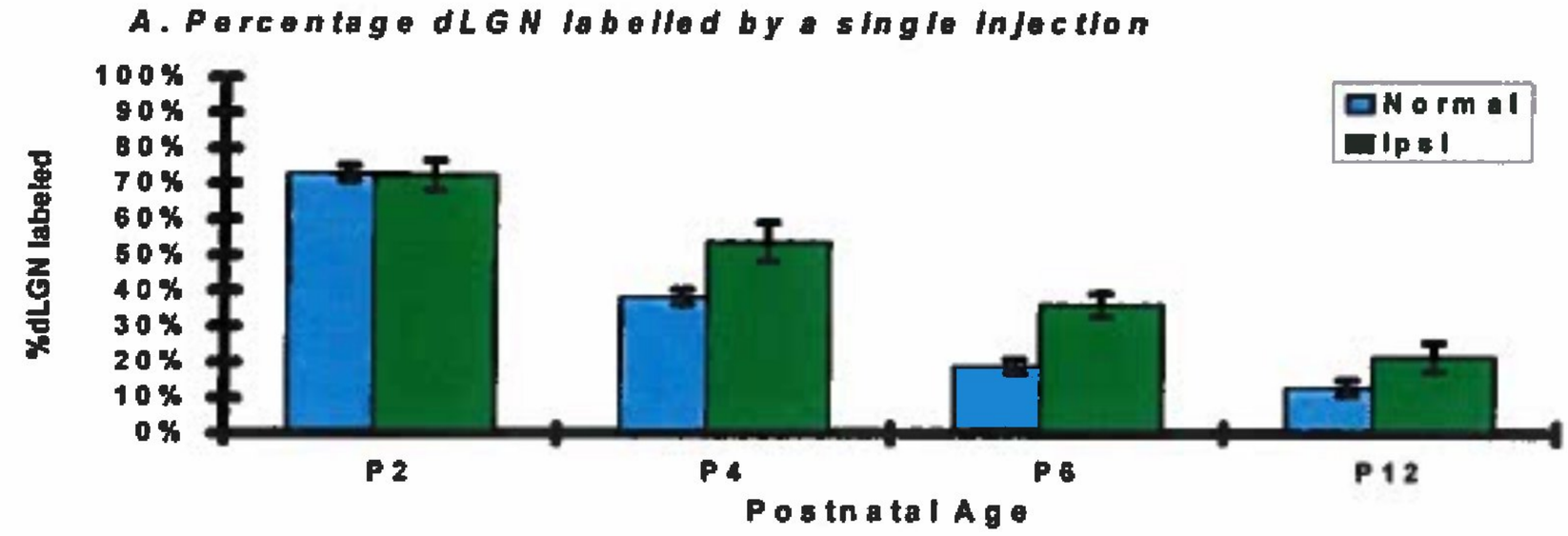


Figure IV.4. A comparison of the development of the pattern of geniculate back-label ipsilateral to the remaining eye versus normal development.

A. At P2, more than 70% of the area of coronal sections are labelled to at least 10% of the peak density, for both projections. First differences appear at P4. For the ipsilateral projection, the spread of label in the dLGN appears to decrease more slowly between P2 and P4. Despite further maturation of the projection, a fairly constant lag in refinement persists up to P12.

B. The nearest neighbour analysis mirrors the result of the measurements of the %area dLGN labelled: although there is no difference between the two distributions at P2, from P4 the ipsilateral projection appears less segregated than in normal development.

C. The percentage of double-labelled on the ipsilateral side does not differ significantly from the normal projection at any of the analysed ages.

Overall, there is no apparent developmental difference in the percentage of double-labelled cells between the ipsilateral and the normal geniculo-cortical topography across the ages (two-way ANOVA; $p < 0.661$), indicating little difference in arbor size. However, the significantly greater scatter and a less segregated projection imply retarded development on the ipsilateral side (two-way ANOVA; $p < 0.0005$ in both cases). The error bars represent the standard error of the mean.

	Number of animals		Percentage dLGN labelled		Percentage nearest neighbour same		Percentage double label	
	IPSI	NORMAL	IPSI	NORMAL	IPSI	NORMAL	IPSI	NORMAL
P2	4	7	**72.3%** *±12.0*	**73%** *±7.6*	**44.5%** *±2.7*	**48.8%** *±4.6*	**17%** *±6*	**16%** *±6*
P4	2	3	**53.7%** *±10.9*	**38%** *±5.2*	**49.6%** *±1.2*	**66.7%** *±14.2*	**7%** *±1*	**7%** *±3*
P6	3	8	**36%** *±8.2*	**19%** *±8.0*	**67.2%** *±12.9*	**80.8%** *±7.4*	**10%** *±6*	**8%** *±6*
P12	4	7	**21.4%** *±11.5*	**13%** *±8.1*	**73.6%** *±7.9*	**90.6%** *±5.1*	**7%** *±4*	**6%** *±7*

Table IV.2. This table summarizes the quantitative results for the development of topography ipsilateral to the remaining eye (green entries). For a direct comparison, the result of the normal development from the previous chapter have been juxtaposed (blue entries). The bold entries represent the means at each age with the standard deviation underneath. See also Figure 4 for discussion of trends and general statistics.

However, by P4 geniculo-cortical ordering appears to have slowed down ipsilateral to the remaining eye. The percentage of dLGN labelled does not drop as rapidly on the ipsilateral side as on the contralateral one (Figure IV.4A). The two populations of label appear more scattered and they also seem to be less segregated. The nearest neighbour analysis underlines a delay in maturation: at P4, after removal of one eye, only 49.6% of labelled cells have a neighbour of the same colour, whereas this is the case for 66.7% of cells in a normal projection. The input from the dLGN to the two injection sites shows still no segregation in contrast to the normal projection. Furthermore the vector analysis shows little developmental change between P2 and P4. Normally, in most sections at this age the two centres of gravity of label start to segregate and the vectors point to the right (medially). However, for the ipsilateral projection, the vector values still cluster around "zero" (Figure IV.5): The foci of label stay closely together, in many cases they are nearly superimposed.

In spite of further refinement in the projection, a developmental lag between the ipsilateral and the normal projection persists. At P6, the results for the nearest neighbour analysis and the extent of dLGN labelled are still trailing behind the expected values (Figure IV.4A+B). There is still a high degree of disorder in the columnar organisation of the ipsilateral projection (Figure IV.5). Although for some sections the vector between the red and the green populations of label extends in the right direction, many vectors still cluster around zero. Thus, at P4 and P6, the development of the projection ipsilateral to the remaining eye appears grossly retarded: in particular, the ipsilateral nearest neighbour value and the mean vector at P4, but not the %dLGN, resemble the P2 normal result; and

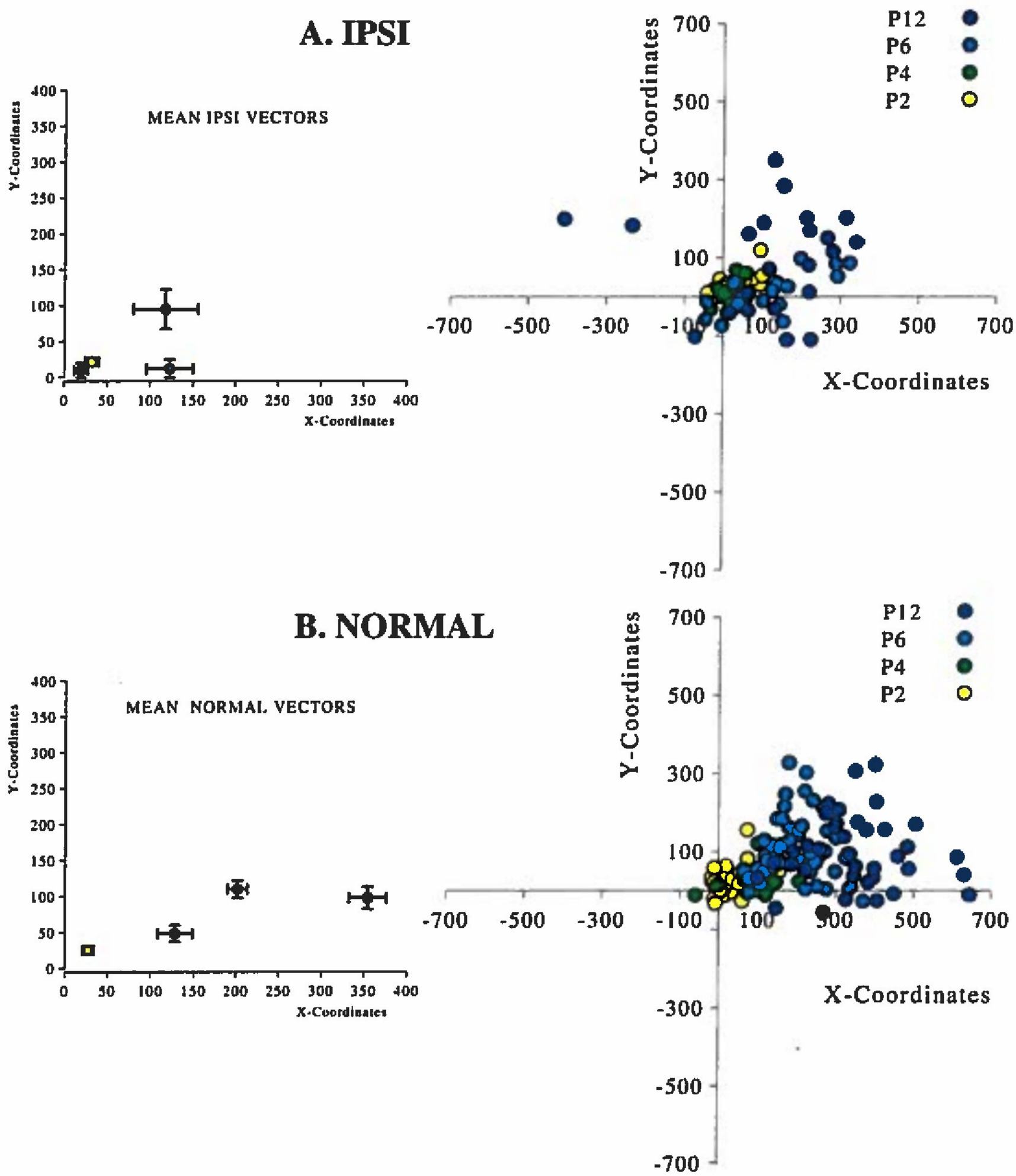


Figure IV.5. In the normal adult hamster, paired injections of retrograde tracers into area 17 back-label two discrete foci of label on coronal sections of the dLGN: the more medial injections labels a more lateral focus in the dLGN and vice versa. The two graphs above show the orientation and length of the vector from the putatively lateral focus of label in the dLGN, i.e. that is labelled from the medial injection, (at the origin), to what should be the more medial focus of label at different postnatal ages (coloured points). The predictability and stability of this pattern is utilised to assess changes of geniculo-cortical topography in the enucleate. The two graphs on the right show all vectors from the analysed sections individually, the small graphs on the left summarize the mean vectors at given ages (error bars represent the standard error of the mean).

A. IPSI. After removal of one eye at birth, ipsilateral to the remaining eye the relationship between the foci of label is disturbed. From the early disordered map at P2, ordering of the back-label is slow: at P4 there is still little topographic organisation discernible. At P6, some vectors point into the right direction, i.e. medially, but they are generally shorter than in the normal animal (see **B.**). When the double focus has emerged at P12, a sizable proportion of vectors cluster around zero, indicating two foci from the lateral injection site flanking a central focus. If the second lateral focus appears on a different section than the first medial one, vectors point to the left.

B. NORMAL. In normal development, there is little topographic organisation at P2. However, from P4 onwards, almost all vectors point to the right, i.e. medially. For similar injection site separations the length of the vector increases during the first two postnatal weeks (see Chapter III, Results).

again at P6, the ipsilateral projection is comparable to the normal projection at P4. The ipsilateral projection does not appear to develop at the same pace as the normal geniculo-cortical projection. At P12, the nearest neighbour values and the percentage of dLGN labelled indicate once again a more disordered map than for the normal projection at the same age (Figure IV.4A+B). Although the percentage dLGN labelled decreases and the nearest neighbour value increases further, there is no further change in the mean vector. This indicates the refinement of a different pattern from the normal projection. The second lateral focus shifts the centre of gravity of the cells labelled from the lateral injection closer to the centre of gravity labelled by the medial injection. But the mean vector does not move back to zero, since the double-focus often has unequal numbers of cells in each focus and also is not present on every section.

Looking at the overall trends, both measures, nearest neighbour analysis and percentage dLGN labelled, differ significantly between the ipsilateral and the normal data (two-way ANOVA, $p < 0.0005$ in both cases). But at all ages and between P4 to P12, there is no major difference in the percentage of cells that are double-labelled (Figure IV.4C), which suggests little change in arbor size. It is interesting to note that, overall, the quantification of segregation and scatter shows a continuous trend towards more order from P4 to P12. The changes with age are significant for both the nearest neighbour values (one-way ANOVA, $p \leq 0.002$) and the percentage dLGN labelled (one-way ANOVA; $p < 0.0005$). The map does not develop first to an approximately normal state with subsequent reorganization into the double focus pattern. Nor does the adult enucleate map emerge

coincident with the normal map. Instead the double focus seems to emerge out of a slowed down process of ordering, at a later stage of development than the normal map.

We must also consider if shrinkage of the dLGN and area 17 could contribute to the greater degree of observed scatter in the back-label. Due to the substantial loss in geniculate afferents a decrease in size of visual cortex and dLGN could render the relative cortical injection sites larger and the pattern of back-label in the dLGN could appear more scattered. In order to avoid artefacts by tissue processing, only the ipsilateral and contralateral dLGN from the same animals were compared. A comparison of the overall area of the dLGN on a complete one in two series of coronal sections indicates that at P4, P6 and P12, but not at P2, the ipsilateral dLGN is 20% smaller on average. It is not clear if this result will prove to be significant, since there is some variation between animals and the sample is quite small. But the values indicate a similar trend as work by Trevelyan and Thompson (1995). They showed that the volume of the adult dLGN ipsilateral to the remaining eye decreases by 27% and the area of striate cortex by 22%. The reduction in size of the dLGN could contribute to the increase in percentage of dLGN labelled and to the reduction in vector length that we see. However, a decrease in area of striate cortex by 20% would increase the relative size of the cortical injection site, which occupies usually about 1.67% of the area of primary visual cortex at P2 in normal animals (see Chapter II), only to approximately 2.1%. And a decrease in the area of striate cortex as well as a reduction of the size of the dLGN should not at all contribute to the decrease in segregation. With constant medio-lateral spacing of the injections sites in cortex, any

reduction in the medio-lateral extent of area 17 actually augments the *relative* separation of the two injections. The nearest neighbour value should increase not decrease.

3.3. A quantitative test for the double focus.

The double-focus pattern can be quantified more directly. The vector between the centres of gravity gives a first indication of qualitative change in the pattern of back-label: sections with a double focus should give us a vector with a length close to zero. Also, in the sections which only show one or the other of the dual focus, the vectors should be long, but pointing in the opposite directions - this is the kind of distribution which can be seen in Figure IV.5. The distinction between the relationship of the back-labelled foci in the normal and the ipsilateral projection is most apparent in the distributions of all the vectors from individual sections.

However, I have also used a Monte Carlo simulation to detect directly if a single injection back-labels more than one discrete cluster of cells. The total variance of the Euclidean distance of the labelled cells is compared to the minimum variance when those cells are divided into two "ideal" clusters. If the labelled cells fall naturally into two foci of label, the drop in total variance after cutting two clusters should be significantly larger (see also Chapter II, 4.4). At P12 in the normal projection, all but 1 out of 51 sections (2%) carry only a single cluster of cells: the drop in variance from one to two clusters is not significant ($p > 0.01$). But the drop in variance is significant for 11 out of 25 sections (44%) ipsilateral to the remaining eye ($p \leq 0.01$). The labelled cells are actually distributed into two separate clusters, i.e. there is a double focus of back-label. Interestingly, although

usually the double focus is only seen in the population of cells that is flanking a central focus, on two sections the more medial injection also resulted in a double focus. It appears, if both injection sites are placed extremely lateral the result can be a dual focus of label flanked by two foci of the second colour.

The Monte Carlo simulation shows that at P12 nearly half of all sections through the dLGN ipsilateral to the remaining eye have a double focus of back-label. Sections with a double focus can be found in all four of the P12 enucleated animals.

4. Discussion

Removal of one eye at birth causes the geniculo-cortical map ipsilateral to the remaining eye to remain crude and scattered during the first postnatal week, which is when normal adult-like geniculo-cortical topography emerges. By P12, an abnormal geniculo-cortical topography like that in the adult enucleate has appeared. A single injection into particular regions of primary visual cortex now yields dual foci of back-label in the dLGN. Thus, changing retinal input alters the geniculo-cortical map twofold: the radical change in retinal input seems both to *delay* and also to *alter* map formation.

This is the first study of the time-course and the development of altered geniculo-cortical topography after deafferentation. The results confirm, what was already implicit in the normal development of the projection described in Chapter III: the abnormal map can be sculpted out of the diffuse initial projection and is not a reactive change to a normal adult-like map. The development of the abnormal map indicates that the retinal input influences geniculate map formation. However, it is not clear if the early scatter at P4 and P6 and the concomitant delay in development is simply a consequence of deafferentation or is a consequence of the formation of the abnormal geniculo-cortical map.

4.1. How does removal of one eye at birth affect the development of the geniculo-cortical map?

Monocular enucleation could influence the developing dLGN in three ways : firstly, through the degeneration of retinal axons, secondly, by the deafferentation of large parts

of the ipsilateral dLGN and finally, through topographic changes in the retino-geniculate maps. Experiments on binocular enucleation and congenitally anophthalmic animals indicate that neither degeneration of retinal axons nor deafferentation alone should dramatically affect the resulting geniculo-cortical topography in the adult (Godement et al., 1979; Kaiserman-Abramof et al., 1980; Guillery et al., 1985). As for the retino-geniculate topography in the rodent, little is known about the development of the normal map, let alone the development and the adult form of the map ipsilateral to the remaining eye in enucleates. What we do know is that monocular enucleation at birth in the hamster has two known consequences for the retinal input to the dLGN ipsilateral to the remaining eye: The retinal input is reduced by 95% and an exuberant uncrossed projection is stabilised throughout the dLGN (Lund et al., 1973; So et al., 1984). Concerning the actual topographic mapping of retinal input in the dLGN in the enucleates, only inferences can be made from the map in the ipsilateral superior colliculus (SC) (Thompson, 1979; Thompson et al., 1995).

(i) Consequences of deafferentation for the adult projection. To discern specific transneuronal effects of enucleation on the geniculo-cortical topography, the change in the retinal signal needs to be related to the observed developmental changes in the geniculo-cortical map, i.e. the prolonged existence of the early scatter and the emergence of the double focus. The presence of a topographic map in congenital and induced anophthalmia implies that the increased scatter is not directly caused by deafferentation (Godement et al., 1979; Kaiserman-Abramof et al., 1980; Guillery et al., 1985). However, the use of single

retrograde tracers (HRP) in these studies cannot exclude the possibility that complete removal of retinal input might have a small effect on topographic precision, or indeed changes the developmental time-course of the map. In fact, some of these papers describe increased scatter of back-label - but, overall, they do indicate that complete removal of retinal input reveals a basic "intrinsic" geniculo-cortical map in the adult. However, other experiments do suggest that retinal input can capture geniculo-cortical ordering when retino-geniculate topography is abnormal (see Chapter I and this chapter, 1. Introduction). This evidence appears to favour a retinal signal instructing topographic mapping, rather than changes due to simply absence of the input. Increased topographic scatter after neonatal monocular enucleation has been reported previously in the adult rat geniculo-cortical projection (Jeffery, 1984). However, only single injections of HRP into area 17 were used. Thus, a double focus could have been misinterpreted as simple scatter. Also quantification of topography is difficult with this technique. The paired injections of tracers are, in this study, used as the basis for classification and quantification of topography (see Chapters I and II).

(ii) The early ipsilateral geniculo-cortical projection. At P6, after monocular enucleation, a single injection results in a more scattered distribution of labelled cells and paired injections reveal a less segregated pattern of back-label. Shrinkage of dLGN and area 17 could contribute to the increase in scatter but cannot account for the decrease in segregation of cortical input (see Results 3.2). The developmental delay in maturation could be induced by deafferentation directly. To verify this hypothesis, the time-course of

geniculo-cortical map formation should be studied in binocular enucleates. Another possibility is that qualitative changes in the retino-geniculate map determine the geniculo-cortical process of ordering.

What do we know about the development of the uncrossed retino-geniculate projection? At the time of birth (the time of enucleation), there is little topographic order in the normal hamster retino-geniculate map (Thompson, *personal communication*), just like in the retino-collicular projection (Thompson and Cordery, 1997). Anterograde tracing of retinal fibres with HRP show that the contralateral and ipsilateral retinal fibres have reached the dLGN. By P1 contralateral fibres would usually have filled the entire dLGN and by P2 the ipsilateral fibres would cover most of the dLGN (So et al, 1984). After removal of one eye at birth, the uncrossed projection expands further and at P4, the ipsilateral dLGN is completely filled by fibres (So et al., 1984). Thus, at a time when the input from the two eyes usually starts to retract and segregate, the ipsilateral projection expands further in the dLGN. This happens at a time, when the developmental lag in topography becomes apparent between the ipsilateral and the normal projection.

It also could be argued that a more scattered retino-geniculate map might be translated into a more scattered geniculo-cortical map. Indeed, as discussed above, the ipsilateral input is abnormally widely spread throughout the dLGN. The map from the retina could be more scattered for several reasons: (i) a relatively small input from the temporal retina expands over a much wider target area, (ii) topographically inappropriately uncrossed fibres survive, (iii) the now unbalanced retinal signal from one eye affects the ordering process. Inappropriately projecting uncrossed axons, which usually disappear,

survive and are stabilised in the SC and the dLGN after monocular enucleation (Thompson, 1979; Thompson et al., 1995; Fawcett et al., 1984), but, at least in the SC, these are mapped topographically (Thompson 1979). The putative retinal signal could cause the developmental changes described by acting through various routes. But in the absence of detailed knowledge concerning the development of the retino-geniculate topography as a whole and of the uncrossed retino-geniculate projection after monocular enucleation in particular this can only be speculative.

The possibility must also be considered that the scatter in the geniculo-cortical topography arises independently of the retino-geniculate map. A reduction in relay neurons projecting to area 17 (around 16% in the adult enucleate, Trevelyan and Thompson, 1995) could result in increased scatter in the projection. Reduced competition for target neurons could result in stabilisation of inappropriate projecting geniculate axons, as has been argued for the retino-collicular projection after monocular enucleation.

(iii) The origin of the double focus. The presence of the duplicate thalamic projection to cortex has to be seen in close connection with the duplication of the physiological map in cortex (Trevelyan, 1992). But the representation of this relationship is complicated by lack of information on the nature of the ipsilateral retino-geniculate projection in the adult enucleates. Work by Thompson (1979) on the SC shows a duplicated retinal map. If the dLGN contains a similar retinal mapping, a simple thalamic mapping rule - retina-independent - would relay the duplicated physiological map to cortex, like in the "Midwestern" Siamese cat or in the albino green monkey (Kaas and Guillery,

1973; Guillery et al, 1984). However, if functional mapping ordered the geniculate projection such that sites with the same receptive field but at opposite ends of the double map in the geniculate project onto the same point in cortex, the thalamic map would be reordered anatomically, as the geniculo-cortical map is reordered in the "Boston" Siamese cat (Hubel and Wiesel, 1971). My predictions would be that in the adult enucleate, the two geniculate sites which are back-labelled from one cortical injection site contain neurons with a similar receptive field location and also that two sites separated in area 17 but which have the same receptive field share geniculate input. It needs to be tested electrophysiologically whether the two geniculate sites of the double focus have similar receptive fields. And recordings from cortex could be combined with bead injections to identify the geniculate origin of input to two cortical sites with corresponding receptive fields across the physiological map reversal.

My developmental results are consistent with the idea that retinal input can instruct geniculo-cortical topography, but does not prove it. It is interesting that the late formation of the geniculo-cortical double focus - after potential map formation and ocular segregation in the normal retino-geniculate map (So et al., 1984; Thompson, *personal communication*) - indicates further that it is the geniculate map which needs to be sorted first before the geniculo-cortical map. This is indirectly supported by the results from late enucleation on the SC: eye removal after P6, after segregation of the input from the two eyes, does not lead to a duplication of the map anymore (Thompson, 1980). Also, in the rat, a double map in the SC was most prominent with prenatal enucleation (Jeffery and Thompson, 1986) - if the map in the dLGN is comparable to the one in the SC, this could explain why the

geniculo-cortical projection after monocular enucleation at birth only showed increased scatter in these animals (Jeffery, 1984).

In summary, all the available evidence points towards a refining role of the retinal signal in the development of the geniculo-cortical map. However, there are still many question marks in the development of the geniculate map itself.

4.2 How relevant is the "retinal signal" to normal development?

Since the geniculo-cortical map seems only to be affected by altering the input from the two eyes not complete removal of retinal input, one might argue that this process is not relevant to the normal development of geniculo-cortical map. However, all the data with its continuous refinement of nearest neighbour and percentage of dLGN labelled values indicate that the aberrant geniculo-cortical map arises slowly out of the initial diffuse projection in a continuous process not unlike the normal map formation. Effects are seen as early as P4, therefore at the same time as the normal map is forming. Furthermore, although the normal adult-like map is reached earlier than the double focus pattern ipsilateral to the remaining eye, at the time the double projection is being formed between P6 and P12, the normal geniculo-cortical map is still being refined (Chapter III). This study, together with work on anophthalmic and albino animals, indicates that the retinal signal is probably not involved in creating a crude overall map but might refine the geniculo-cortical topography. In the case of a major disturbance in the retinal input the balance might shift towards retina-dependent mechanism(s).

4.3 About the role and the nature of "the retinal signal".

Although the removal of one eye renders the geniculo-cortical projection ipsilateral to the remaining eye quite abnormal, two things need to be noted. Firstly, an initial crude map develops in spite of the removal of most of the retinal input. Thus, factors independent of the retina signal must govern the generation of a crude map. The absence of major abnormalities in the geniculo-cortical topography after binocular enucleation underlines this (Guillery et al., 1985). Secondly, the retinal-dependent signal is not only implied in the change in geniculo-cortical topography itself but also in the degree of refinement and order in the abnormal map. The system can create an ordered map in the face of a grossly changed input. Most of the suddenly available cortical space is utilised without massive enlargement of the axonal arbors (the percentage of double-labelled neurons is unchanged). The capacity of the thalamo-cortical projections to capture changes in visual input is evident in such diverse experiments as on albinism and on rerouting visual fibres to cortical areas of other sensory modalities. In Siamese cats, the "Midwestern" pattern seems to directly translate a retino-geniculate abnormality into a disrupted cortical map (Kaas and Guillery, 1973), but in the "Boston" pattern, the geniculo-cortical input reorders onto a continuous cortical map of the visual field (Hubel and Wiesel, 1971). In the ferret, retinal fibres rerouted into auditory thalamus seem to provide a signal that generates a crude visual map in primary auditory cortex (Roe et al, 1990). The evidence suggests a balance between preserving retina-independent mechanisms of map formation and adaptive retina-dependent mechanisms. The timing of the changes after monocular enucleation further indicates that

the balance between the two might shift in development from the retina-independent in favour of retina-dependent mechanism(s).

The most likely candidate for the signal itself is neural activity. Early in development waves of spontaneous activity sweep across the retina (Meister et al, 1991; Wong et al, 1993) and could provide the coherent signal needed by Hebbian synapses to refine a topographic map (Hebb 1949, Willshaw and van der Malsburg, 1976). In order to test if it is indeed retinal activity which provides the signal to refine the geniculo-cortical map after eye removal into a double projection, I blocked neural activity in the developing retina while the geniculo-cortical projection was forming. The results are discussed in the following chapter.

V. Retinal activity and the development of geniculo-cortical topography after monocular enucleation at birth.

1. Introduction

2. Material and Methods

3. Results

3.1 The effect of retinal activity blockade on the development of abnormal topography ipsilateral to the remaining eye.

3.2 The effect of retinal activity blockade on the development of normal topography contralateral to the remaining eye.

4. Discussion

4.1 Is retinal activity essential for abnormal map formation after enucleation?

4.2 Is retinal activity necessary for normal development of geniculo-cortical topography?

4.3 Implications

1. Introduction

Monocular enucleation at birth severely alters the development of the geniculo-cortical map. The previous chapter described how a double projection to a single point in cortex arises out of an early disordered input. But the question remains what is the nature of the signal that is changed by enucleation. This chapter attempts to dissect out the possible role retinal activity might play in the abnormal and also normal development of geniculo-cortical topography.

Earlier work in rodents on the superior colliculus (SC) and the somatosensory system suggests altered patterns of neuronal activity can convey the signal for rearrangement and refinement of a topographic projection in development. Intraocular injections of the sodium channel blocker tetrodotoxin (TTX) prevent the selective elimination of topographic errors in the retinal projection to the SC without altering the overall level of retinal ganglion cell death (O'Leary et al., 1986; O'Leary et al., 1986b; Thompson and Holt, 1989). Monocular and binocular injections of TTX also prevent the refinement of the uncrossed projection into ordered patches in rostral SC. However, monocular injections of TTX, unlike monocular enucleation did not result in an expanded uncrossed projection (Thompson and Holt, 1989). It is not clear if this is a result of incomplete activity blockade or if other factors are involved. A refining role for neuronal activity in central map formation is also supported by Fox et al. (1996). They showed electrophysiologically small-scale topographic disorder in the thalamic projection to the barrel cortex of the rat. Blocking cortical activity resulted in functional input from

whiskers to the wrong barrels. Cortical activity is furthermore necessary for the developmental rearrangement of the cortical barrels after removal of a whisker (Schlaggar et al., 1994). These results suggest that retinal activity might play a similar role in normal and abnormal geniculo-cortical map formation.

The importance of retinal activity in the development of the geniculo-cortical map was tested by blocking retinal activity in the remaining eye during map formation. After removal of one eye at birth, the remaining eye received daily injections of TTX from P2, when the projection is still disordered, until P12, when topography was assessed by paired injections of fluorescent tracers. During the first two postnatal weeks, an abnormal pattern of geniculo-cortical topography usually emerges on the side ipsilateral to the remaining eye, showing a double focus of back-label from one injection (Chapter IV), while the contralateral side develops essentially normal (Chapter III). Thus, the role of activity on normal and abnormal geniculo-cortical map formation could be examined in the same animals.

2. Material and Methods.

For this study, hamster pups from more than one litter were used. The numbers of animals assessed in this study are as follows:

- Topography ipsilateral to the remaining eye

  TTX treatment n = 5

  Citrate controls n = 3

- Topography contralateral to the remaining eye

  TTX treatment n = 6 (n = 4 for nearest neighbour analysis)

  Citrate treatment n = 4 .

TTX or citrate buffer were administered through glass-pipettes by an air-pressure injection system from P2 to P12 daily. For the injections, the eye was punctured with an insect pin. Injections were made as long as possible without parting the eyelid, which was usually done from P9 onwards. The dosage of the daily injections of TTX varied with age and was based on estimates of eye-size to yield a final concentration of 10^{-6} M in the eye. This concentration injected into the eye blocks visually-evoked response in the superficial layers of the SC in the hamster at P16 just after eye-opening (Thompson and Holt 1989). The volumes injected ranged between 25 and 100 nl of a 10^{-3} M solution in citrate buffer. The control animals received similar amounts of citrate buffer alone.

At the time the cortical bead injections were made, the injected eye was checked for gross abnormalities. However, none were found in the animals in this study.

3. Results

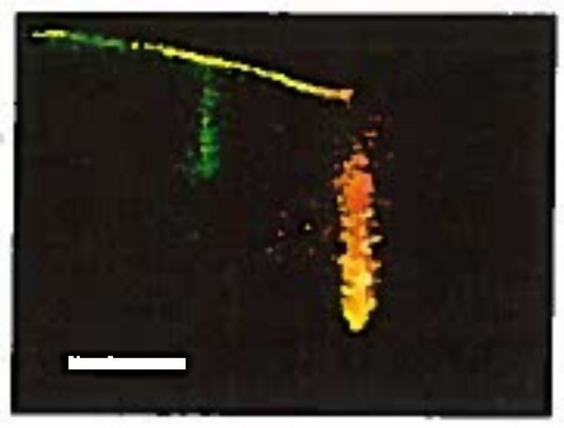
After removal of one eye at birth, hamster pups received daily injections of TTX into the remaining eye between P2 and P12. At P12, paired injections of red and green microbeads were placed into area 17 of both hemispheres. The pattern of back-label in the dLGN was assessed. Thus, I could investigate the effect of retinal activity blockade on abnormal map formation, ipsilateral to the remaining eye, and on normal geniculo-cortical development, contralateral to the remaining eye.

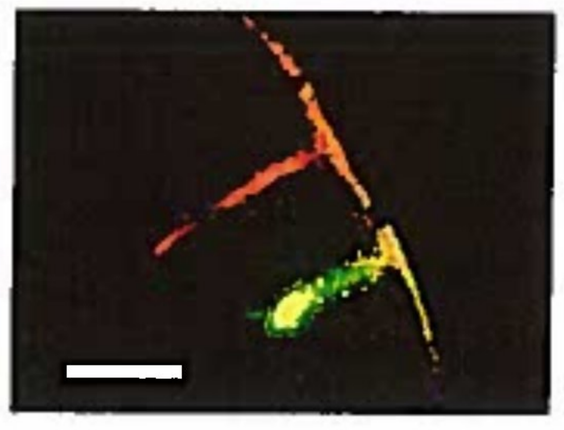
3.1 The effect of retinal activity blockade on the development of abnormal topography ipsilateral to the remaining eye.

By P12 in untreated animals, the geniculo-cortical projection ipsilateral to the remaining eye shows on some coronal sections, a double focus of back-label from a single injection placed very laterally or medially into area 17. The following section investigates the effect of retinal injections of TTX on the formation of this double focus pattern.

(i) Qualitatively, the ipsilateral double-focus appears absent. Paired injections into area 17 after monocular enucleation at birth and TTX into the remaining eye reveal a scattered pattern of back-label. In Figure V.1 (left), the two injection sites label cells over a large extent of the dLGN. The foci of label are big, especially the green one, and overlap to a great degree. However, the clusters of label shift from the dorso-medial end of the dLGN on more caudal sections to the ventral border of the nucleus on more rostral sections, as would be expected for a topographically ordered geniculo-cortical projection.

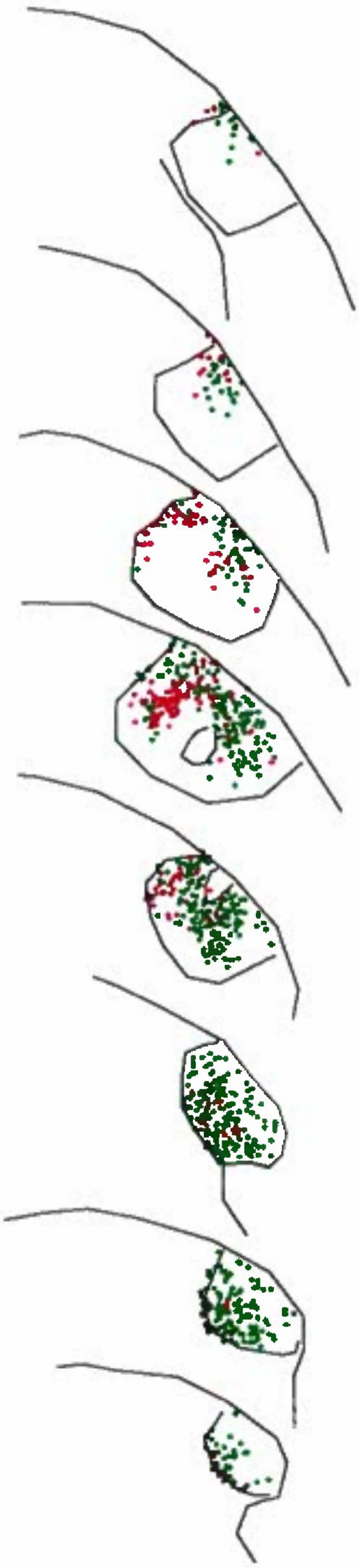
Figure V.1. This figure shows the pattern of retrograde label in one in two series of sections through two dLGN ipsilateral to the remaining eye after monocular enucleation at birth. Above are photomicrographs of the respective bead injection sites in cortex. The animal on the left received daily intraocular injections of TTX into the remaining eye between P2 and P12. The one on the right had citrate buffer injected as a control. The TTX-treated animal shows a scattered pattern of back-label with large overlapping foci in the dLGN instead of the typical double focus seen in the control on the right. In the control animal the lateral green injection back-labels two discrete foci of cell which flank a central red focus of label. The scale bars represent 500 µm.





TTX

Citrate





D

M

500 Microns

Figure V.1

The lateral, red injection does not give rise to an obvious double focus, although the distribution of labelled cells on sections 3 and 4 from the top might hint at a double focus pattern. But cells labelled from the medial green injection are found at both, the medial and the lateral margin of the red focus. The distribution of label is also too disorganised to resemble the normal enucleate projection at this age (see below and Chapter IV), it appears more like the immature ipsilateral map at P6, shown in the previous chapter.

However, in an animal that received matched volumes of citrate buffer from P2 to P12, the typical double-focus pattern can be seen at this age. In Figure V.1 (right), a single lateral green injection into area 17 results in two distinct foci of back-label in the dLGN. These two foci flank a central red cluster of label from the more medial injection site. The projections for the two cortical sites are largely segregated in the dLGN - even though one cortical site gets input from two points in the dLGN.

In summary, daily retinal injections of TTX during development appear to disturb the formation of the abnormal geniculo-cortical map after monocular enucleation at birth. Whereas in control animals the ipsilateral projection displays the typical double-focus of back-label, in the TTX-treated animals this pattern cannot be observed. Instead, labelled cells appear more scattered and the red and the green populations are less segregated.

(ii) Measuring the double focus. The question is can the presence or absence of the double-focus be determined quantitatively. One way to study the clustering of label in the dLGN is by superimposing iso-density contours onto the red or green populations of label on geniculate sections. Local clusters of high density of label are made visible by these contour lines. Is there still some bias towards the double-focus pattern within the observed

scatter? Figure V.2 illustrates the contour analysis of sections taken from TTX treated and citrate treated enucleates. The sections from the TTX animal do not show a double focus of label, the iso-density contours circumscribe a continuous area. But in the control animals the contour lines accentuate the double focus.

In the previous chapter, a cluster analysis was used to assess if a single population of back-label consists of one or two clusters of cells (Chapter II and IV). I have used the same test on the TTX and citrate-treated animals. In TTX-treated animals, 4 out of 36 coronal sections (11%) show a significant double focus in the cluster analysis ($p \leq 0.01$), in contrast to 6 out of 19 sections (32%) in the three control animals (Table V.1). Furthermore, two out of the five TTX-treated animals show no double-focus at all, whereas all the control animals have at least one section carrying the double focus. The appearance of some double foci in the TTX-treated animals could mean that some other factors apart from retinal activity are involved in its formation. However, it seems more likely that in those animals the blockade of activity was not complete.

Table V.1. The table summarizes the results of the Monte Carlo analysis. The percentage of sections with a double focus ($p < 0.01$) is shown for TTX treated, Citrate controls and uninjected animals (from Chapter IV). Intraocular injections of TTX greatly reduce the percentage of geniculate sections on which a double focus is seen.

	TTX	Citrate	Ipsilateral (unmanipulated)
number of animals	5	3	4
percentage of sections with a double focus	11%	32%	44%

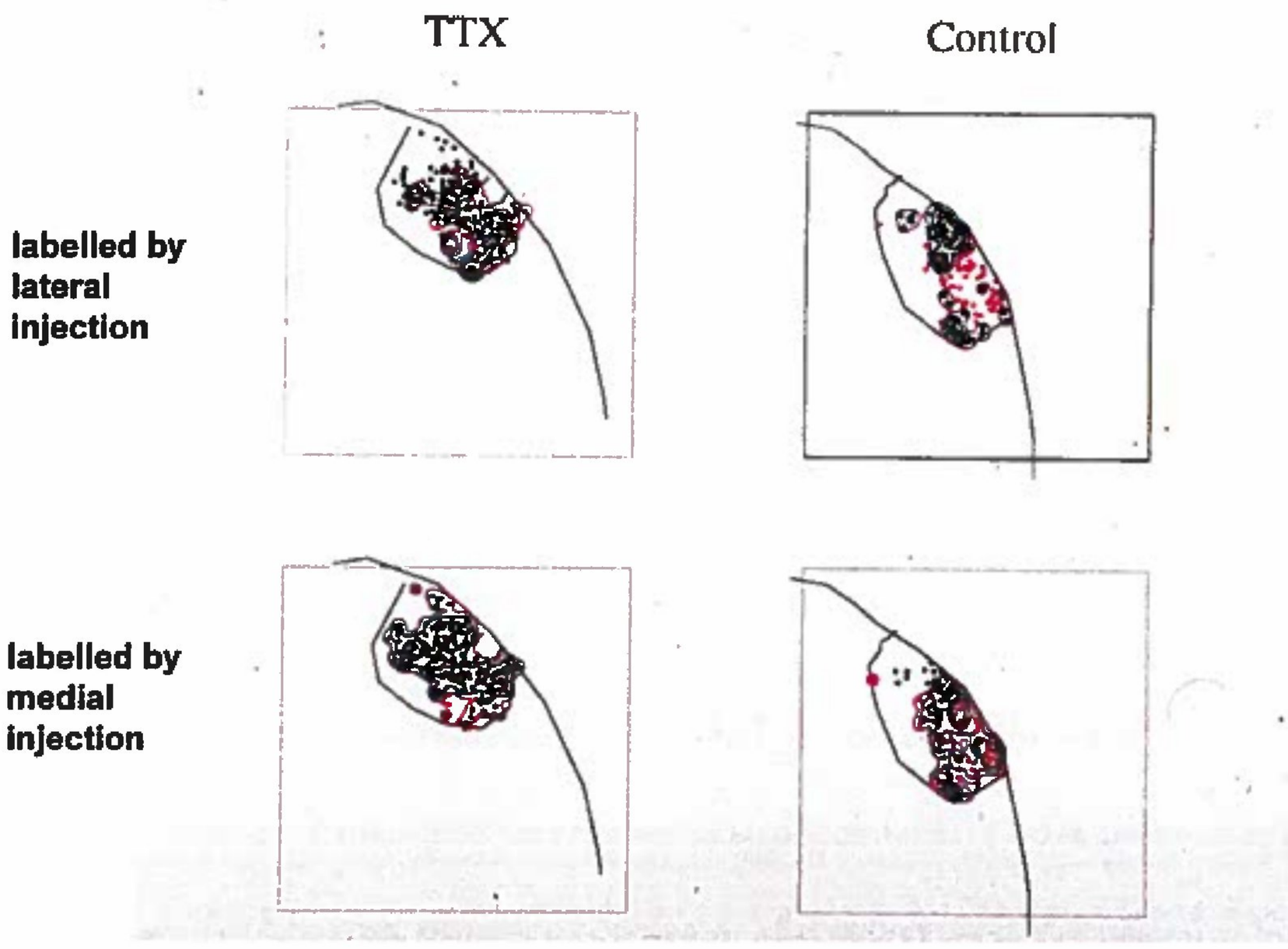


Figure V.2. The sections above were taken from central dLGN of the animals displayed in Figure V.1. On the left, iso-density contours were superimposed onto the red population (lateral injection) and the green population (medial injection) of cells after TTX treatment. Underneath are the contour lines on their own. On this section no double focus can be detected for either population of label. Although the red label (top left) appears to form multiple clusters of higher density, these lie within the area densely labelled by the green injection. In contrast to this, the control section on the right sports clearly a double focus of green label (lateral injection; top section in both panels) flanking the red label.
The colours of the contours in rising density: **pink < blue < black.**

Overall, the qualitative and the quantitative observations in this section, show that retinal activity is necessary for the formation of abnormal topography after monocular enucleation.

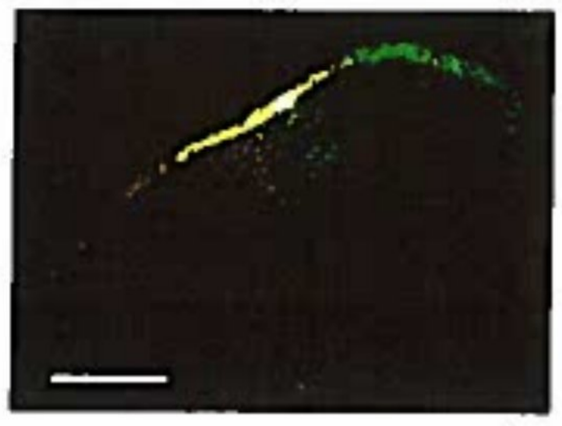
3.2 The effect of retinal activity blockade on the development of normal topography contralateral to the remaining eye.

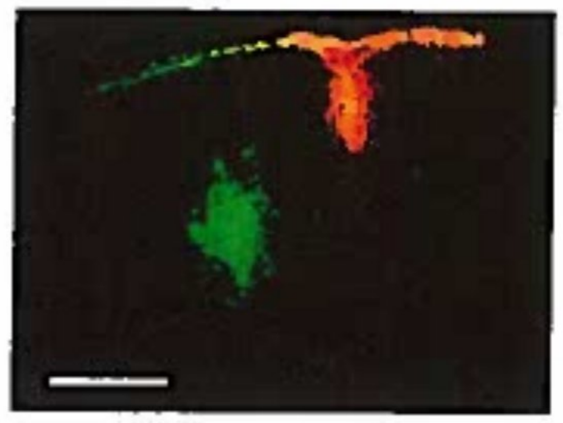
(i) Qualitatively, the contralateral geniculo-cortical map appears more disordered after retinal activity blockade. In untreated animals, contralateral to remaining eye, the geniculo-cortical map develops essentially normally after monocular enucleation at birth (Chapter III). It does so also with control injections of citrate into the remaining eye (Figure V.3). Paired, medio-laterally spaced injections back-label two discrete foci of labelled cells on coronal sections of the dLGN (Figure V.3, right).

After daily injections of TTX into the remaining eye, similar injections into contralateral area 17 still yield a crude topographic map. However, many foci on coronal sections seem to occupy a larger medio-lateral extent of the dLGN, and the red and green foci of label overlap greatly . The input to the two injection sites appears less segregated with the red and the green cells being intermingled. Overall, the contralateral geniculo-cortical topography appears more disordered after TTX treatment. But the effect can vary greatly between animals.

(ii) Quantitatively, little effect of TTX-treatment can be measured on topographic order in the geniculo-cortical map. The use of paired tracer injections provides the tools with which to quantify topography (see Chapter II). Segregation of input to different sites

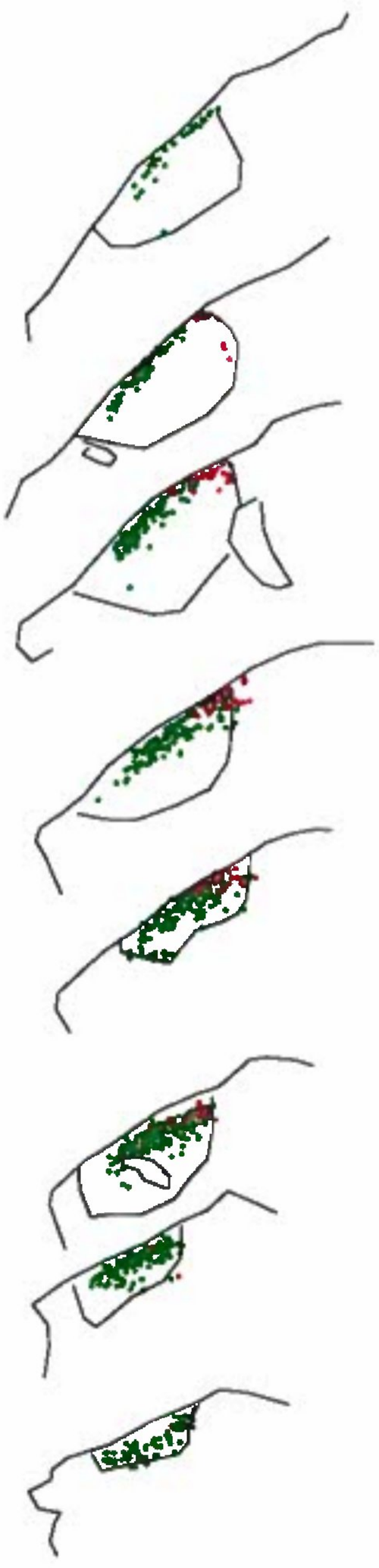
Figure V.3. This figure depicts the pattern of retrograde geniculate label on coronal sections after cortical bead injections (top) contralateral to the remaining eye. The animal on the right received daily injections of citrate into the remaining eye between P2 and P12. It shows a normal pattern of label in the dLGN with two discrete segregated foci of back-label. On the left, the TTX-treated animal has at first glance as well a basically normal map. However, the red and the green populations of cells overlap to a larger degree and appear less segregated. The injection sites are also closer to each other than in the control, but they are small and discrete. The scale bar represents 500 µm.

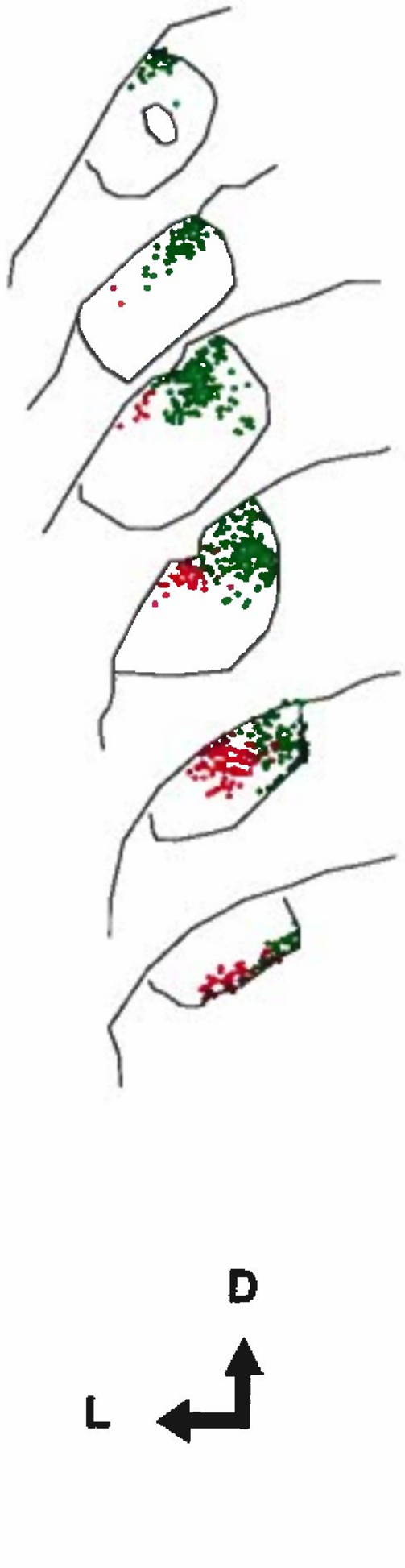




TTX

Citrate





D

L

500 Microns

Figure V.3

of area 17, the injection sites, can be measured by using a nearest neighbour analysis. This measure estimates the probability that a labelled cell has as its nearest neighbour a cell of the same colour. An indication about the arbor size of geniculate terminals can be obtained from the percentage of double labelled cells.

For the nearest neighbour analysis, only 4 of the 6 animals studied, could be included, since the great imbalance in the relative number of red and green labelled cells might have affected their neighbour value (see Chapter II). The graph (Figure V.4A) shows a smaller nearest neighbour value for the TTX treated animals, indicating less segregation in the projection. Also, the percentage of double-labelled cells seems to be much greater in the TTX-treated animals versus normals (Figure V.4B). However in both cases, the results are not statistically significant, although especially for the double-label result only by a very small margin (unpaired t-test, $p < 0.11$ for nearest neighbour; $p < 0.075$ for double label). One reason for the non-significance might lie in the great variability between individual results, for example for the nearest neighbour analysis the individual results span from 60.4% to 87.85%. Similarly, the results for the percentage of double-label lie between 10% and 41%. Such ranges were not seen in either the control animals nor in normal development (Chapter III). Low nearest neighbour values are usually associated with high double label values in the same animals. While it cannot be excluded that this still represents natural fluctuations of the results, it seems more likely that the effectiveness of the TTX treatment varied between animals. Other possible factors include injection site separation and retinal damage, which will discussed below (see Discussion). A careful analysis of all these factors will be necessary.

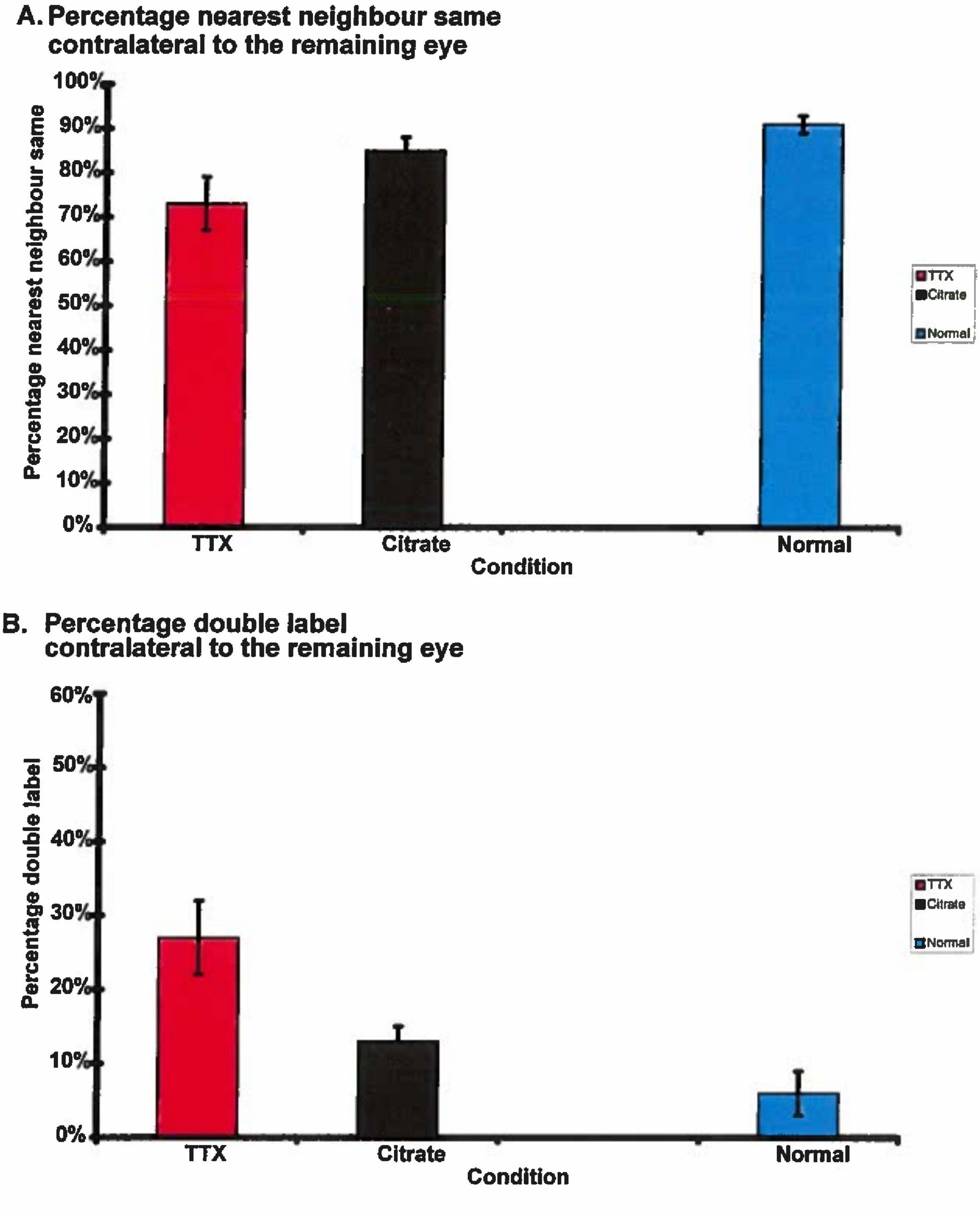


Figure V.4. This figure shows the results of the nearest neighbour analysis and the percentage of double label for the dLGN contralateral to the remaining eye after TTX treatment. For reference, the data from the normal development have been added at the far right (blue). The error bars represent the standard error of the mean.

A. TTX treatment (n=4) appears to decrease the nearest neighbour value over the citrate controls (n=4). This indicates a less segregated projection. However, this difference is not statistically significant (t-test, $p < 0.11$).

B. The percentage of double-labelled cells also appears larger for the TTX treated animals (n=6) than in the citrate controls (n=4) with 27% versus 13%. Again this result is not statistically significant, but the double label only fails the t-test by a narrow margin (t-test, $p < 0.075$).

In summary, the results from individual animals indicate an effect of TTX treatment on the segregation of geniculo-cortical input to cortex in the formation of a normal, non-duplicated map. However, the overall effect on all animals studied is not significant.

4. Discussion

The results in this study show that retinal activity is involved in the development of abnormal geniculo-cortical topography in the hamster ipsilateral to the remaining eye after monocular enucleation at birth. Blocking retinal activity by intraocular injections of TTX during map formation interferes with the emergence of the double-focus of back-label. The map which is seen appears scattered and immature. A significant effect of retinal activity on normal map formation contralateral to the remaining eye cannot be detected in the overall population of treated animals. But individual animals can show a large increase in the scatter in the geniculo-cortical projection after TTX treatment.

Retinal activity is argued for as the major effector of the changes described in this chapter after retinal TTX injections, but the presence of changes in the ipsilateral geniculo-cortical projection (or their absence in the contralateral projection) could also be the result of three possible artefacts. What is seen could be the effect of retinal damage, of activity-dependent changes of axonal transport or due to incomplete action potential blockade. However, the same protocol and dosage of TTX was used as by Thompson and Holt (1989). Their result shows no overall effect on retinal ganglion cell death, which makes it very unlikely that the injection procedure or the TTX cause retinal damage. Furthermore, there were no apparent problems with anterograde HRP transport in their study. Thus, at least partially, axonal transport seems unaffected. I can not entirely exclude incomplete activity blockade as the source of the variability of the contralateral result. However, the estimated concentration of TTX in the eye has been shown to block action potentials in the

neonatal rat optic nerve (Foster et al., 1982) and blocked visually-evoked responses in recordings from the SC at eye-opening in hamsters (Thompson and Holt, 1989). There are also the changes with retinal TTX in the ipsilateral map in this chapter. I have, furthermore, preliminary results from a study using elvax impregnated with the NMDA-channel blocker MK-801 over ipsilateral cortex after enucleation at birth. It appears that blocking the NMDA-component of activity in visual cortex also interferes with the development of the abnormal double-focus pattern. This strengthens the case for a role of patterned activity in the formation of the abnormal ipsilateral projection even further and would exclude the artefacts described above.

4.1 Is retinal activity essential for abnormal map formation after enucleation?

The qualitative and the quantitative results on the abnormal projection are very clear. Despite hints of a double focus in some animals, overall retinal activity blockade seems to have prevented the formation of a double focus pattern in most animals. Also, the pattern of back-label from paired injections is more scattered and overlapping, it appears comparable to the immature map seen at P6 ipsilateral to the remaining eye (see Chapter IV). This would suggest that refinement of the map is delayed and "frozen" in an immature state. How permanent these changes would be in the absence of further TTX treatment is not known.

My results confirm earlier work in the somatosensory system, which showed that developmental rearrangement of the barrel pattern in cortex after peripheral whisker removal is inhibited by cortical blockade of activity (Schlaggar et al., 1994). However, in

this study I also show it is the peripheral pattern of neuronal activity that is important for the developmental rearrangement in the thalamo-cortical projection.

4.2 Is retinal activity necessary for normal development of geniculo-cortical topography?

My results from the contralateral projection are not conclusive. The data from individual animals indicate that retinal activity is important for the refinement of the projection. However, for the whole population the result is not significantly different from the controls. Factors that have to be taken into consideration are, for example the effectiveness of the retinal blockade of activity in individual animals (see above). The results from the ipsilateral projection also showed traces of a double focus in some animals despite the TTX-treatment. If the TTX-treatment led to a more complete blockade in some animals in contrast to others, the changes in the projection on both sides of the brain should be correlated. In this case I would expect to find traces of a double focus ipsilateral to the remaining eye in the same animals that also should show little change in topography on the contralateral side. Also the projection studied is not entirely normal, since the ipsilateral retinal input to the geniculate has been lost. It might be possible that some parts of the projection, possibly those from dorso-medial dLGN that would normally receive uncrossed input, show a stronger effect than others. Finally, since the increase in double-labelled cells indicates an increase in axonal arbor size, it might be possible that my quantitative measures are only sensitive to the changes at small medio-lateral spacings of the injections. Results from the somatosensory system indicate that blocking activity results only in

topographic errors over a small range (Fox et al., 1996). The nearest neighbour value and the percentage double label for TTX and citrate animals should then be analysed as a function of injection site separations. In general a larger number of experiments is necessary to draw firm conclusions.

4.3 Implications.

Whereas neuronal activity clearly seems to play a role in rearrangement of thalamo-cortical topography, its possible role in normal development is still elusive. The resemblance of the ipsilateral map after activity blockade to early immature topography implies that retinal activity is important for the sculpting of the abnormal map beyond a certain stage, at which a crude map is in place. Therefore, the balance between activity-dependent and activity-independent developmental mechanisms seems to shift late in the process of geniculo-cortical map formation to favour the influence of retinal activity. However, if retinal activity was also involved in the normal refinement of the map, a more disordered geniculo-cortical topography should be seen in the absence of retinal driving. This could not be found. It could constitute a safety-net to adapt the geniculo-cortical map to changes in the pattern of input. However, it would seem an immense waste of resources if this mechanism would only be in place to deal with major developmental manipulations like enucleation.

A different question is whether the retino-geniculate projections ipsilateral to the remaining eye is also affected by the TTX treatment and if this induces the geniculo-cortical changes in topography. Does the loss of the double focus in the geniculo-cortical

projection also mean that the dual map in cortex was also lost? If the changes in ipsilateral topography could be replicated with elvax (see above) and they would be stabile, cortical recordings in the adult could investigate this.

The development of geniculo-cortical topography described in this and previous chapters takes place before eye-opening, which is around P15 in the hamster. Thus, if we turn to the origin of retinal activity, the most likely candidate appears to be intrinsic correlated activity which is generated spontaneously in the retina before eye-opening (Maffei and Galli-Resta, 1990 - in the rat; Meister et al., 1991 and Wong et al., 1993 - in the ferret). However, the next chapter is going to suggest that visual experience through the closed eyes also generates early retinal activity.

VI. Visual driving of cortical neurons through the unopened eyelids in ferrets

1. Introduction

2. Material and Methods

2.1 Animals

2.2 Surgery and Anaesthesia

2.3 Recordings

2.4 Analysis

3. Results

3.1 Neurons in primary visual cortex respond to light through the naturally closed eyelid

3.2 At least a third of the visually-responsive neurons respond differentially to orientation

3.3 Directionality of responses

4. Discussion

4.1 The nature of the response

4.2 The origin of the oriented response

4.3 Development of orientation- and direction-tuning

4.4 Implications

1. Introduction

Altering retinal activity can influence the development of visual pathways and areas. One example is in the previous chapter. It is generally believed that the major watershed between innate and intrinsic factors alone governing the development of visual pathways and the onset of influences of visual experience is the time of eye-opening. In many carnivores and rodents this does not happen until days, or even weeks, after birth. Although some reports suggested that visually-driven neuronal activity can reach visual cortex through the yet unopened eyelids of kittens (Huttenlocher, 1967; Fregnac and Imbert, 1984), animals have been treated as visually inexperienced until the eyes opened. However, if the eyelids of ferrets are artificially opened, neurons in the dLGN and in primary visual cortex not only respond to visual stimuli about a week before natural eye-opening (Chapman and Stryker, 1993), but also show evidence of orientation-tuning. Since the visual system is functional early, could its functioning have a developmental role? An important step in answering this question is to see whether neurons can actually be driven through the naturally closed eyelids. I wanted to test if information from visual stimuli can reach primary visual cortex in ferret kits and if so, how neuronal activity is patterned.

Another question in its own right is whether the orientation-tuning of neurons in primary visual cortex is innate or requires visual experience. How early can visual driving and orientation-tuning be detected and is their emergence coincident? The degree of orientation-selectivity in the earliest possible recordings - in contrast to adults - as well as a qualitative analysis of the tuning and the receptive field structures could help us to

determine how orientation tuning develops. Chapman and Stryker (1993) found that their recordings from primary visual cortex of 23-26 day old ferrets showed orientation-selectivity in about 25% of the recorded units in their sample. Since these represented the earliest recordings, made before eye-opening (the eyelids were artificially opened), they concluded that visual experience is not necessary for basic orientation tuning. A similar conclusion was reached by Blakemore and Van Sluyters (1975), when they classified about 25% of units (as a percentage of spontaneously active units) in the visual cortex of kittens just after eye-opening as orientation-selective. However, the development of orientation-tuning in parts of the neuronal population as well as the sharpening of responses is influenced by visual experience and patterns of retinal input in both ferrets and cats (Blakemore and Van Sluyters, 1975; Chapman and Stryker, 1993; Welikey and Katz, 1997).

In the following experiments, action potentials were recorded from area 17 in ferret kits between postnatal day 21 (P21) and 24 (P24). At these ages the eyelids remained closed. The responses of cortical neurons to large moving squarewave gratings presented through the unopened eyelids were analysed. Ferrets usually open their eyes between P30 and P35, thus the earliest recordings were made about one and a half weeks before natural eye-opening. Three questions will be addressed in this chapter: Firstly, can cortical neurons be driven through the *unopened* eyes? Secondly, how is the early neuronal activity in cortex patterned? And finally, what is the degree of orientation-selectivity, if any, of visually responsive cortical cells early in development?

2. Material and Methods

2.1 Animals

Pigmented ferret kits from time-mated females (Marshall Farms, New Rose, NY; Glaxo; University Laboratory of Physiology, Oxford, UK) were studied between postnatal day P21 and P24. All animals were housed from birth in the Animal House of the University Laboratory of Physiology Oxford under a light/dark cycle of 16 hours light and 8 hours dark. The litters were in an enclosed wooden box with an opening into the cage. The average level of luminance was around 93 cd/m^2 in the room, where animals were kept. For the cortical recordings 6 animals were used. All ferret kits had firmly closed eyes at the time of recording. At the time of recording the weight of the animals ranged between 82g and 138g.

2.2 Surgery and Anaesthesia.

Anaesthesia was induced with alphaxalone 0.9% and alphadolone acetate 0.3% (Saffan, Pitman-Moore, Uxbridge, UK; i.m., 1.5ml/kg). This was followed by 0.1 ml of atropine sulphate (BP 0.6mg/ml; C-Vet, Leylands, UK) i.p. to prevent possible respiratory depression. The radial vein of the front leg was cannulated. During the subsequent surgery, anaesthesia was maintained by intermittent intravenous administration of Saffan (diluted 1:2 in 0.9% saline). Transecting the skin along the throat, the trachea was visualised. The trachea was usually intubated through the mouth and the tube was tied in to give more stability and a better seal; in some animals however, a tracheotomy was performed and the

tube was inserted directly into the trachea. For recordings from area 17, craniotomies were made roughly 1 mm forward from the triangular bony sutures at lambda and about 7 mm lateral in one or both hemispheres.

The ferret was then transferred to the recording table. Its head was immobilised in a stereotaxic holder with a bite bar and two ear bars. Since the skull was still quite fragile at this age (not yet fully calcified) and the meatus has not yet opened, the ear bars were either very blunt or had special plastic buffers. The animal's temperature was monitored by an anal probe which controlled a heating blanket in a feedback loop. The temperature was maintained around 37.5°C. An ECG was taken throughout the experiment. During the recordings, anaesthesia was maintained by a continuous infusion with a solution of medetomidine (Dormitor, 11µg/kg/hr) and Ketamine (2.5mg/kg/hr) in 0.9% sterile saline. The animal was paralysed with gallamine tri-ethiodide (Flaxedil, 10mg/kg/hr). In some experiments, the dose was halved by reducing the speed of the infusion. During paralysis the tracheal tube was connected to a respirator which supplied the animal with room air (respiratory rate typically 28-35 strokes per minute) and measured the end-tidal CO_2 (maintained at 2%; stroke volume 2 ml).

The doses of anaesthesia administered were tested extensively in the same set-up in the absence of paralysis. The depth of anaesthesia was also monitored during paralysis. Anaesthesia is sufficient when pinching of the animal's footpad does not affect the heart rate and/or the CO_2 readings. In the absence of paralysis, there was no movement or withdrawal.

2.3 Recordings

Action potentials were recorded extracellularly with glass-coated tungsten microelectrodes with a 5 μm exposed tips (Merrill and Ainsworth, 1972). The dura over cortex was cut and the electrode was advanced roughly perpendicularly to the surface. Units were initially identified by their responses to the moving spot of light provided by an ophthalmoscope. Visual stimuli were in many cases presented to both eyes. Only in some experiments, one eye was covered, usually the one ipsilateral to the recorded visual cortex. Visual stimuli were presented on a display screen (average luminance 85 cd/m^2 at 90% contrast) which covered most of the putative visual field of the ferret. High contrast (90-99% Michelson contrast) squarewave gratings of low spatial (0.03 cycles per degree) and low temporal frequency (0.25 cycles per second) were used. This spatial frequency is one order of magnitude lower than the typical preferred frequency in adult ferret striate cortex (Baker et al., submitted). The gratings were displayed in four different orientations each moving in two directions (Figure VI.1). Additionally, a uniform display of zero contrast controlled for spontaneous activity. In a typical experiment, all nine stimuli were shown in a pseudo-randomized order, mostly at 5 cycles at a time (in few experiments 10 or 20 cycles). When each had been presented, the sequence was re-randomized and the

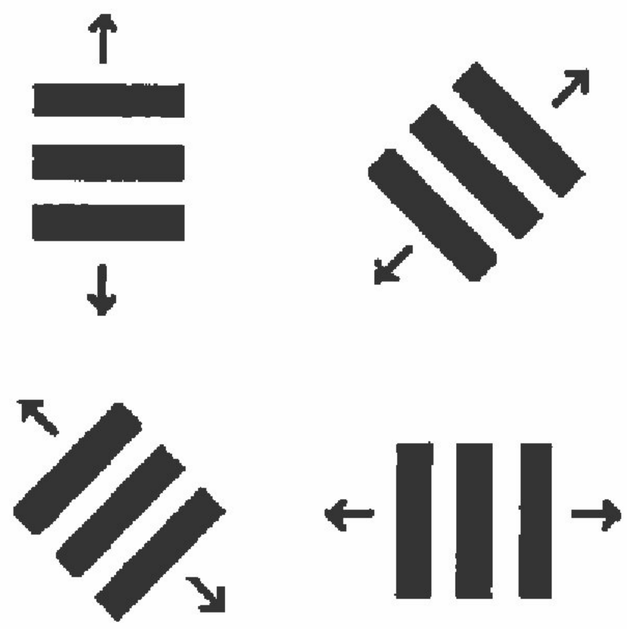


Figure VI.1. Above is a schematic representation of the eight stimuli used: squarewave gratings of four different orientations moving in two directions, perpendicular to the grating pattern itself.

procedure was repeated. In total, at least three repetitions or 15 stimulus cycles were presented - in most cases more. The times of the neuron's action potentials were recorded with reference to the timing of the stimuli, and peri-stimulus-histograms (PSTHs) were compiled. Single units were isolated using a Schmidt trigger: isolated spikes above a certain peak height were selected and displayed on a storage scope where they were checked both for differences in shape and also that no spikes fall in the refractory period of the triggered action potential .

During the experiments, lesions were made - most commonly when the end of an electrode penetration was reached or at various levels on the way up. Thus, tracts and depths of recordings could be reconstructed later on.

2.4 Analysis

The responses of isolated single units were first tested for significant changes in the spike rate with orientation (one way ANOVA, $p< 0.05$). Then the remaining cells were checked with an unpaired Student's t-test ($p < 0.05$) for significant elevation of response rate for all pooled orientations over the baseline (spontaneous activity during presentation of zero contrast display). This sequence was adopted since a small number of highly tuned cells which respond only to a single direction fail the t-test, but clearly pass the ANOVA (see for example Figure VI.8 left). Those cells were included in the further analysis, since their responses are highly tuned and also modulated with the phase of the stimulus.

Another more continuous classification of orientation tuning is an orientation selectivity index (OSI) based on a Fast Fourier Transform (Worgotter and Eysel, 1987).

Whereas the ANOVA only shows that there is modulation of the response with different stimuli, the OSI extracts the second harmonic and thus tests for a regular pattern of modulation with two peaks 180° out of phase. In order to be able to compare my results to those obtained from ferret kits at a similar age after artificial opening of the eye by Chapman and Stryker (1993), a modified version employed in that specific study was used. The OSI was obtained by first deducting the spontaneous rate from the average firing rate at each orientation. Then, the amplitude of the second harmonic (A2) of the tuning curve was extracted (Fast Fourier Transform, Excel, Version 7.0a for Windows 95) and normalized by division through itself and the average firing rate (A0):

OSI = (A2/(A0+A2)) *100 (Chapman and Stryker).

Chapman and Stryker (1993) argue, that this equation yields an OSI between 0 and 100. However, it only does so provided that there is a sufficient background of spontaneous activity (Figure VI.2), which is mostly absent for my units. But also their own results hardly ever seem to exceed OSI values greater than 70. Possible differences in the results obtained by Chapman and Stryker and my own could lie in the higher number of orientations they sample. It is conceivable, because I only sample eight different orientations that I could miss the peak of the tuned responses and the tuning curve would be broader. My OSI values would be generally lower. However this the opposite of what I find.

Traditionally, units where classified as non-orientated, orientation-biased if they showed a preference for one orientation but also responded to all other orientations, or orientation-tuned if they did not show any responses to the perpendicular orientation. To

Testing the OSI on simulated data.

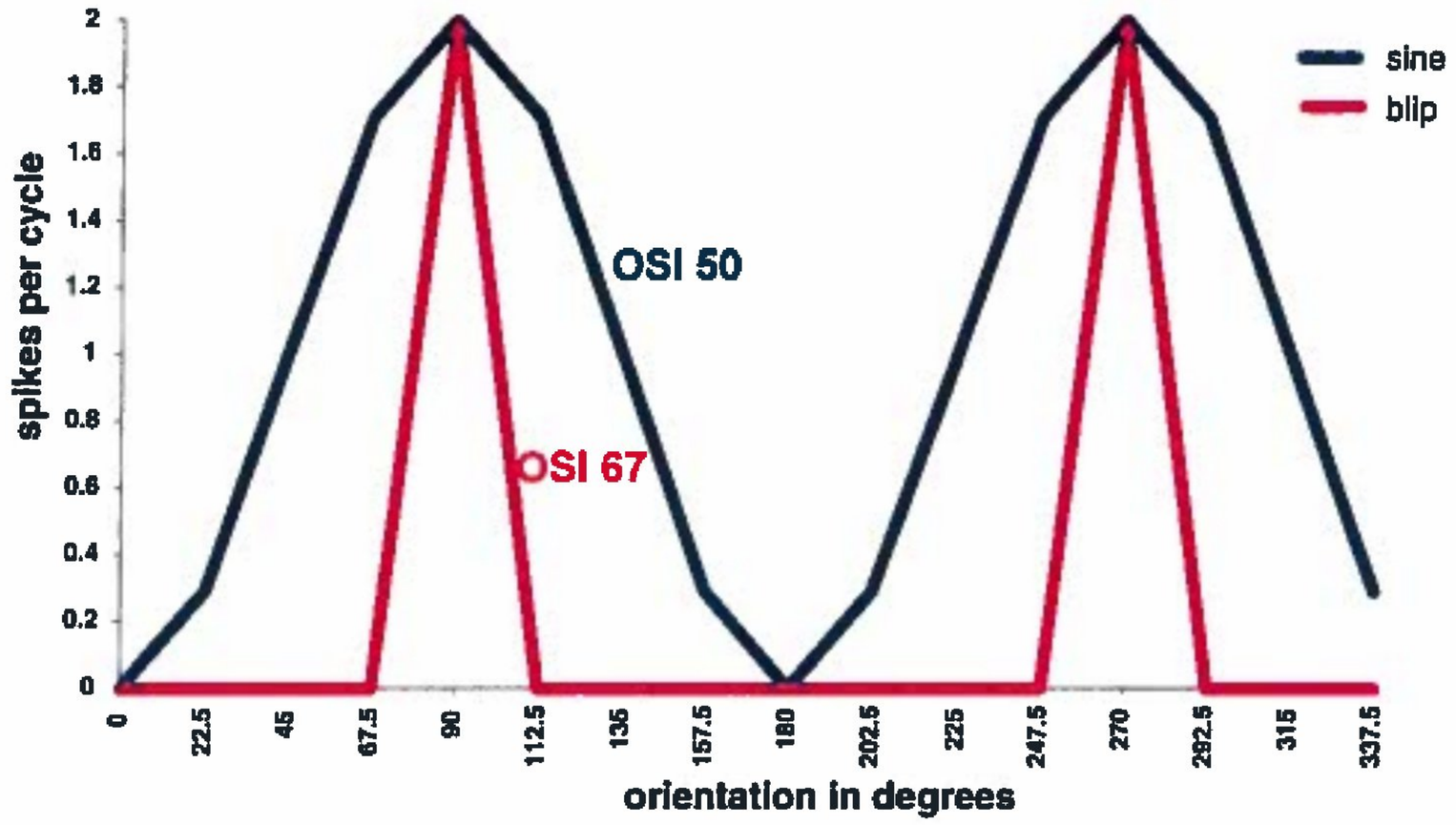


Figure VI.2. The range of the OSI was tested by calculating it for simulated tuning curves: a double-sinewave (sine) and a tight, peaky function (blip) either sampled with 8 or with 16 orientations.

A. If there is little spontaneous background as in my data, inhibition of the spontaneous activity as part of the tuning is impossible. The result is a relatively low maximum OSI value in both cases: an OSI of 50 for the sinewave function and an OSI of 67 for the tightest orientation curve possible with the given sampling points. A value of 100 - given as maximum for this function by Chapman and Stryker - cannot be achieved for this kind of data.

B. A value of 100 can be reached when, for example, there is some spontaneous background activity which is inhibited at the trough of the sinewave function. The average activity (A0) goes down to zero, when the spontaneous activity is deducted.

map OSI values onto this scheme is not straightforward, but as a rough guide cells could be classified as *orientation-biased* above an OSI of 25 and *orientation-tuned* from an OSI of 50. Chapman and Stryker (1993) group all cells with an OSI score of 25 and higher as *orientation-selective*. It is more difficult to distinguish between orientation-biased and orientation-tuned cells, but looking at the tuning curves of the individual units and Figure VI.2, at least neurons with an OSI of 50 and upwards should be classified as orientation-tuned.

In a similar way to the OSI a directionality index (DSI) was calculated based on the amplitude of the first harmonic (A1) of the Fast Fourier Transform (modified from Worgotter and Eysel, 1987):

$$DSI = (A1/(A0+A1)) *100.$$

Since the results for the recorded units span a similar range to the OSI (0-70), comparisons between the OSI and DSI distribution should be possible. But in both cases, it will be necessary to compare the results obtained with a representative sample of neurons from adult ferrets. Interestingly, highly directional units also achieve high OSI scores, but units which yield a high OSI value will not necessarily obtain a high DSI score .

3. Results

3.1 Neurons in primary visual cortex respond to light through the naturally closed eyelid.

Recordings were made from neurons in primary visual cortex in ferret kits between P21 and P24 with the naturally closed eyelids intact. Around this time, the earliest visual responses have been recorded after eyelids were artificially opened (Chapman and Stryker, 1993). Units were searched for and selected on the basis of whether they responded to a bright moving spot of light. Visual stimuli were usually presented to both eyes, only sometimes to one eye alone. Most units were recorded below 350 μm from pial surface into cortex - probably from layer IV and below. In total, I recorded from 62 units in 6 ferrets aged 21 to 24 days of which 38 units showed significant responses to the squarewave gratings (ANOVA or unpaired t-test, $p<0.05$, Figure VI.3). The majority of units has a very low average response rate around as little under 0.1 spike per cycle (spc) to about 3 spc; few neurons show higher average response rates of up to 7 spc (see also Figure VI.6). Many neurons appear to show phase-specificity: the pattern of action potentials modulates with the phase of the presented grating as can be revealed with a scatterplot of the timing of the spikes (Figure VI.3). However, in a typical cycle of 4 seconds discrete clusters of spikes occupy as much as a quarter of the cycle, which might indicate a somewhat sluggish response with long latencies. The scatterplot also reveals a high failure rate with many presentations of the stimulus for which no action potential was fired. These features are roughly comparable to what was observed in early recordings in

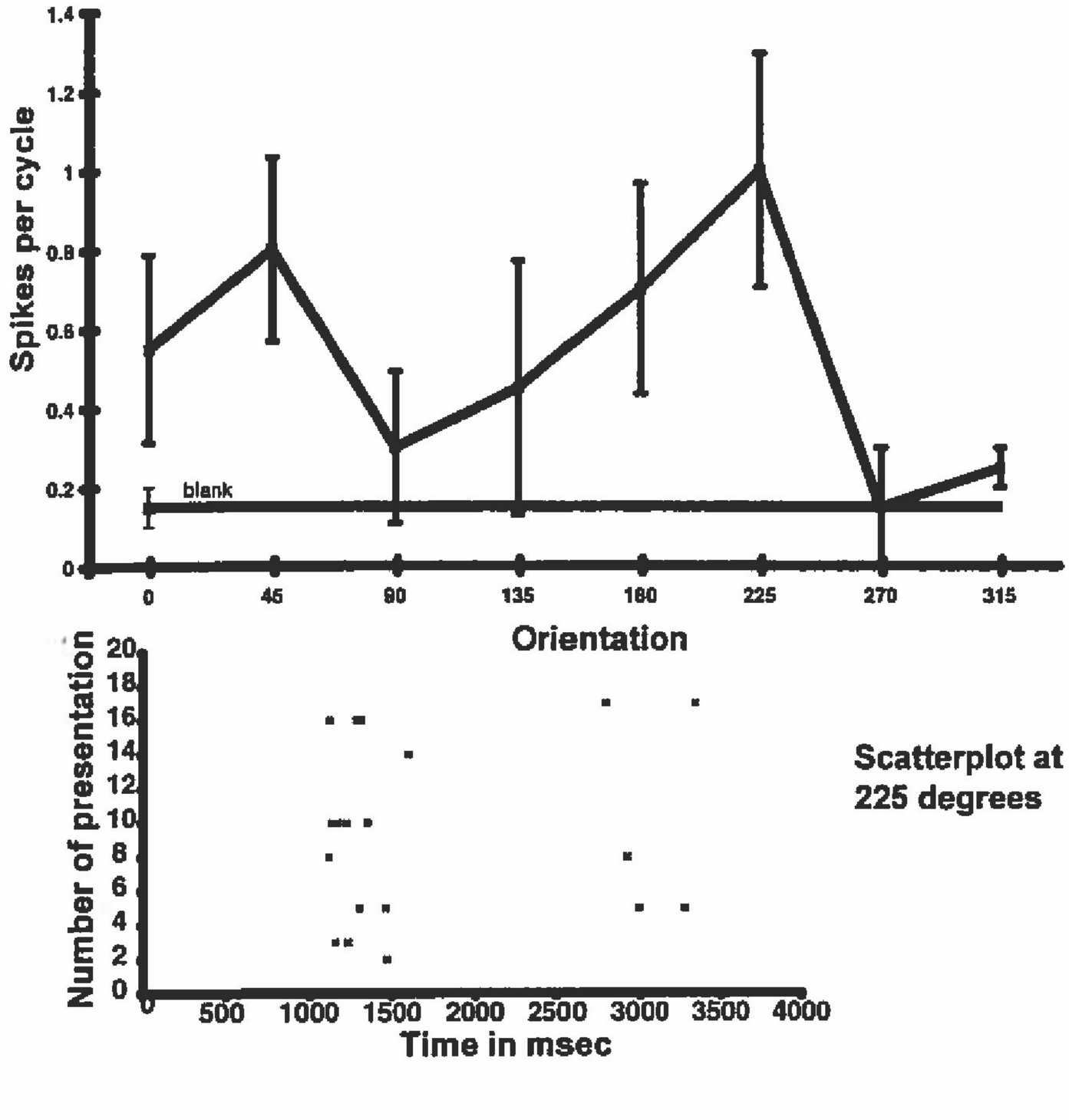
Figure VI.3. This figure gives two examples of tuning curves which scored differently with the two statistical tests used. The t-test looks at the difference between the background activity and visual stimulation (responses across all orientations are pooled), whereas the one-way ANOVA establishes if there is a significant change in response rate with orientation. The error bars represent the standard error of the mean.

A. The first unit fails the ANOVA-test, but shows increased activity with visual stimulation. The tuning curve itself suggests some orientation-bias, but the variance in the response for specific stimuli probably causes failure on the ANOVA-test. The scatterplot for the preferred direction shows phase-locking of the response, but there is also a high failure rate for individual presentations of the stimulus.

B. The unit in this figure shows both a general increased response with visual stimulation and modulation of the response with different orientations. The scatterplot shows action potentials in response to larger portions of the cycle, but responses still cluster into two areas.

This figure underlines one of the major problems with the orientation-selectivity index (OSI). Information about variance of responses is discarded and only the shape of the tuning curve itself is evaluated. Thus, both tuning curves give similar OSI values.

A. Failed ANOVA, passed t-test



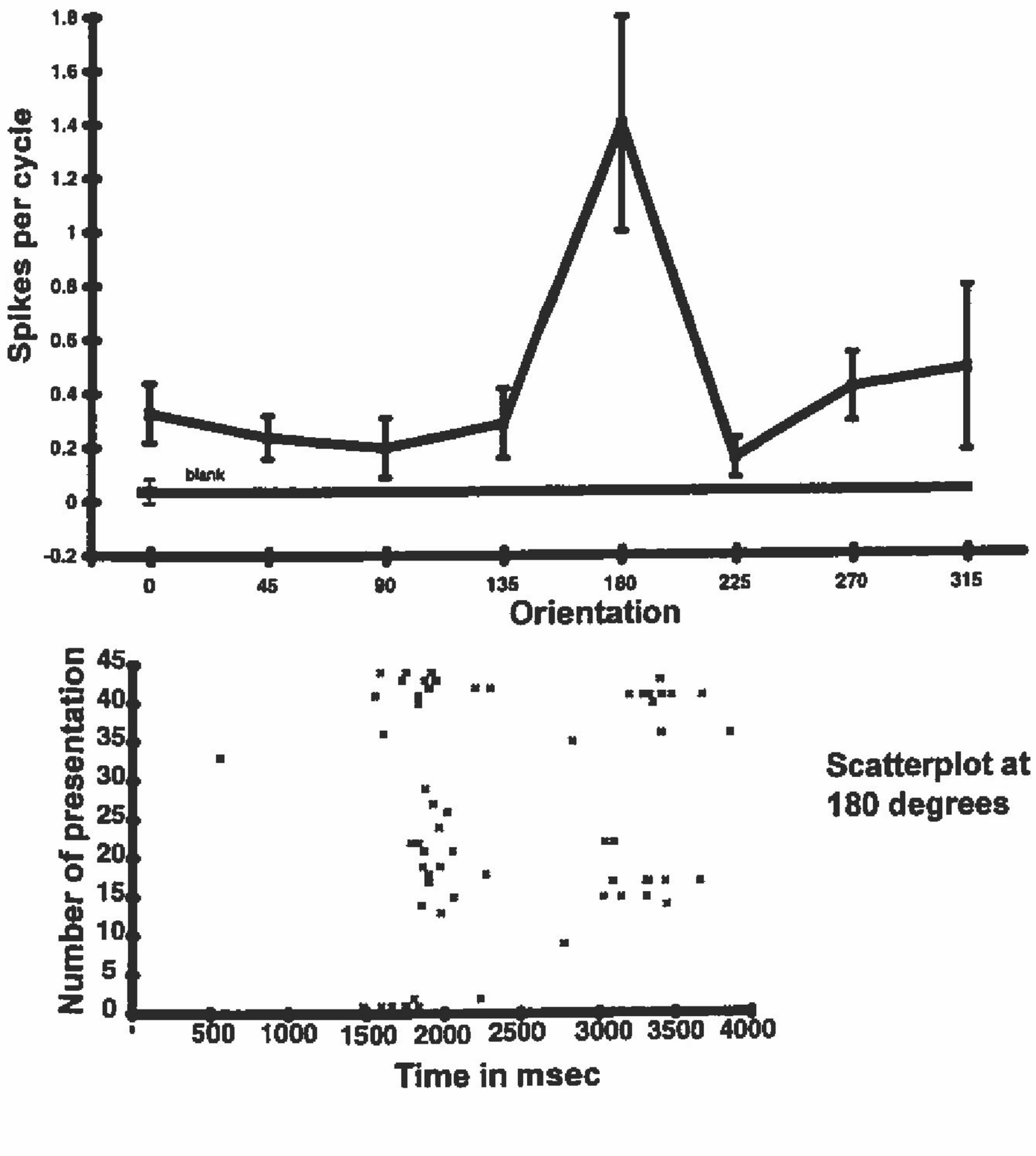
Orientation tuning at P23
Kf5-2,cell 10, depth 420

ANOVA p < 0.18
t-test p < 0.0001

OSI = 47

Scatterplot at 225 degrees

B. Passed ANOVA, passed t-test.



Orientation tuning at P21
KF5-1, cell 1B, depth 400

ANOVA p < 0.001
t-test p < 0.00006

OSI = 42

Scatterplot at 180 degrees

Figure VI.3

kittens previously (Huttenlocher, 1967; Blakemore and Van Sluyters, 1975).

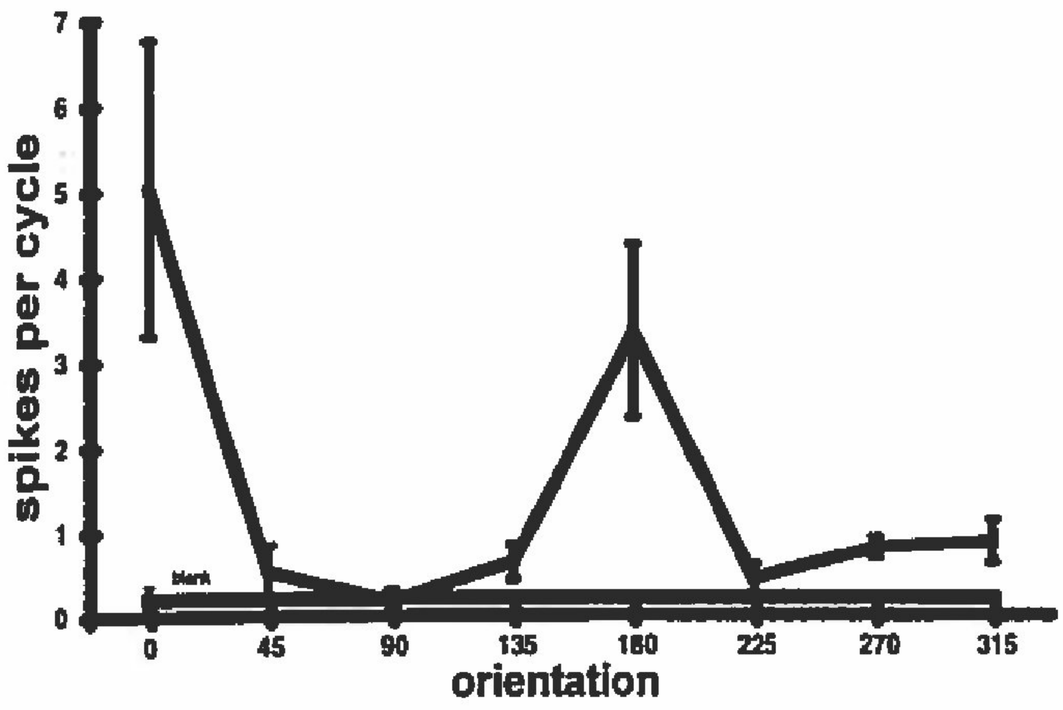
These results show a differentiated response of the recorded units to the visual stimuli presented. But little can deduced from the data above about what patterning the tuning has. The following sections look for regular modulation in the tuning curve, such as displayed by orientation-biased or -tuned cells or directional cells.

3.2 At least a third of the visually-responsive neurons respond differentially to orientation.

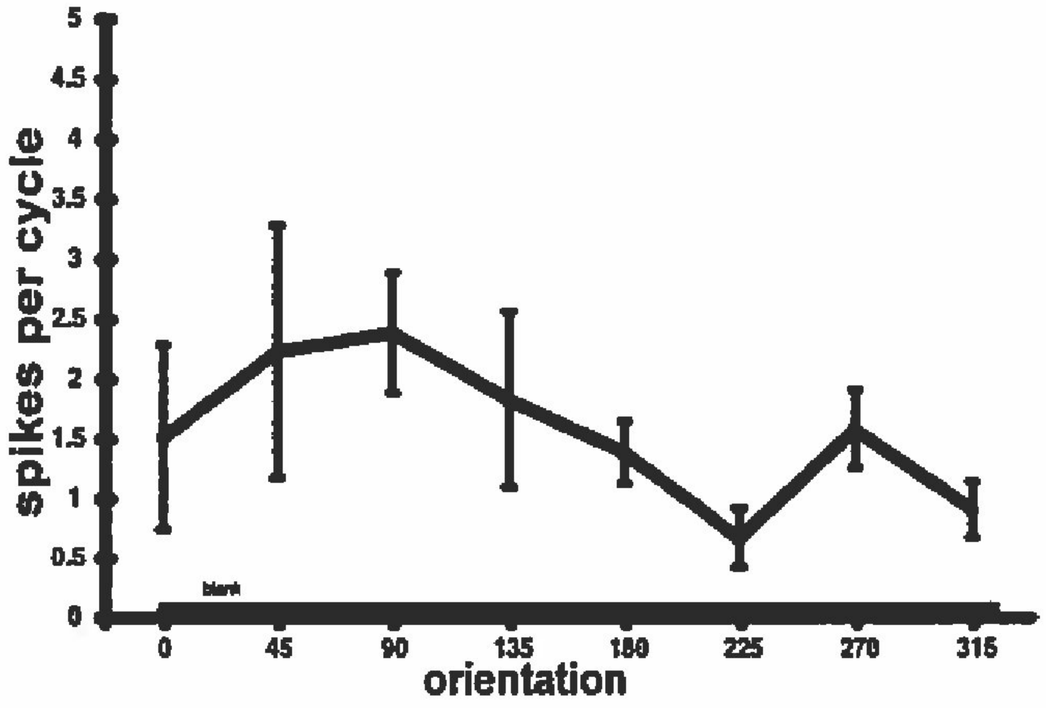
Amongst the 38 neurons, more than a third, 13, show a significant variation in spike rate per cycle across different orientations (one-way ANOVA, $p < 0.05$). This is a very stringent test which allows little variance in the spike rate for any given direction. Even so, a third of all recorded cells pass the ANOVA. More recently, instead of using rigid categories, studies tended to look at the distribution of cells on a continuous orientation selectivity index (OSI : after Worgotter and Eysel, 1987; Chapman and Stryker, 1993).

(i) The OSI. This index assesses the weight of the second harmonic if the tuning curve is decomposed by a Fourier analysis. Figure VI.4A shows a high scoring unit: the tuning curve has two narrow peaks 180° out of phase. On the right is a unit that scores low on the OSI (Figure VI.4B). The peak response is very broad around 90° and not really matched by a similar peak at 270°. Despite the less modulated scatterplot, it seems unlikely that the neuron on the right is simply badly isolated, since the scatterplot for the small peak shows fairly tight modulation of the pattern of spikes at the peak response and there is also very little spontaneous activity. However, the scatterplots indicate a shift in eye-position

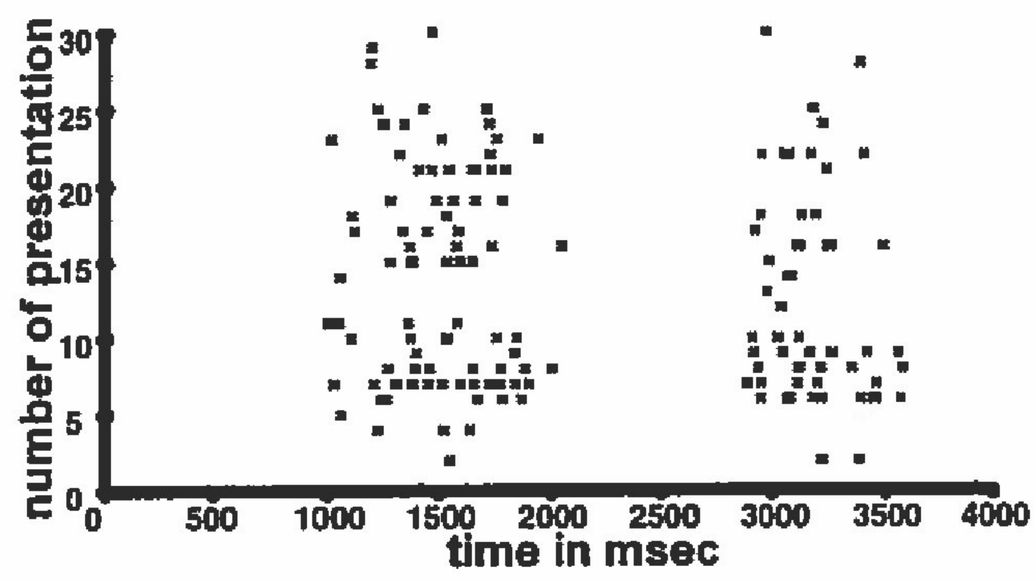
A. Orientation tuning at P21 - OSI 60



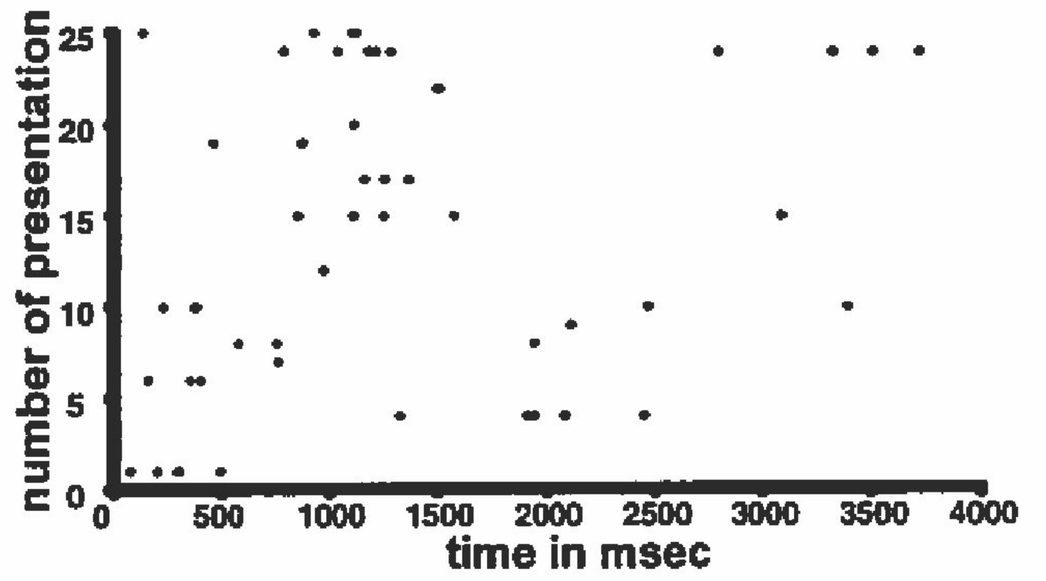
B. Orientation tuning at P23 - OSI 15



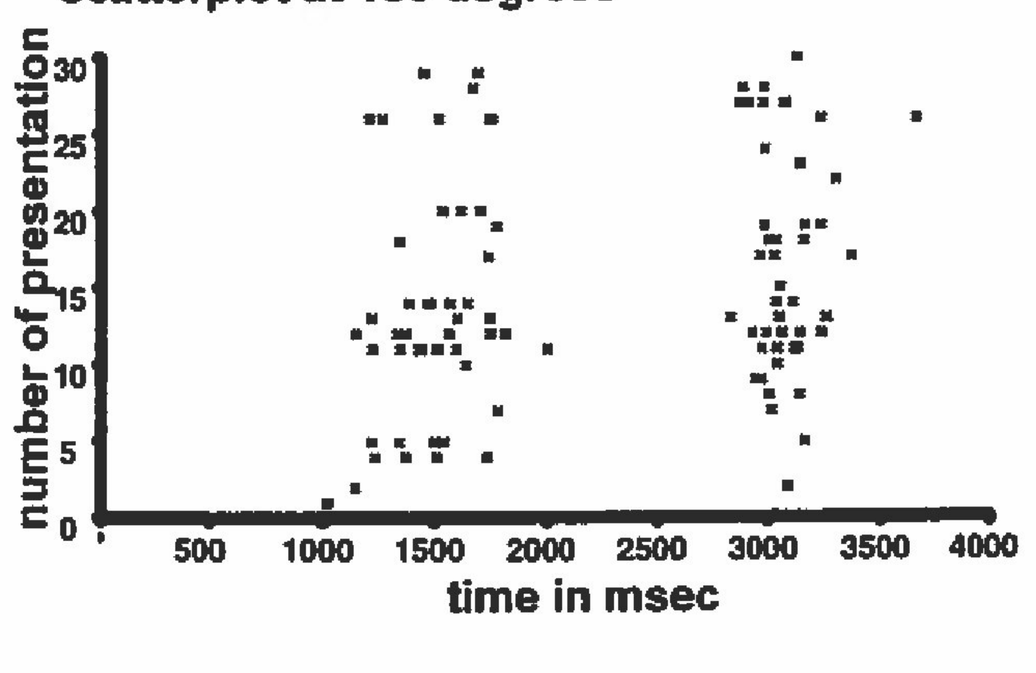
Scatterplot at 0 degrees



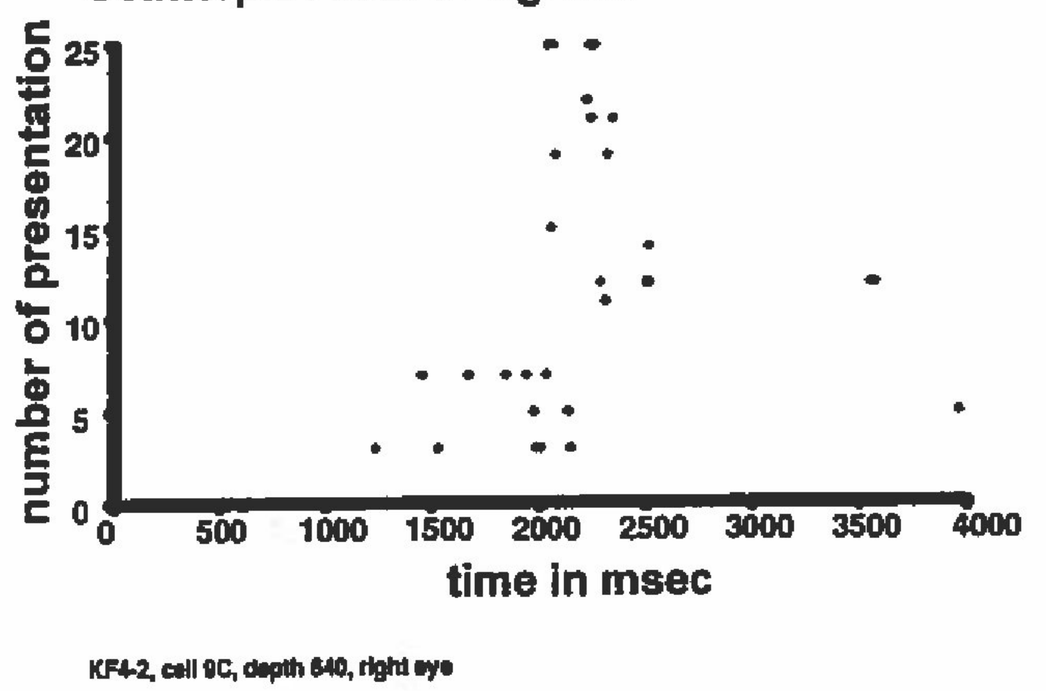
Scatterplot at 90 degrees



Scatterplot at 180 degrees



Scatterplot at 270 degrees



KF5-1, cell 8, depth 740

KF4-2, cell 9C, depth 640, right eye

Figure VI.4. This figure shows the response of units from the opposite ends of the OSI spectrum.

A. The unit on the left is highly tuned to horizontal gratings, it scores 60/100 on the OSI. The peak responses are 180 degrees apart and narrowly tuned. The changes in response to different orientations are highly significant, too (one-way ANOVA, $p < 0.0001$). Furthermore, the scatterplots show the responses of the neuron are also modulated with the phase of the grating.

B. The unit on the right appears less well tuned and scores with 15/100 rather low on the OSI. The peak at 90 degrees is very broad and is not matched by a similar response 180 degrees out of phase. Also, the scatterplots reveal - at least at 90 degrees - little modulation of the response. This unit fails the ANOVA.

Error bars represent the standard error of the mean.

around the tenth presentation of the grating. Although the scatterplot do not show changes in firing associated with the possible shift, I can not exclude that this affected the tuning.

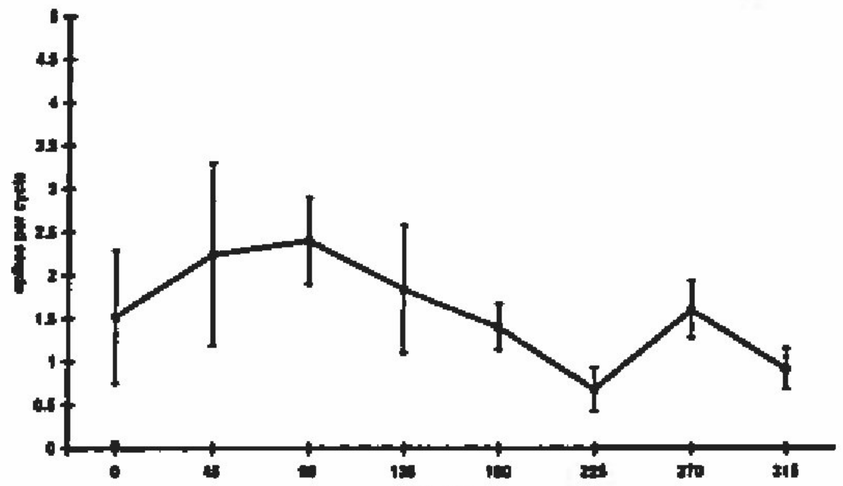
The whole population of units cover a wide range on the OSI (Figure VI.5). Some units are included more than once if they have been tested through both eyes, the left eye and the right eye separately, since different OSI scores can be found in tuning curves obtained through either eyes. The examples around the central histogram show tuning curves from different parts of the distribution. Units with an OSI of 25 and higher are classified by Chapman and Stryker (1993) as orientation-selective - more than half of the recorded units fall into this category. This would be also the group which would comprise orientation-biased and orientation-tuned cells. Not surprisingly, most of the units that pass the ANOVA-test cluster around the upper end of the histogram. About 42 % in my sample of 38 units have an OSI value of 50 (29% of the observations in Figure VI.5) and higher and thus, should be classified as orientation-tuned. A major problem with the OSI is that it discards any information about variance at each point of the tuning curve and only assesses the shape of the tuning curve itself. Thus, it would be best to consider the results from the OSI in conjunction with the ANOVA-test, which compares the variances. That still leaves about third of units in my sample as orientation-selective.

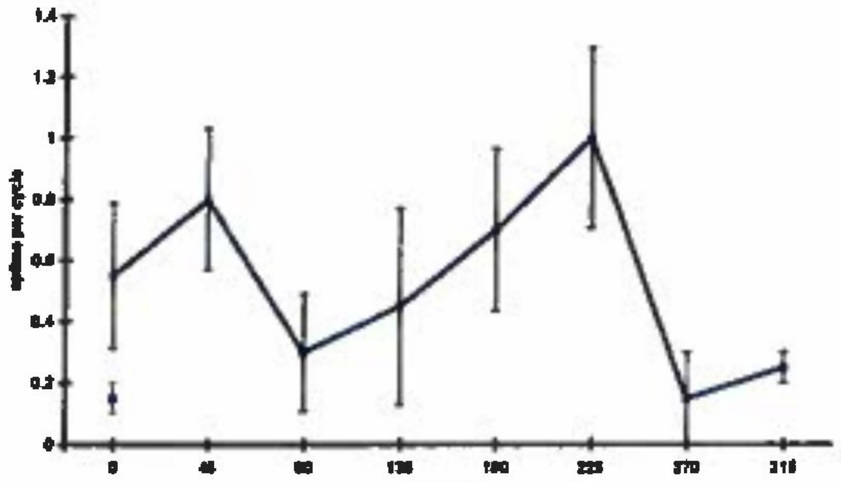
Does the firing rate affect orientation-tuning? If, for example, units with a low OSI all show higher response rates than units with a high OSI score, this might suggest that bad isolation (i.e. recordings from more than one neuron) was the reason for low OSI scores. However, most units with a low OSI score fall into the normal range of average response rates to visual stimuli as well as the normal range of peak responses (Figure VI.6). The

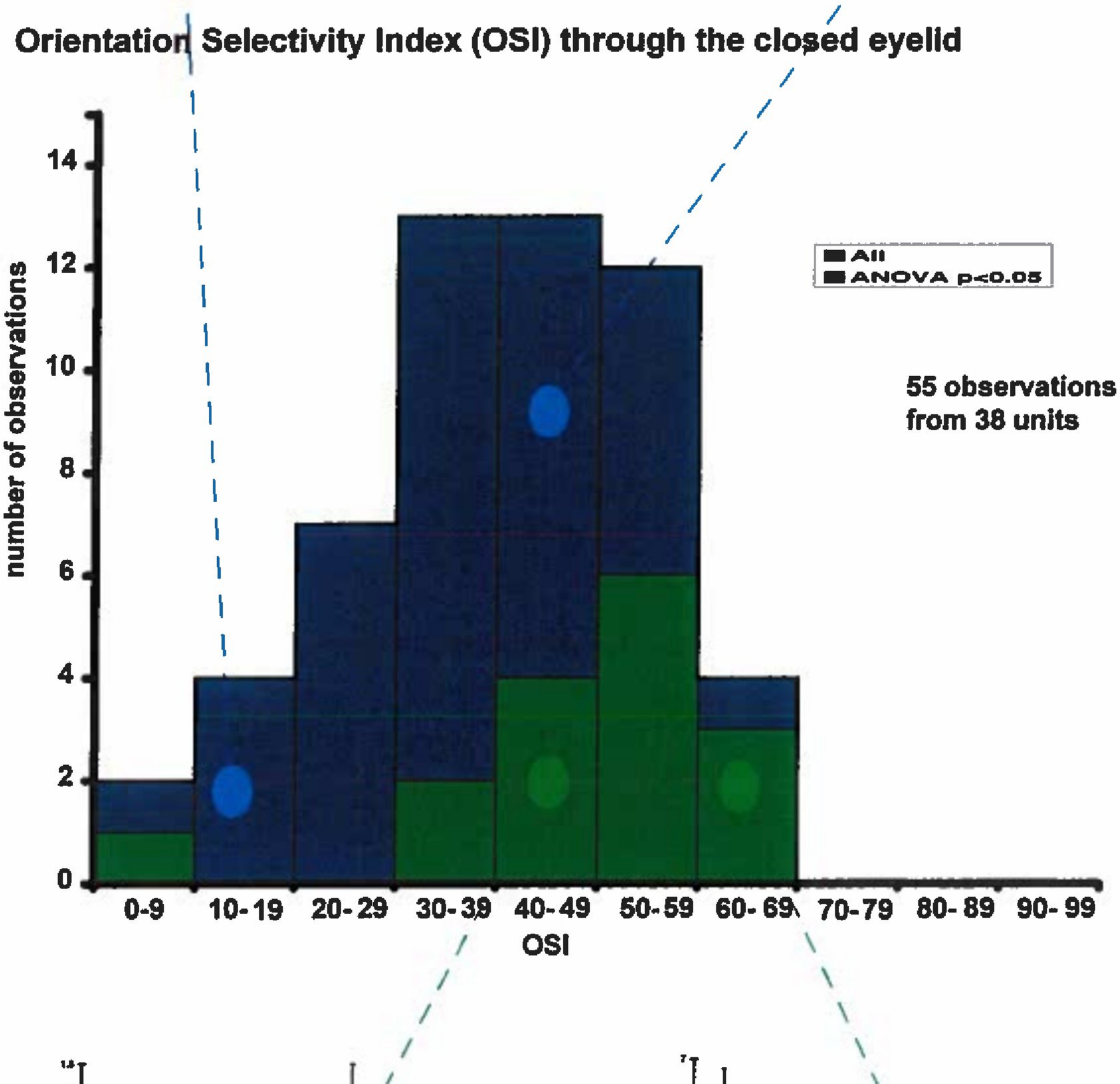
Figure VI.5. The histogram shows the distribution of recorded units along the OSI (some units are represented more than once if they have been analysed separately through the two eyes). In total 55 observations from 38 cells are represented. The blue bars comprise all units that showed a significant response to visual stimulation, whereas the green bars represent the subset which showed significant changes with orientation (ANOVA, $p < 0.05$). Single units passing the ANOVA cluster in the upper half of the distribution showing some congruence of the two measures. Around the histogram there are examples of tuning curves which score differentially on the OSI (error bars represent the standard error of the mean).

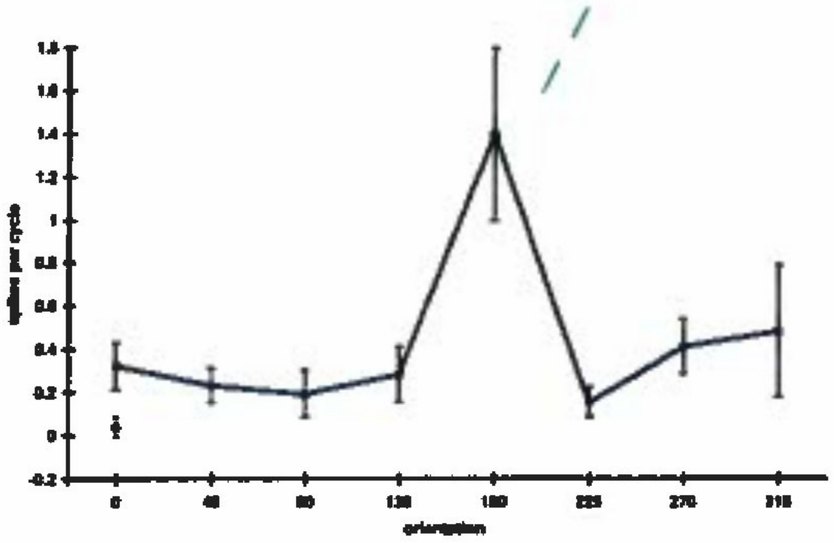
Chapman and Stryker (1993) use a value of 25 and higher on the scale to select units as orientation-biased or tuned. For my data-set this would mean more than 50% of the cells recorded would fall into this category - more than double the percentage reported in their study.

However, the examples of tuning curves in the top right and bottom left hand corner demonstrate a basic problem of the OSI. It is good for assessing the shape of the tuning curve, but in doing so it discards the variance of the individual responses.






Orientation Selectivity Index (OSI) through the closed eyelid
number of observations
14
12
10
8
6
4
2
0
All
ANOVA p<0.05
55 observations
from 38 units
0-9
10-19
20-29
30-39
40-49
50-59
60-69
70-79
80-89
90-99
OSI



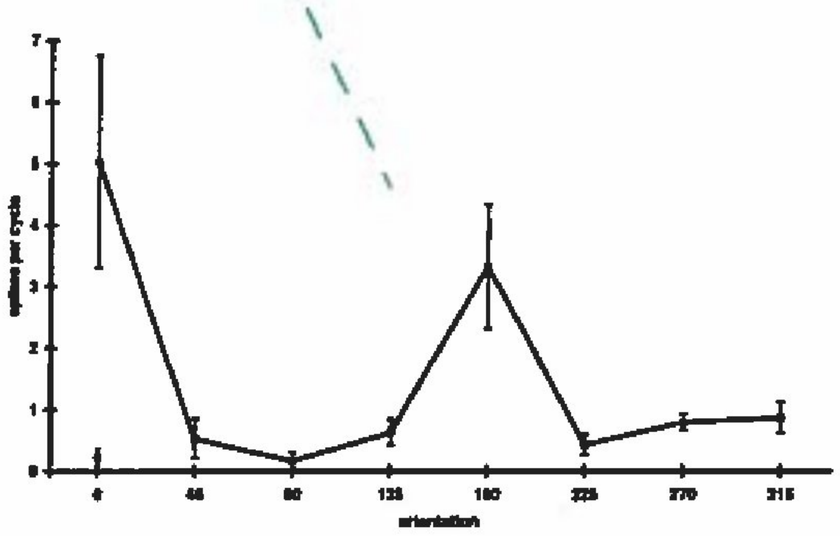
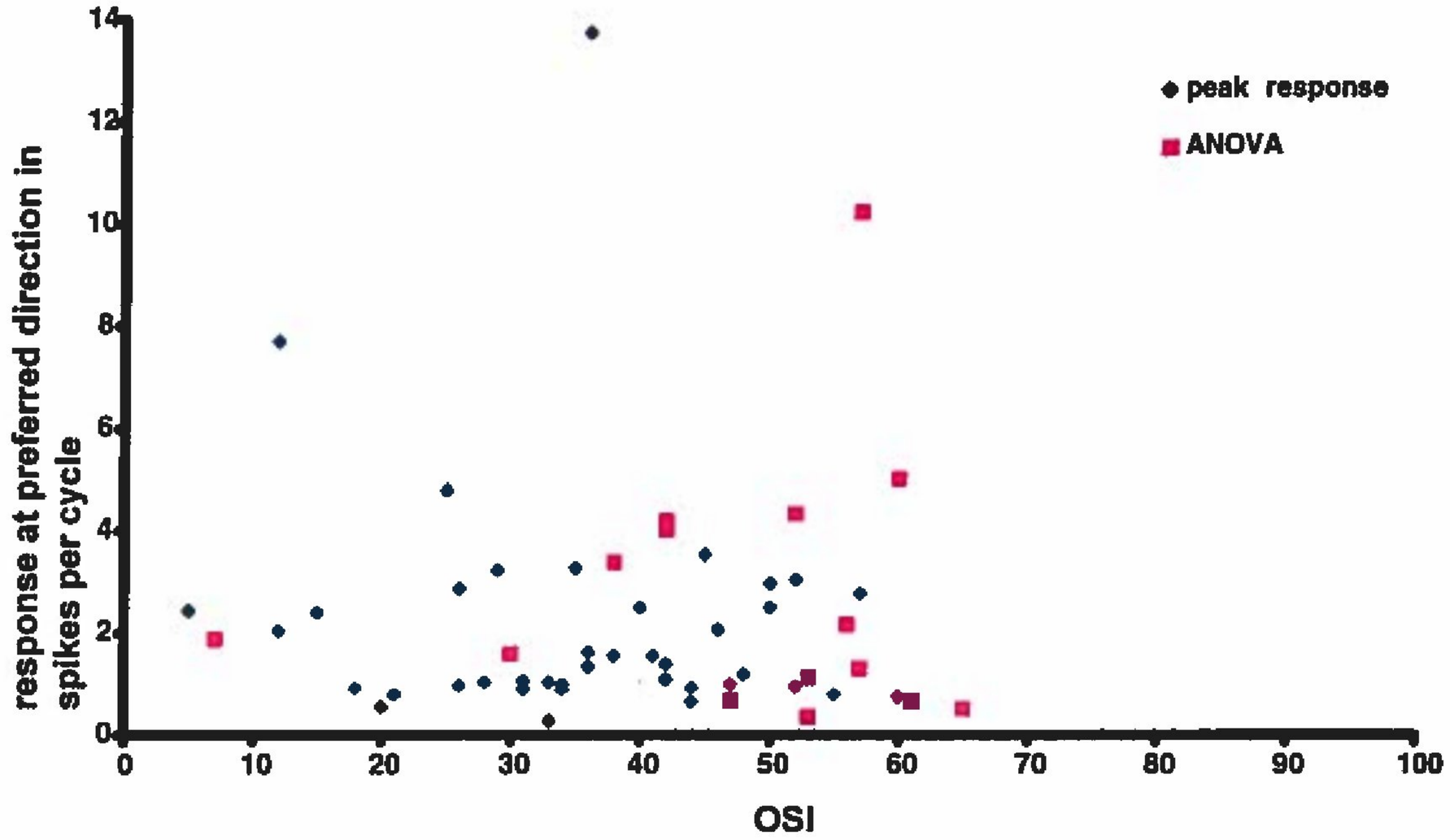


Figure VI.5

A. OSI versus response at preferred direction



B. OSI versus average firing rate

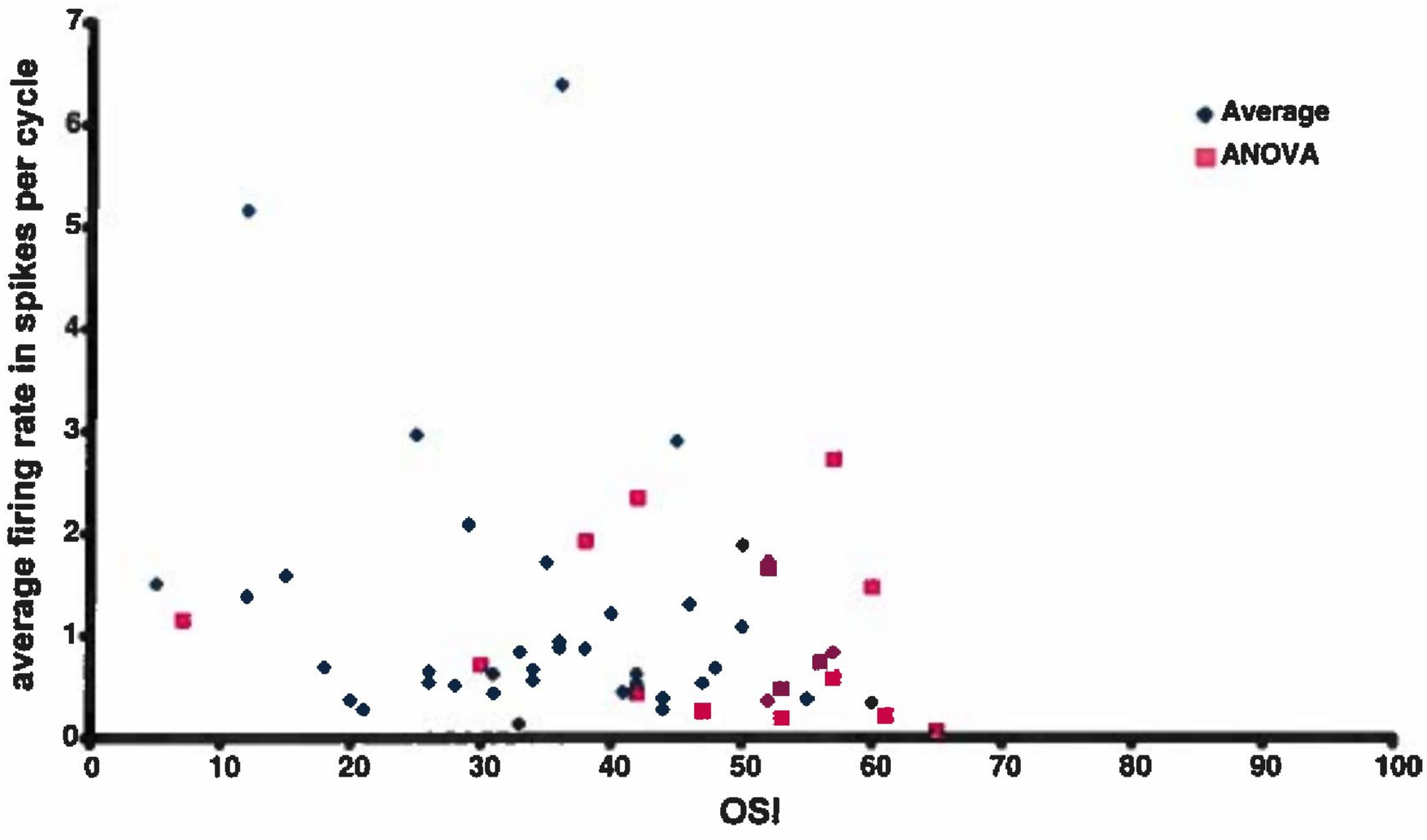


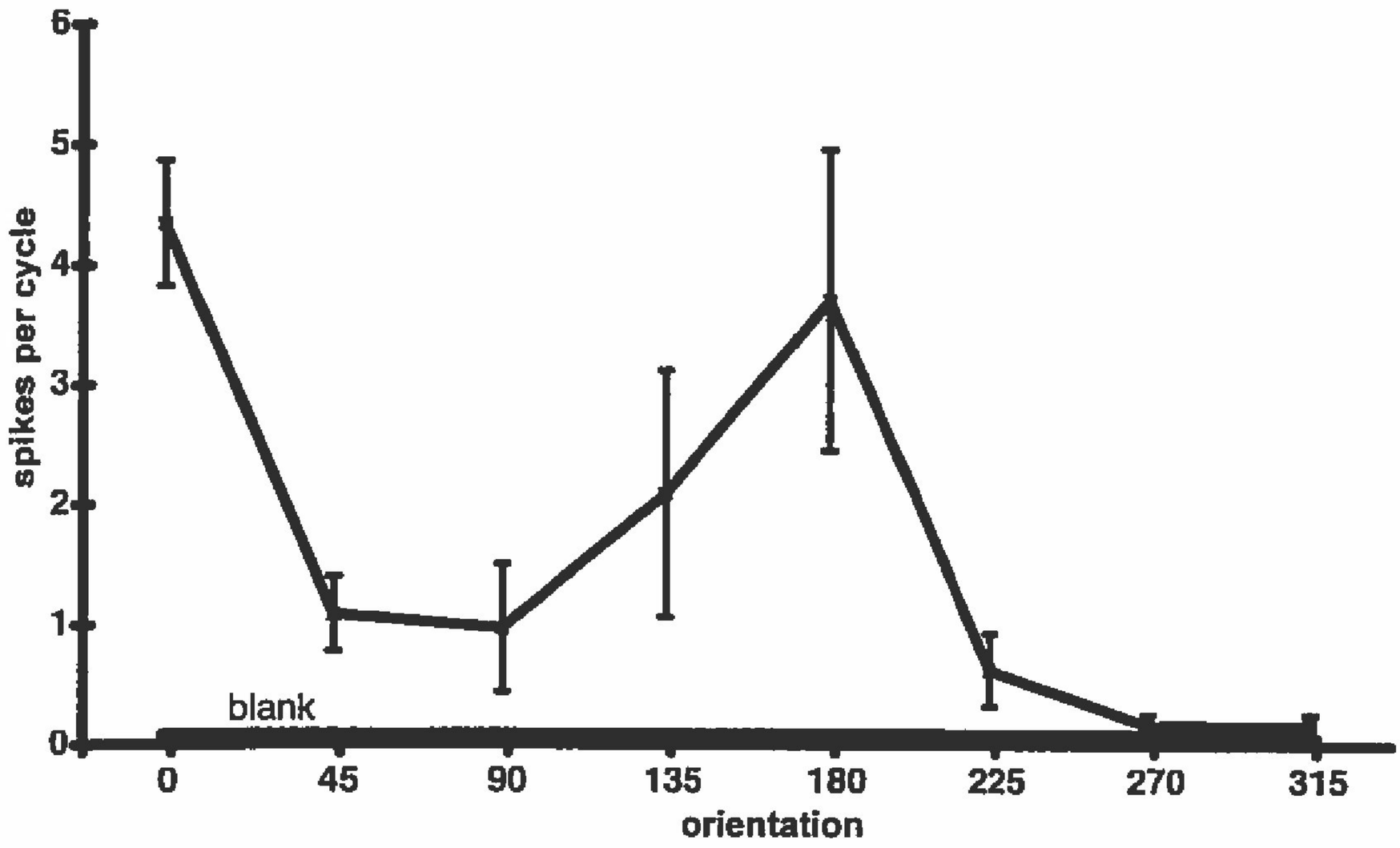
Figure VI.6. The degree of orientation-selectivity of a unit can be influenced by its level of activity or by its isolation. To investigate if there is any such relationship, the score on the OSI is compared with the spike rate at the peak response **(A)** as well as with average activity across all stimuli presented **(B)**. Most units over a wide range of OSI values show very low average and peak firing rates. At the lowest OSI values, the few units recorded do not show the lowest spike rates. However, they fall into the normal range of responses. Units passing the ANOVA test have similar response rates to neurons that are less well tuned to orientation.

The level of activity of a unit seems not to influence its tuning. Some of the neurons at the low end of the OSI might be less well isolated - but their spike rates still fall into the range of the rest of the data.

example in Figure VI.4B also shows that low OSI scores are not necessarily connected to a high background of spontaneous activity. Response rates at these ages are generally very low, apart from few exceptions peak responses lie below 4 spikes per cycle (spc). There are no obvious correlations between OSI score or ANOVA result and level of activity of a unit.

(ii) Is the orientation-tuning really neuronal? It is not quite clear if the selective responses to gratings of different orientations stem from neuronal orientation-tuning or might be influenced by optical filtering. The distribution of the tuning curves across the different orientations shows a bias towards horizontals. This could have multiple reasons. It could lie in the morphology of the closed eyelid, or the immature optics of the eye (see discussion). Another possibility is that most of the neurons were recorded when the stimulus was presented to both eyes. In this case, only a horizontal bar might activate both eyes at the same time and therefore, preferentially stimulate binocular neurons in primary visual cortex. However, in some experiments, the same, horizontally-tuned cell was tested through both eyes first and then with one eye covered by a black patch. In these cases, the neurons preserved their orientation-preference (Figure VI.7).

In one experiment, opening the eyelid while recording from a single cell led to a shift (45 degrees) of one peak in the tuning curve. This could indicate some filtering by the eyelid. However, this is a very difficult experiment to do and this is only an isolated observation. It is possible that the eye-position shifted when the eye was opened. More experiments like this are needed to draw firm conclusions. But if the neurons in cortex were only responding to the filtered light let through by the eyelid, directional responses



Orientation tuning at P21
KF5-1, cell 7, depth 740

Figure VI.7. A single unit in area 17 was tested for orientation-selectivity through the closed eyelids with either both eyes not additionally covered (A.) or with the right eye covered (B.). If the horizontal tuning seen is due to stimulation of both eyes by a horizontal grating, it would be expected to disappear when the unit is examined with one eye covered. However, in both cases the neuron shows strong tuning to horizontal gratings.
Error bars depict the standard error of the mean.

should be mostly absent, since only the change in level of luminance but not its direction should matter. However, directional responses are described in the following section.

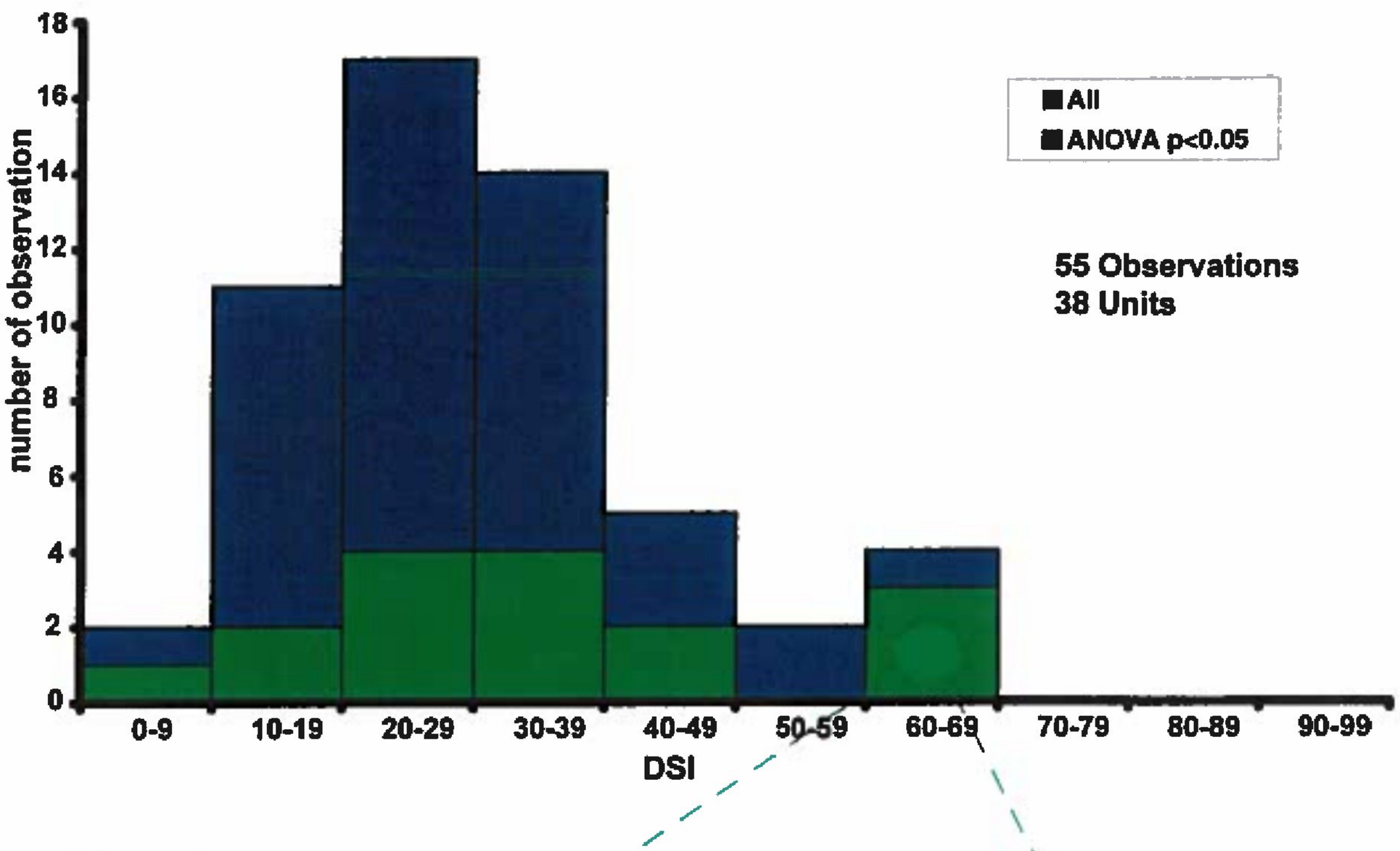
3.3 Directionality of responses

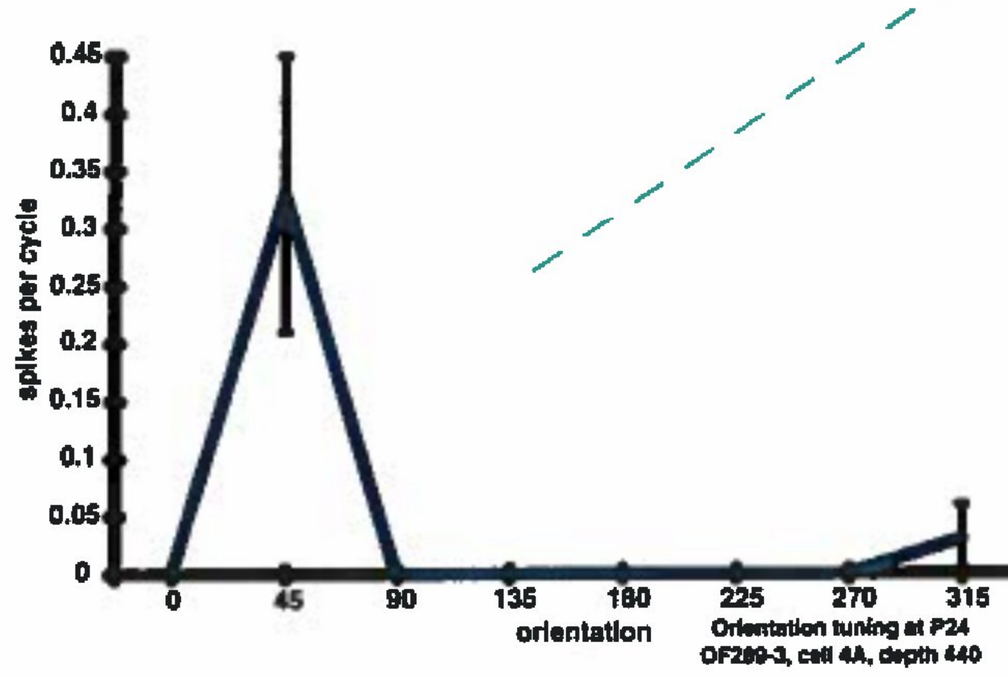
Another regular pattern of tuning in primary visual cortex is directionality of responses. It is not clear if directionality constitutes only a specific case of orientation-tuning or if it is a completely different mechanism. To test if directional responses are present as early as orientation-selective cells, the DSI based on the first harmonic was calculated for all units used in the previous section. Figure VI.8 shows that responses are distributed over a similar range than for the OSI (0-70). However, the bulk of the units lies in the lower third of the scale in contrast to the OSI where the bulk of the units cluster higher up on the scale. It appears that the second harmonic is a stronger component of most tuning curves than the first harmonic. This suggests, direction selectivity might be less developed than orientation-selectivity. However, the examples of clearly directional units underneath the summary graph show that there are only a few units highly tuned for the direction of the stimulus. It is possible that directionality arises later in area 17 than orientation-selectivity. But as for orientation-tuning, the results need to be compared to data from adult ferrets. The relationship of orientation-selectivity to direction-selectivity needs to be assessed in the adult with comparable quantitative measures.

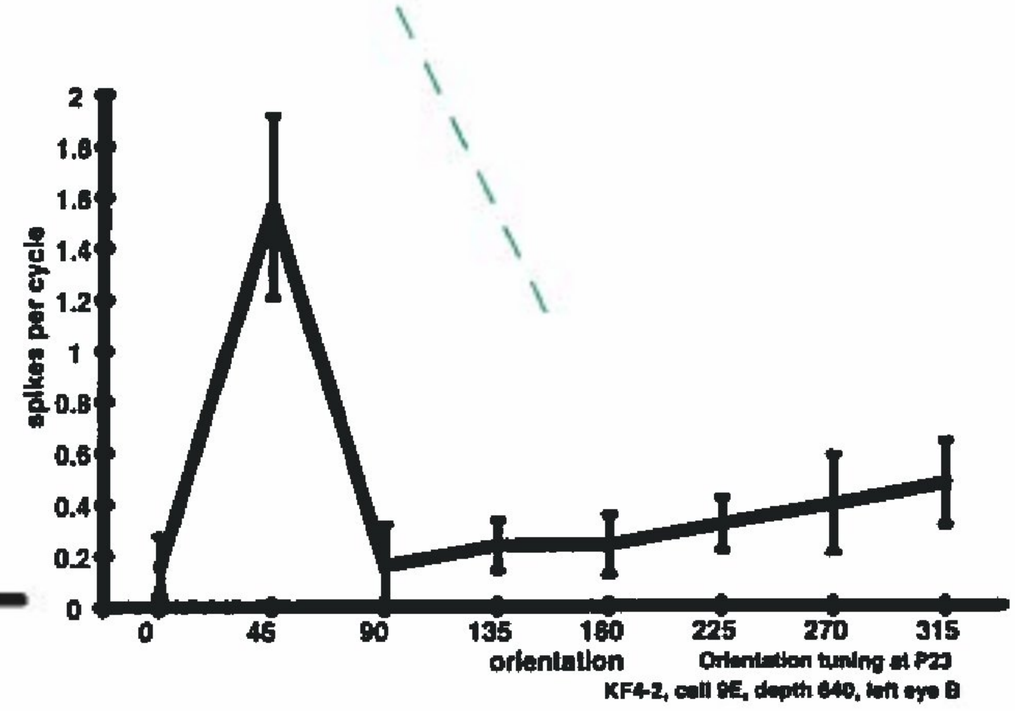
Figure VI.8 The histogram shows the distribution of recorded units along the DSI (some units are represented more than once if they were recorded through different eyes). The blue bars (including the green bars) contain all units that passed t-test or ANOVA, whereas the green bars alone give the responses which showed significant changes with orientation (ANOVA, $p < 0.05$). Comparing this histogram with the distribution along the OSI, overall the recorded units score lower, it appears that units are less directional. Also, single units passing the ANOVA, do not cluster at the upper end of the scale.

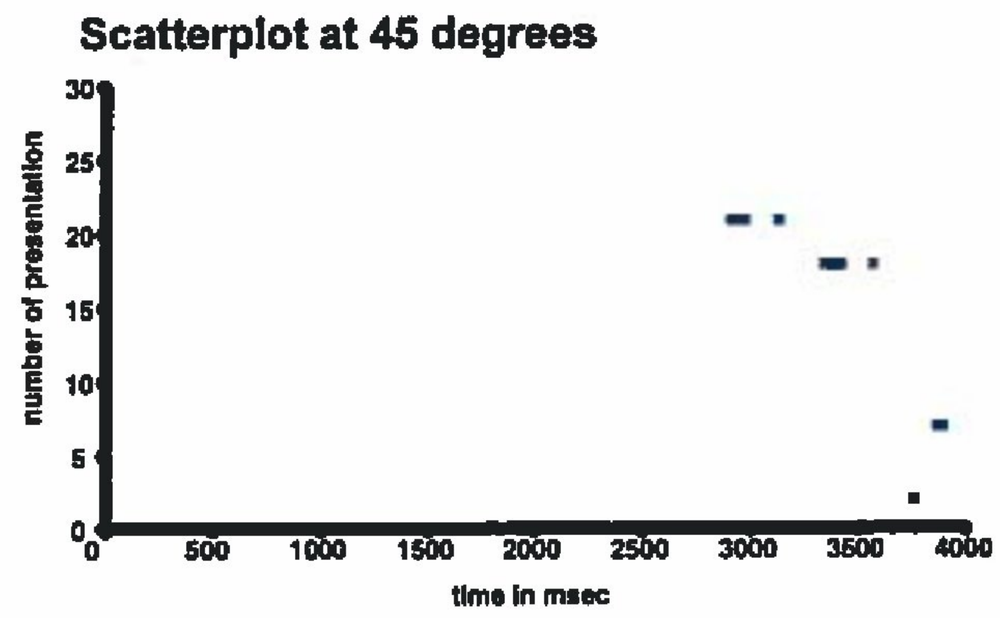
At the bottom of the graph are two examples of two highly directional cells from different animals (the error bars represent the standard error of the mean). The one on the left also shows phase-locking at the preferred direction and a high failure rate of the response. The unit on the right has a higher firing rate at the preferred direction but the action potentials are more widely scattered along the cycle of the grating. Highly directional cells can be found as early as orientation-tuned cells but are scarcer than orientation-tuned neurons.

Direction selectivity index (DSI) through the closed eyelids









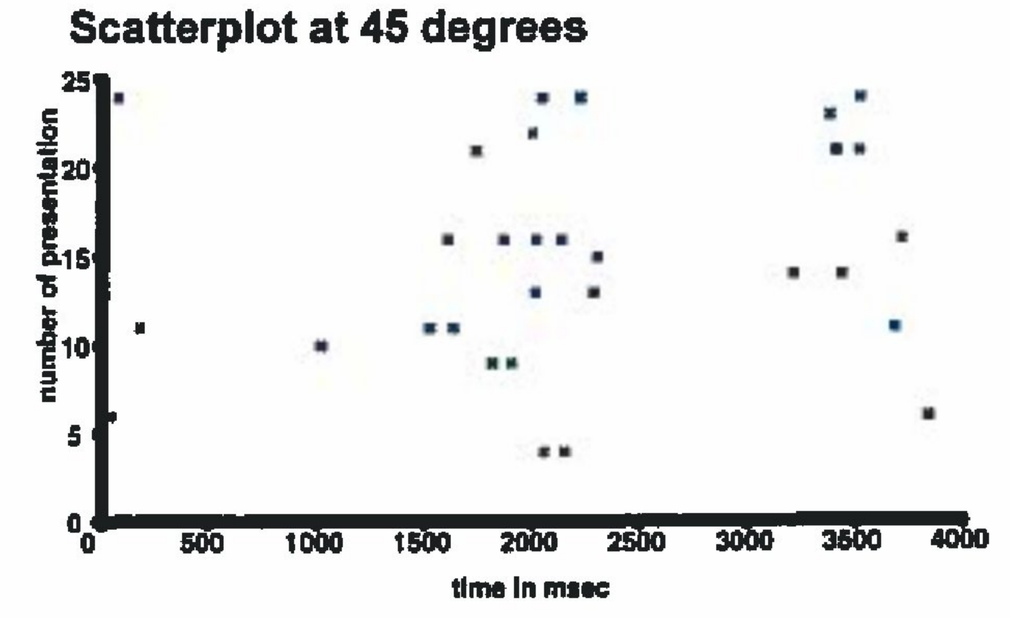


Figure VI.8

4. Discussion

Cortical neurons in area 17 of ferret kits can be driven by light *through the closed eyelids* as early as P21, about one and a half weeks before eye-opening. Moreover at the ages P21-P24, at least a third of all the units which responded to squarewave gratings show significant orientation-tuning with the high contrast stimuli used in this study. Furthermore, the spiking of the units is often modulated by the phase of the displayed grating.

4.1 The nature of the responses.

There is a significant elevation of the spike rate correlated to the visual stimuli and the response of neurons in striate cortex appears to be modulated by the orientation of the presented grating. Although all the analytical tools have their individual weaknesses, eg. the ANOVA does not take the periodicity of orientation tuning into account and the OSI discards the variance of the response to individual directions, the tests taken together show that a group of neurons exhibit orientation-selective responses early in development to stimuli presented through the unopened eyelids. This is also supported by the modulation of the spiking along one cycle of the stimulus: the response varies with the phase of the grating. Furthermore, neurons can also be found which show a directional response.

As far as comparisons are possible, the general features of the kind of responses, the sluggishness, long latencies, high failure rate and the orientation-selectivity appear similar to studies in the kitten around eye-opening (Huttenlocher, 1967; Blakemore and

Van Sluyters, 1975; Fregnac and Imbert, 1984). However, there seem to be some discrepancies with the study most closely associated to mine. Chapman and Stryker (1993) appear to find in visual cortex of ferret kits with artificially opened eyelids a similar degree of orientation-selectivity. They suggest 25% of units in their sample are orientation-selective when the eyelids are open. This result is probably also expressed in percent of visually-responsive units, but this is not entirely clear in their study. However, they only used the criterion of the OSI (OSI> 25), on which overall their neurons score much lower at the same age. The data-set in this study assessed by the same criterion would yield a result of about 50% or more - and this while the eyelids are still closed. There are multiple possible reasons for this. It is difficult to compare percentages of orientation-selectivity, because of different sampling and selection strategies. For example, Blakemore and Van Sluyters (1975) also arrive at 25% orientation-tuned units in visual cortex at eye-opening in the kitten, but these are 25% of the spontaneously active neurons. However, it appears that Chapman and Stryker also selected visually-responsive neurons (their paper is not entirely clear on this point). And the fact remains that overall, the units in my sample score higher on the OSI through the closed eyelid. The closed eyelid could have introduced some optical tuning (see next section). Another reason could also lie in the less stable set-up (no paralysis; intermittent shots of anaesthetic) Chapman and Stryker are using. In my experience, only if the animal is completely immobilised and the vital signs are stable, is it possible to record single units from area 17 at this age. Incidentally, their average response rates appear much higher than mine. This could be due to a difference in depth of anaesthesia. However, pentobarbitone sodium is known for causing cortical depression

of activity. In fact, the anaesthetic regime used in this study was chosen over pentobarbitone because of problems with the isolation of single units. The higher spike rates of Chapman and Stryker's data might rather suggest poor isolation of units. This in turn would also explain their low OSI scores.

4.2 The origin of the oriented response.

The question remains whether the tuning of the recorded responses represents neuronal tuning of cortical cells or whether it is an artefact which should rather be attributed to optical filtering by eyelids and the immature eye itself. Some bias towards a horizontal orientation introduced by the morphology of the closed eyelids and the early optics cannot be excluded. But, despite a general preponderance of horizontally tuned units in my sample, cells selective to all different orientations can be found, albeit verticals are represented more weakly. In the developing kitten visual cortex, experiments have shown that different orientations are also not equally represented when tested in the first few weeks after eye-opening, but in this case oblique gratings lose out against horizontals and verticals (Thompson et al., 1983; Blakemore and Van Sluyters, 1975). The phase modulation of the spikes along the grating suggests also a neuronal origin. Recordings from dLGN with closed and opened eyelids should resolve the question of whether the closed eyelids and the optics of the eye introduce any orientation filtering of visual input. Since geniculate neurons are not orientation-selective in the adult, any orientation-tuning detected should be attributed to optical filtering.

The structure of the receptive field for the cortical neurons should also be

investigated through the closed eyelid and compared to the structure as seen through the opened eyelid. This could help to clarify the nature of the orientation-selectivity found.

4.3 Development of orientation- and direction-tuning.

A high percentage of orientation-tuned cells was found in visual cortex even at the earliest recordings, assuming the orientation-selectivity is neuronal in nature. The ANOVA-test suggests that a third of the visually-responsive units are orientation-selective, looking at the OSI, it could be even more. Orientation-selective cells with an OSI of greater than 25 represent about 50% of my sample. The earliest recordings at P21 are around a time, when finally almost all geniculate fibres are firmly established in layer IV (Smith and Thompson, submitted). The segregation of on- and off-layers in the dLGN is also completed around this time. In the retina, the spontaneous bursts of activity become unsynchronized between P21 and P30 (Wong et al., 1993). The considerable degree of orientation-tuning found at this time could be taken to indicate that orientation-selectivity in some neurons is intrinsic, as has been believed to follow from Chapman and Stryker's results. However, my results also show that cortical neurons respond to the oriented gratings through the closed eyelid at the same time. Thus, visual experience could influence and could have influenced the development of the orientation-tuning present at P21. Earlier recordings need to be made, and orientation-selectivity needs to be assessed at the time when the first visual driving of cortical neurons can be detected. Interestingly, in the Siberian hamster, photic responses in the supra- chiasmatic nucleus can be found as early as P3, through the closed eyelids (Duffield et al., 1995) - this is the time when in the

Syrian hamster topography in the geniculo-cortical map is formed (Chapter III). This implies that information about light-levels can be detected at even an earlier stage in development.

Recent work on the nature of orientation-tuning in adult primary visual cortex, suggests that very precise geniculate input to layer IV is necessary for the receptive field structure underlying orientation-tuning (Chapman et al., 1991; Reid and Alonso, 1995; Ferster et al., 1996). How the required precision of this wiring of single cells could be achieved genetically is difficult to imagine. However, it could be possible that sparse input to cortical neurons "randomly" creates some orientation-selective cells or the differential, intrinsic bursting of ON and OFF retinal ganglion cells could set-up a basic receptive field structure (Wong et al., 1997). In essence, only one ON and one OFF dLGN-neuron with slightly displaced receptive field are needed to create a very basic orientation-selective cell. Dark-rearing experiments in kittens (Blakemore and Van Sluyters, 1975) as well as results from cortical infusion of TTX in ferrets (Chapman and Stryker, 1993) suggest that although some degree of orientation-selectivity is independent of visual experience, retinal activity is necessary for maturation of orientation-tuning: in both paradigms less neurons in area 17 are orientation-tuned and the existing tuning is very broad. And at least in the experiment on ferret, the blockade of visual cortical activity did not start early enough to rule out completely the influence of visual-experience on the earliest orientation-selective cells. Chapman and Stryker's TTX infusions commenced between P21 and P23. But in my recordings at P21 I found visual driving and orientation-tuning in cortex. Earlier retinal blockade as well as dark-rearing from birth would be necessary to assess the full effect of

intrinsic retinal activity and retinal driving on the development of orientation-selectivity.

Similar issues apply for directionality of neurons in area 17. Directional units seem to be sparse between P21 and P24, but a few are certainly present. It will be interesting to assess their laminar location. It is not clear if direction-selectivity develops independently or arises from initially orientation-selective units.

4.4 Implications

Patterned activity has been deemed to be very important for the development of the visual system since the 1970s. It has been implicated in OD-column plasticity in cortex, in the segregation of eye-specific layers and ON and OFF layers in the dLGN (Sretavan and Shatz, 1986; Hahm et al., 1991), in the refinement of altered topographic maps (see Chapter V) as well as in shaping receptive field properties in area 17 (Blakemore and Van Sluyters, 1975). This study suggests that visually-driven, patterned activity could be present in parts of the developing visual system much earlier than previously assumed. Irrespective of whether the patterning arises from the optics or is neuronal in origin, the neuronal responses in cortex are modulated by the orientation as well as the phase of the grating. Thus, there is temporal and probably also spatial patterning of neuronal activity in cortex. However, it is not clear whether the natural environment of ferret kits can also stimulate visual cortex. The light-levels of the gratings used are comparable to those of an in door laboratory housing. And towards the end of the third postnatal week, ferret kits also start their first exploratory ventures out of the nest (Porter and Brown, 1985), just before the age at which recordings were done for this chapter. A closer look at the natural habitat and

behaviour of the ferret's closest wild relatives, the Spanish polecat, might be helpful. If these results also hold true for natural stimuli, visual experience could influence the development of visual structures much earlier than previously thought.

In this light, two recent studies are very interesting. Although a map of orientation columns in area 17 only seems to be detectable after natural eye-opening in the ferret (Chapman et al., 1996), Gödecke and Bonhoeffer (1996) suggested common experience is not necessary for the developmental alignment of the orientation maps from the two eyes in kittens. This result was based on a reverse occlusion paradigm starting at eye-opening. My results however suggest common experience for the two eyes before this time. Interestingly, in binocular suture experiments, the map obtained through optical imaging developed at the same rate for three weeks if eyelids were sutured or not and only later the binocular suturing altered the developmental rate of map formation (Crair et al.,1997). On the basis of these results it was proposed that visual experience is not important in the first few weeks after eye-opening to set-up maps of orientation-selectivity in area 17 of kittens. However, it has been suggested before that a low frequency stimulus could also penetrate the sutured eye-lid (Spear et al., 1978; Loop and Sherman, 1976). Around the time of eye-opening, a weak low frequency signal might be sufficient or even better suited to influence development. The patterning of neuronal activity described in this chapter could be utilised in a variety of developmental tasks in visual cortex, for example the temporal modulation of the firing in topographic map refinement, the spatial patterning by the orientation of the stimulus for structuring the receptive field and both in aligning the topographic and the orientation map in visual cortex.

VII. Conclusions

1. Map formation in area 17

2. Early activity in visual development

VII. Conclusions

My thesis shows the emergence of the geniculo-cortical topography from an early disordered input to the subplate and lower cortical layers. These results confirm that the subplate could indeed be the place where an exchange of neighbours takes place to generate the necessary map reversal between geniculate and area 17 (Connolly and Van Essen, 1984; Nelson and LeVay, 1985) and they contradict the suggestion of passive relay of topography from the dLGN. The detailed mechanics of the ordering process, however, still proves to be elusive. My work on the enucleate indicates that retinal-dependent and -independent mechanisms can affect the geniculo-cortical mapping process. Although blockade of retinal activity does not prevent geniculo-cortical map formation, the early geniculo-cortical map is plastic and retinal activity plays a role in its rearrangement and refinement. Finally, the previous chapter described visual driving of cortical neurons before natural eye-opening in ferret kits as well as orientation-selectivity of those cells for stimuli presented through the closed eye-lid. Thus, visual experience could influence the development of the visual system much earlier than previously assumed.

The question remains where do we go from here? In the individual chapters I have already started to discuss what specific experiments still need to be done to lead the work presented here to a conclusion. At the end of my thesis, I would like to discuss where I would like to take my results, what future experiments need to be done to get closer to the answers of how geniculo-cortical topography develops and to find out more about the characteristics and the role of early activity in the developing visual system.

1. Map formation in area 17

(i) What cues guide map formation in cortex? My results describe an early disordered geniculo-cortical input to visual cortex. The adult geniculo-cortical map is sculpted out of the early disorder either by stabilisation of axon terminals or by directed growth of nerve terminals. Axon morphology of growing geniculo-cortical fibres in subplate and lower cortical layers needs clarification. Although most results point towards a sculpting of the geniculo-cortical map from multiple short collaterals as described underneath hamster visual cortex (Naegele et al, 1988; see Chapter III, Discussion), it has not been proven that the geniculate-cortical fibres have multiple short collaterals. Studies on the somato-sensory system are contradictory (Agmon et al., 1993; Catalano et al., 1996).

The next step is to identify the mechanics of directed growth and/or selection of collaterals. The development of order from disorder can be visualized in the geniculo-cortical system of the hamster and various tools like the nearest neighbour or the density analysis are available to quantify topography. Therefore, this system provides an ideal model in which to manipulate factors which have been implicated in map formation and early plasticity. Many of these, like growth factors or drugs which block neuronal activity or confound particular transmitter systems, could be packed into the slow-release plastic elvax (Smith et al., 1994) and thus be applied directly to the neonate cortex at a time when the map is still disordered. Growth-factors could, via localised release as posed by Thoenen (1995), provide a selective incentive for stabilisation of synapses or could play a more general permissive role for ingrowth into area 17. It has also been shown recently

that the expression of BDNF and NGF can be regulated by activity (Lindholm et al., 1994). NT4-5 and BDNF have already been implicated in the regulation of ocular dominance plasticity (Cabelli et al, 1995), and BDNF and NT-3 in the control of dendritic growth of pyramidal neurons in cortex (McAllister et al., 1997). Another interesting candidate for a general switch to regulate map formation in cortex is 5-HT. 5-HT is taken up by developing thalamic terminals and temporarily accumulated in their cell bodies (Lebrand et al., 1996). Work in the mouse somatosensory cortex shows that perinatal up-regulation of 5-HT interferes with the generation of barrel cortex (Cases et al., 1996). In this particular study, transgenic mice deficient for Monoamine oxidase A (MAO-A) or systemic injections of clorgyline, a MAO-A inhibitor, were used to block MAO-A and thus the breakdown of 5-HT. This is the only paradigm so far to succeed in preventing barrel cortex formation. It should be interesting to see if and how up-regulation of 5-HT affects geniculo-cortical development. Because of its systemic effects, in particular on the kidneys, it would be preferable to apply clorgyline via elvax directly.

Work on retino-collicular topography suggests a major signal for mapping might lie in molecular gradients of surface molecules on the neurons themselves (see I. Introduction). So, another general approach would be the search for differential expression pattern along different axes of the area 17 map. It might be interesting to investigate geniculo-cortical topography in knock-out mice with deficiencies in specific transmitter systems using the anatomical tools employed in this thesis. Also, animals should be assessed in which specific layers in cortex were eliminated by early methylazoxymethanol

(MAM) treatment. In such animals, the role of the subplate or specific cortical layers for map formation can be investigated.

(ii) How similar are thalamo-cortical mapping processes across different senses?

Another important question lies in the generality of the findings from the geniculo-cortical map. The concept of a protocortex, which is supported by experiments on cortical transplants and on rerouting of visual input to auditory cortex, suggests that there should be common features in the developmental strategies (O'Leary et al., 1992 ; Sur et al, 1988). It is essential to compare notes: so far, it has always been suggested that even the early thalamo-cortical input in the rodent is topographically ordered (Agmon et al., 1995; Catalano et al., 1996). However, ingrowing fibres were described to run tangentially in the subplate or the lower cortical layers of mice and rats, which suggests earlier, at least local, disorder (Agmon et al., 1993; Catalano et al. 1991, 1996). It would be interesting to investigate somato-sensory thalamo-cortical topography with paired microbead injections, either prenatally in the mouse or rat, if possible, or in the newborn hamster. Interestingly, the results concerning the role of activity in map refinement and rearrangement parallel each other in the visual and the somatosensory system, although the somatosensory system could potentially be influenced much earlier by sensory stimulation than the visual system (Fitzgerald, 1986). However, early spontaneous waves of activity are present in the retina and the dLGN.

(iii) The role of retinal activity. The results in chapters IV and V suggest that retinal activity plays a role in the refinement and the rearrangement of the geniculo-cortical map rather than in its basic set-up. A parallel result was found for sensory driving in the

development of barrel cortex by blocking cortical activity (Schlaggar et al., 1994; Fox et al., 1996). The issue of intra-cortical or intra-geniculate spontaneous activity in development has been raised by work on horizontal connections in visual cortex (Ruthazer and Stryker, 1996) and needs further investigation. However, effects in cortex by cortical TTX alone do not tell us very much about the origin of the activity, because it wipes out all input as well as the intrinsic activity. Such experiments include the possibility that it is the retinal component that was important. Intracortical activity could be blocked by the direct release of TTX from elvax over area 17 and topographic development investigated with paired bead injections. It is also not resolved what is the nature of the retinal activity which is important for the generation of the ipsilateral map after monocular enucleation. Spontaneous waves are a possible source, but in the light of the results in Chapter VI, early visual driving before eye-opening is another possibility. It would be very interesting to find out how early visual experience begins in the Syrian hamster.

The double tracer injections together with the various quantitative analyses provide a very sensitive tool to investigate even small changes in topographic precision. Thus, topography and scatter after binocular enucleation or binocular TTX injection could be re-evaluated. If retinal activity is involved in geniculo-cortical map refinement, an effect should be seen. The same tools could be employed to compare and contrast the extent of early and adult plasticity after peripheral manipulations like retinal lesions. It would be interesting to see if the effects only differ in extent and time-scale or if separate mechanisms act in developmental and adult plasticity.

2. Early activity in visual development

The interest in retinal activity in development comes in phases, the most recent boost in its popularity stems from the finding that well before eye-opening spontaneous retinal waves sweep across the ferret retina (Meister et al., 1991; Wong et al., 1993). However, that also steered the focus away from visual experience - a lot of the more recent work on the development of visual cortex tries to make the point that visual experience has no or only a secondary role to intrinsic factors. Examples are the development of long range connections in ferret visual cortex (Ruthazer and Stryker, 1996) and the development of orientation preference maps in area 17 and 18 in kittens (Gödecke and Bonhöffer, 1996; Gödecke et al., 1997; Crair et al., 1997). However, in many experiments manipulation of visual driving started around the time of eye-opening or binocular suturing was employed. We need to reconsider the experimental set-up of studies looking at the development with binocular lid-suture and dark rearing and also question whether features present at eye-opening like orientation-selectivity have indeed developed independently of visual driving.

(i) The role of spontaneous and visual driving before eye-opening. To get a clearer idea about its possible role in development, the spatio-temporal features of early visual driving need to be investigated. Questions concerning the onset of visual driving, the transition from spontaneous waves to visual experience and a comparison between the stimuli used in the laboratory and the natural environment of ferret kits need to be addressed. Furthermore, it is not known how the spontaneous retinal waves are transmitted to cortex. Multiple electrode recordings could provide the data about the spatio-temporal

activity patterns in visual cortex of spontaneous as well as visual evoked activity. Such results could be a starting point for developmental models of formation of topography as well as of the generation of orientation-selectivity or of disparity selective cells.

(ii) Development of orientation-tuning. Since Chapman and Stryker's (1993) demonstration of orientation-tuning of cortical neurons after early, artificial opening of eyelids, opinion has swung towards a more important role for intrinsic mechanisms in the development of orientation-tuning. My evidence strengthens their argument for a certain degree of innate orientation-tuning in corroborating their results, but also weakens it, since my recordings also indicate onset of visual experience before eye-opening. I also strongly believe that recording of cortical neurons is technically possible before P21. It needs to be seen what degree of orientation-selectivity can be found in the earliest possible recordings. It is also important to determine the receptive field structure of these orientation-tuned neurons - and possible changes up to and after eye-opening. This line of research might lead us to how orientation-selectivity develops. Specific questions are: is the early input sparse and how much does it change over the weeks around eye-opening.

The two main areas of my work seem in apparent conflict. On one hand I showed that development of basic topography is independent of activity, on the other hand I propose that visual experience could influence development prior to eye-opening. However, these two ideas could come together in the refinement of topographic maps. Also early retinal activity is clearly involved in the generation of aberrant maps after retinal manipulations. And finally, there is still the problem of "micro-topography", the mapping of appropriate input into one cortical cell and how these emergent cortical maps of

properties like orientation tuning need to be registered with the retinotopic map itself. Similar developmental mechanisms could govern tasks as diverse as refinement of the geniculo-cortical topography and the generation of receptive field properties.

REFERENCES

Adams NC, Lozsadi LD, Guillery RW (1997) Complexities in the thalamocortical and corticothalamic pathways. Eur J Neurosci 9: 204-209.

Agmon A, Yang LT, O'Dowd DK, Jones EG (1993) Organized growth of thalamocortical axons from the deep tier of terminations into layer IV of developing mouse barrel cortex. J Neurosci 13: 5365-5382.

Agmon A, Yang LT, Jones EG, O'Dowd DK (1995) Topological precision in the thalamic projection to neonatal mouse barrel cortex. J Neurosci 15: 549-561.

Baker GE, Thompson ID, Krug K, Smyth D and Tolhurst DJ (1998) Spatial-frequency tuning and geniculocortical projections in the visual cortex (Areas 17 and 18) of the pigmented ferret. Eur J Neurosci *in press*.

Barlow HB, Blakemore C, Pettigrew JD (1967) The neural mechanism of binocular depth discrimination. J Physiol Lond 193: 327-342.

Barlow HB, Pettigrew JD (1971) Lack of specificity of neurones in the visual cortex of young kittens. J Physiol Lond 218: 98P-100P.

Blakemore C, Molnar Z (1990) Factors involved in the establishment of specific interconnections between thalamus and cerebral cortex. Cold Spring Harb Symp Quant Biol 55: 491-504.

Blakemore C, Van Sluyters RC (1975) Innate and environmental factors in the development of the kitten's visual cortex. J Physiol Lond 248: 663-716.

Cabelli RJ, Hohn A, Shatz CJ (1995) Inhibition of ocular dominance column formation by infusion of NT-4/5 or BDNF. Science 267: 1662-1666.

Cases O, Vitalis T, Seif I, De-Maeyer E, Sotelo C, Gaspar P (1996) Lack of barrels in the somatosensory cortex of monoamine oxidase A-deficient mice: role of a serotonin excess during the critical period. Neuron 16: 297-307.

Catalano SM, Robertson RT, Killackey HP (1991) Early ingrowth of thalamocortical afferents to the neocortex of the prenatal rat. Proc Natl Acad Sci (USA) 88: 2999-3003.

Catalano SM, Robertson RT, Killackey HP (1996) Individual axon morphology and thalamocortical topography in developing rat somatosensory cortex. J Comp Neurol 366: 36-53.

Chalupa LM, Snider CJ, Kirby MA (1996) Topographic organization in the retinocollicular pathway of the fetal cat demonstrated by retrograde labeling of ganglion cells. J Comp Neurol 368: 295-303.

Chan SO, Guillery RW (1994) Changes in fiber order in the optic nerve and tract of rat embryos. J Comp Neurol. 344: 20-32.

Chapman B, Stryker MP (1993) Development of orientation selectivity in ferret visual cortex and effects of deprivation. J Neurosci 13: 5251-5262.

Chapman B, Stryker MP, Bonhoeffer T (1996) Development of orientation preference maps in ferret primary visual cortex. J Neurosci 16: 6443-6453.

Chapman B, Zahs KR, Stryker MP (1991) Relation of cortical cell orientation selectivity to alignment of receptive fields of the geniculocortical afferents that arborize within a single orientation column in ferret visual cortex. J Neurosci 11: 1347-1358.

Cheng HJ, Nakamoto M, Bergemann AD, Flanagan JG (1995) Complementary gradients in expression and binding of elf-1 and mek-4 in development of the topographic retino-tectal projection map. Cell 82: 371-381.

Cline HT (1991) Activity-dependent plasticity in the visual systems of frogs and fish. Trends Neurosci 14: 104-111.

Connolly M, Van Essen D (1984) The representation of the visual field in parvocellular and magnocellular layers of the lateral geniculate nucleus in the macaque monkey. J Comp Neurol 226: 544-564.

Cooper ML, Blasdel GG (1980) Regional variation in the representation of the visual field in the visual cortex of the Siamese cat. J Comp Neurol 193: 237-253.

Crair MC, Gillespie DC, Ruthazer ES, Stryker MP (1997) Matching orientation maps develop in cat visual cortex without visual experience but maintained responsiveness requires experience. Neurosci Abs 23: 694.3.

Crossland WJ, Uchwat CJ (1982) Neurogenesis in the central visual pathways of the golden hamster. Brain Res 281: 99-103.

Drescher U, Kremoser C Handwerker C, Loschinger J, Noda M, Bonhoeffer F (1995) In vitro guidance of retinal ganglion cell axons by RAGS, a 25kDa tectal protein related to ligands for Eph receptor tyrosine kinases. Cell 82: 359-370.

Duffield GE, Dickerson JM, Alexander IH, Ebling-FJ (1995) Ontogeny of a photic response in the suprachiasmatic nucleus in the Siberian hamster (Phodopus sungorus). Eur J Neurosci 7: 1089-1096.

Dursteler MR, Blakemore C, Garey LJ (1979) Projections to the visual cortex in the golden hamster. J Comp Neurol 183: 185-204.

Fawcett JW, O'Leary DD, Cowan WM (1984) Activity and the control of ganglion cell death in the rat retina. Proc Natl Acad Sci (USA) 81: 5589-5593.

Ferster D, Chung S, Wheat H (1996) Orientation selectivity of thalamic input to simple cells of cat visual cortex. Nature 380: 249-252.

Fitzgerald M (1987) Spontaneous and evoked activity of fetal primary afferents in vivo. Nature 326: 603-605.

Florence SL, Jain N, Pospichal MW, Beck PD, Sly DL, Kaas JH (1996) Central reorganization of sensory pathways following peripheral nerve regeneration in fetal monkeys. Nature 381: 69-71.

Fox K, Schlaggar BL, Glazewski S, O'Leary DD (1996) Glutamate receptor blockade at cortical synapses disrupts development of thalamocortical and columnar organization in somatosensory cortex. Proc Natl Acad Sci (USA) 93: 5584-5589.

Freeman RD, Ohzawa I (1992) Development of binocular vision in the kitten's striate cortex. J Neurosci 12: 4721-4736.

Fregnac Y, Imbert M (1984) Development of neuronal selectivity in primary visual cortex of cat. Physiol Rev 64: 325-434.

Friauf E, McConnell SK, Shatz CJ (1990) Functional synaptic circuits in the subplate during fetal and early postnatal development of cat visual cortex. J Neurosci 10: 2601-2613.

Ghosh A, Shatz CJ (1992) Pathfinding and target selection by developing geniculocortical axons. J Neurosci 12: 39-55.

Godecke I, Bonhoeffer T (1996) Development of identical orientation maps for two eyes without common visual experience. Nature 379: 251-254.

Godecke I, Kim DS, Bonhoeffer T, Singer W (1997) Development of orientation preference maps in area 18 of kitten visual cortex. Eur J Neurosci 9: 1754-1762.

Godement P, Saillour P, Imbert M (1979) Thalamic afferents to the visual cortex in congenitally anophthalmic mice. Neurosci Lett 13: 271-278.

Guillery RW, Hickey TL, Kaas JH, Felleman DJ, Debruyn EJ, Sparks DL (1984) Abnormal central visual pathways in the brain of an albino green monkey (Cercopithecus aethiops). J Comp Neurol 226: 165-183.

Guillery RW, Kaas JH (1971) A study of normal and congenitally abnormal retinogeniculate projections in cats. J Comp Neurol 143: 73-100.

Guillery RW, Ombrellaro M, LaMantia AL (1985) The organization of the lateral geniculate nucleus and of the geniculocortical pathway that develops without retinal afferents. Brain. Res. 352: 221-233.

Hahm JO, Langdon RB, Sur M (1991) Disruption of retinogeniculate afferent segregation by antagonists to NMDA receptors. Nature 351: 568-570.

Hebb DH (1949) The Organization of Behavior. John Wiley, New York.

Herrmann K, Shatz CJ (1995) Blockade of action potential activity alters initial arborization of thalamic axons within cortical layer 4. Proc Natl Acad Sci (USA) 92: 11244-11248.

Horder TJ, Martin KA (1978) Morphogenetics as an alternative to chemospecificity in the formation of nerve connections. A review of literature, before 1978, concerning the control of growth of regenerating optic nerve fibres to specific locations in the optic tectum and a new interpretation based on contact guidance. Symp Soc Exp Biol 32: 275-358.

Huang K, Guillery RW (1985) A demonstration of two distinct geniculocortical projection patterns in albino ferrets. Brain Res 352: 213-220.

Hubel DH, Wiesel TN (1962) Receptive fields, binocular interaction and functional architecture in cat's visual cortex. J Physiol Lond 160: 106-154.

Hubel DH, Wiesel TN (1963a) Single cell responses in striate cortex of kittens deprived of vision in one eye. J Neurophysiol 26: 1003-1017.

Hubel DH, Wiesel TN (1963b) Receptive fields of cells in striate cortex of very young, visually inexperienced kittens. J Neurophysiol 26: 994-1002.

Hubel DH, Wiesel TN (1971) Aberrant visual projections in the Siamese cat. J Physiol Lond. 218: 33-62.

Huttenlocher PR (1967) Development of cortical neuronal activity in the neonatal cat. Exp Neurol 17: 247-262.

Jeffery G (1985) Retinotopic order appears before ocular separation in developing visual pathways. Nature 313: 575-576.

Jeffery G (1984) Transneuronal effects of early eye removal on geniculo-cortical projection cells. Brain Res 315: 257-263.

Jeffery G, Thompson ID (1986) The effects of prenatal and neonatal monocular enucleation on visual topography in the uncrossed retinal pathway to the rat superior colliculus. Exp. Brain.Res. 63: 351-363.

Kaas JH, Guillery RW (1973) The transfer of abnormal visual field representations from the dorsal lateral geniculate nucleus to the visual cortex in Siamese cats. Brain Res 59: 61-95.

Kaiserman-Abramof IR, Graybiel AM, Nauta WJ (1980) The thalamic projection to cortical area 17 in a congenitally anophthalmic mouse strain. Neuroscience 5: 41-52.

Kennedy H, Salin P, Bullier J, Horsburgh G (1994) Topography of developing thalamic and cortical pathways in the visual system of the cat. J Comp Neurol 348: 298-319

Krug K, Smith AL, Thompson ID (1998) The development of topography in the hamster geniculo-cortical projection. J Neurosci *accepted pending revision.*

Krug K, Thompson ID (1996) Mechanisms involved in the normal and abnormal development of geniculo-cortical topography in the Syrian hamster. Soc Neurosci Abs 22: 404.11.

Krug K, Trevelyan AJ, Thompson ID (1995) A study of abnormal geniculo-cortical topography in the anaesthetised Syrian hamster. J Physiol 485:9P.

Lebrand C, Cases O, Adelbrecht C, Doye A, Alvarez C, El-Mestikawy S, Seif I, Gaspar P (1996) Transient uptake and storage of serotonin in developing thalamic neurons. Neuron 17: 823-835.

Linden DC, Guillery RW, Cucchiaro J (1981) The dorsal lateral geniculate nucleus of the normal ferret and its postnatal development. J Comp Neurol 203: 189-211.

Lindholm D, Harikka J, da-Penha-Berzaghi M, Castren E, Tzimagiorgis G, Hughes RA, Thoenen-H (1994) Fibroblast growth factor-5 promotes differentiation of cultured rat septal cholinergic and raphe serotonergic neurons: comparison with the effects of neurotrophins. Eur J Neurosci 6: 244-252.

Loop MS, Sherman SM (1976) Visual discriminations during eyelid closure in the cat. Brain Res 128: 329-339.

Lund RD, Cunningham TJ, Lund JS (1973) Modified optic projections after unilateral eye removal in young rats. Brain Behav Evol 8: 51-72.

Maffei L, Galli-Resta L (1990) Correlation in the discharges of neighboring rat retinal ganglion cells during prenatal life. Proc. Natl. Acad. Sci. (USA) 87: 2861-2864.

McAllister AK, Katz LC, Lo DC (1997) Opposing roles for endogenous BDNF and NT-3 in regulating cortical dendritic growth. Neuron. 18: 767-778.

Meister M, Wong RO, Baylor DA, Shatz CJ (1991) Synchronous bursts of action potentials in ganglion cells of the developing mammalian retina. Science 252: 939-943.

Merrill EG, Ainsworth A (1972) Glass-coated platinum-plated tungsten microelectrodes. Med Biol Eng 10: 662-672.

Mesulam MM (1982) Principles of horseradish peroxidase neurohistochemistry and their applications for tracing neural pathways. In: Tracing neural connections with horseradish peroxidase (Mesulam MM, ed.), pp1-151. Chrichester, UK: Wiley.

Miller B, Chou L, Finlay BL (1993) The early development of thalamocortical and corticothalamic projections. J Comp Neurol 335: 16-41.

Molnar Z, Blakemore C (1995) How do thalamic axons find their way to the cortex? Trends Neurosci 18: 389-397.

Mooney R, Penn AA, Gallego R, Shatz CJ (1996) Thalamic relay of spontaneous retinal activity prior to vision. Neuron 17: 863-874.

Naegele JR, Jhaveri S, Schneider GE (1988) Sharpening of topographical projections and maturation of geniculocortical axon arbors in the hamster. J Comp Neurol 277: 593-607.

Nakamoto M, Cheng HJ, Friedman GC, McLaughlin T, Hansen MJ, Yoon CH, O'Leary DD, Flanagan JG (1996) Topographically specific effects of ELF-1 on retinal axon guidance in vitro and retinal axon mapping in vivo. Cell 86: 755-766.

Nakamura H, O'Leary DD (1989) Inaccuracies in initial growth and arborization of chick retinotectal axons followed by course corrections and axon remodeling to develop topographic order. J Neurosci 9: 3776-3795.

Nelson SB, LeVay S (1985) Topographic organization of the optic radiation of the cat. J Comp Neurol 240: 322-330.

O'Leary DD, Crespo D, Fawcett JW, Cowan WM (1986) The effect of intraocular tetrodotoxin on the postnatal reduction in the numbers of optic nerve axons in the rat. Brain Res 395: 96-103.

O'Leary DD, Fawcett JW, Cowan WM (1986) Topographic targeting errors in the retinocollicular projection and their elimination by selective ganglion cell death. J Neurosci 6: 3692-3705.

Porter V, Brown N (1985) The complete book of ferrets. Pelham Books, p. 93, p. 172.

Reese BE, Baker GE (1993) The re-establishment of the representation of the dorso-ventral axis in the chiasmatic region of the ferret. Vis Neurosci 10: 957-968.

Reid RC, Alonso JM (1995) Specificity of monosynaptic connections from thalamus to visual cortex. Nature 378: 281-284.

Reid RC, Alonso JM (1996) The processing and encoding of information in the visual cortex. Curr Opin Neurobiol 6: 475-480.

Roe AW, Pallas SL, Hahm JO, Sur M (1990) A map of visual space induced in primary auditory cortex. Science 250: 818-820.

Ruthazer ES, Stryker MP (1996) The role of activity in the development of long-range horizontal connections in area 17 of the ferret. J Neurosci 16: 7253-7269.

Scholes JH (1979) Nerve fibre topography in the retinal projection to the tectum. Nature 278: 620-624.

Schlaggar BL, O'Leary DD (1994) Early development of the somatotopic map and barrel patterning in rat somatosensory cortex. J Comp Neurol 346: 80-96.

Sengelaub DR, Jacobs LF, Finlay BL (1985) Regional differences in normally occurring cell death in the developing hamster lateral geniculate nuclei. Neurosci Lett 55: 103-108.

Simon DK, O'Leary DD (1991) Relationship of retinotopic ordering of axons in the optic pathway to the formation of visual maps in central targets. J Comp Neurol 307: 393-404.

Simon DK, O'Leary DD (1992) Development of topographic order in the mammalian retinocollicular projection. J Neurosci 12: 1212-1232.

Simon DK, Prusky GT, O'Leary DD, Constantine Paton M (1992) N-methyl-D-aspartate receptor antagonists disrupt the formation of a mammalian neural map. Proc Natl Acad Sci (USA) 89: 10593-10597.

Smith AL, Krug K, Thompson ID (1994) The development of normal and abnormal geniculo-cortical topographies in the Syrian hamster. Soc Neurosci Abs 20: 695.10.

Smith AL, Thompson ID (1997) Differential patterning of ionotropic glutamate receptor subtypes during establishment of thalamocortical connectivity in the developing ferret primary visual cortex. (*submitted*).

So KF, Woo HH, Jen LS (1984) The normal and abnormal postnatal development of retinogeniculate projections in golden hamsters: an anterograde horseradish peroxidase tracing study. Brain Res 314: 191-205.

Spear PD, Ton L, Langsetmo A (1978) Striate cortex neurons of binocularly deprived kittens respond to visual stimuli through the closed eyelids. Brain Res 155: 141-146.

Sperry RW (1963) Chemoaffinity in the orderly growth of nerve fibre patterns and connections. Proc Natl Acad Sci (USA) 50: 703-710.

Sretavan DW, Shatz CJ (1986) Prenatal development of cat retinogeniculate axon arbors in the absence of binocular interactions. J Neurosci 6: 990-1003.

Sretavan DW, Shatz CJ (1986) Prenatal development of retinal ganglion cell axons: segregation into eye-specific layers within the cat's lateral geniculate nucleus. J Neurosci 6: 234-251.

Thompson ID (1979) Changes in the uncrossed retinotectal projection after removal of the other eye at birth. Nature 279: 63-66.

Thompson ID (1980) Plasticity in the uncrossed retinotectal projection of the Syrian hamster. D Phil Thesis, Cambridge University.

Thompson ID, Cordery P (1997) Cell death and the elimination of topographic errors in the hamster retino-collicular projection. J Physiol 501.P.

Thompson ID, Cordery P, Holt CE (1995) Postnatal changes in the uncrossed retinal projection of pigmented and albino Syrian hamsters and the effects of monocular enucleation. J Comp Neurol 357: 181-203.

Thompson I, Holt C (1989) Effects of intraocular tetrodotoxin on the development of the retinocollicular pathway in the Syrian hamster. J Comp Neurol 282: 371-8.

Thompson ID, Kossut M, Blakemore C (1983) Development of orientation columns in cat striate cortex revealed by 2-deoxyglucose autoradiography. Nature 301: 712-715.

Torrealba F, Guillery RW, Eysel U, Polley EH, Mason CA (1982) Studies of retinal representations within the cat's optic tract. J Comp Neurol 211: 377-396.

Trevelyan AJ (1992) Development of the mammalian geniculo-cortical projection. D.Phil Thesis, Oxford University.

Trevelyan AJ, Thompson ID (1992) Altered topography in the geniculo-cortical projection of the golden hamster following neonatal monocular enucleation. Eur J Neurosci 4: 1104-1111.

Trevelyan AJ, Thompson ID (1995) Neonatal monocular enucleation and the geniculo-cortical system in the golden hamster: shrinkage in dorsal lateral geniculate nucleus and area 17 and the effects on relay cell size and number. Vis Neurosci 12: 971-983.

Van der Loos H, Woolsey TA (1973) Somatosensory cortex: structural alterations following early injury to sense organs. Science 179: 395-398.

Waite PM, Li L, Ashwell KW (1992) Developmental and lesion induced cell death in the rat ventrobasal complex. NeuroReport 3: 485-488.

Walter J, Henke-Fahle S, Bonhoeffer F (1987) Avoidance of posterior tectal membranes by temporal retinal axons. Development 101: 909-913.

Walter J, Kern-Veits B, Huf J, Stolze B, Bonhoeffer F (1987) Recognition of position-specific properties of tectal cell membranes by retinal axons in vitro. Development 101: 685-96.

Weliky M, Katz LC (1997) Disruption of orientation tuning in visual cortex by artificially correlated neuronal activity. Nature 386: 680-685.

Willshaw DJ, von der Malsburg C (1976) How patterned neural connections can be set up by self-organization. Proc Soc Lond B Biol Sci 194: 431-445.

Wong RO, Herrmann K, Shatz CJ (1991) Remodeling of retinal ganglion cell dendrites in the absence of action potential activity. J Neurobiol 22: 685-697.

Wong RO, Meister M, Shatz CJ (1993) Transient period of correlated bursting activity during development of the mammalian retina. Neuron 11: 923-938.

Wong RO, Oakley DM (1996) Changing patterns of spontaneous bursting activity of on and off retinal ganglion cells during development. Neuron 16: 1087-1095.

Woolsey TA, Van der Loos H (1970) The structural organization of layer IV in the somatosensory region (SI) of mouse cerebral cortex. The description of a cortical field composed of discrete cytoarchitectonic units. Brain Res 17: 205-242.

Worgotter F, Eysel UT (1987) Quantitative determination of orientational and directional components in the response of visual cortical cells to moving stimuli. Biol Cybern 57: 349-355.

Yates PA, Friedman G, O'Leary DDM (1996) Chick retino-tectal map develops primarily by arborisation of collateral branches. Neurosci Abs 22: 765.4.